© 2018
Lizahira Rodriguez-Colon
ALL RIGHTS RESERVED

ROLE OF G9A METHYLTRANSFERASE IN THE DNA DAMAGE RESPONSE SIGNAL

By

LIZAHIRA RODRIGUEZ-COLON

A dissertation submitted to the

School of Graduate Studies

Rutgers, The State University of New Jersey

In partial fulfillment of the requirements

For the degree of

Doctor of Philosophy

Graduate Program in Cellular and Molecular Pharmacology

Written under the direction of

Shridar Ganesan

And approved by

_____

_____

_____

_____

New Brunswick, NJ
May 2018

ABSTRACT OF THE DISSERTATION

Role of G9a methyltransferase in the DNA damage response signal

by LIZAHIRA RODRIGUEZ-COLON

Dissertation Director:

Shridar Ganesan

DNA damage induces a choreographed set of local changes in histone modifications which leads to efficient recruitment of DNA repair factors. The regulation of these chromatin modifications at DNA breaks is critical to maintain genome integrity. Recent studies in our lab have identified a role for G9a methyltransferase in regulating DNA repair. The overall aim of this project was to elucidate how G9a activity regulates this pathway and to identify the effects of its inhibition in this process. It was shown that G9a localizes to sites of DNA damage in an ATM-dependent fashion and that inhibition of G9a activity affects early recruitment of multiple DNA repair factors. We found that catalytic inhibition of G9a using UNC0638 results in increased ATM activation. This led to increased "spreading" of pH2AX and MDC1 signals seen at regions of localized DNA breaks induced by UV-laser scissors, which was dependent upon ATM activation. This was also associated with increased levels of H3K36me2 and H3K56Ac. Biochemical data showed that G9a interacts and regulates HDAC1/2 activity during the DNA damage response. G9a inhibition led to decreased HDAC1 methylation, and increased ATM acetylation. These data suggest that G9a activity regulates the extent of ATM activation induced by DNA breaks and is required for

efficient recruitment of downstream DNA repair factors. Overall our data suggests that G9a plays a critical role in regulation of ATM-dependent signaling during the DNA damage response and raises the possibility of using G9a inhibitors in the clinical setting as part of novel cancer therapies.

Acknowledgements

I want to start by thanking my thesis advisor, Dr. Shridar Ganesan, for giving me the opportunity to join his lab. Thank you for your guidance, patience, and for being an important part in my development as a scientist. Also, I want to thank the members of my thesis committee, Dr. Bing Xia, Dr. Sharon Pine, and Dr. Jerome Langer for the advices and scientific discussions that were key to the success of this project. I want to thank my mentors at the Bridge to the Doctoral Degree Program, Dr. Beatrice Haimovich, Dr. Paul Copeland, and Dr. Jerome Langer for being there since the beginning of this journey and encouraging my professional development every step of the way. Being part of the bridge program and being made all the difference and was truly a key to my success in graduate school.

I want to thank the current and former members of my lab: Bratati Ganguly, Ming Yao, Jeremy Tang, Jinesh Geeya, Husam Al-Hraishawi, and specially to Atul Kulkarni, for being a mentor during the lasts years, and Vasudeva Ginjala for taking me in and making me part of his G9a project, work that is presented in the first chapter of this thesis and is part of the publication Ginjala, V. and Rodriguez-Colon, L. *et al* 2017. I want to thank Jacqueline Harris, Perry Dominguez and Tina Cicollela for all the help and patience during these years. I also want to acknowledge NIH-Bridge to the doctoral degree: UPR to UMDNJ grant (NIGMS/NIH Grant R25 GM058389), the Rutgers University Pipeline grant (R25 GM055145) and the Steve A. Cox Foundation Scholarship for the financial support.

I want to give special thanks to every mentor I had along the way, whose influences, in part, have shaped who I am and my journey. Alexis Osoria Lopez, for being the mentor I needed and believing in me when I didn't know how capable I was. You saw in me the potential and made sure I could see it too. Carlos Saavedra, for always believing in me and giving me the opportunity to develop my leadership through 4-H Club. Dr. Carlos Rios-Velazquez, for giving me the opportunity to do research for the first time and being a mentor in science and in life. Dr. Emil Bogeman, for believing in me and giving the opportunity to do my first internship. Your support and constant advice were key in this journey.

Most importantly, thanks to my family for being there for me every step of the way. My mom, Gloaida Colon, you always believed in me and you never got tired of telling me "Tu puedes". I have no words to describe how thankful I am of your constant support and unconditional love. My dad, Luis Rodriguez, thanks for believing in me and supporting me and for every advice along the way. Fernando Juarbe and Leyda Burgos (ma), thank you both for being like parents to me, for your love and unconditional support, and for treating me like a daughter. I am blessed for having you in my life. My aunt Julia Colon (mami Mery) for being almost like a mother to me. My brothers and sisters, Luis Emmanuel, Luis Pablo, Mariely Enid, and Dolly Janet for all the support. Special thanks to my boyfriend, Luis A. Bermudez Bosch; your unconditional love and constant support made this last year one more exciting and the load more bearable. I don't think there was a greater motivator than you. Thanks for believing in me and for pushing me to give my best, especially during the hard times. Thanks to my friends Eva N. Rubio, Jennifer

Casiano, Patricia Irizarry, Edgar Ferrer, Letzibeth Mendez, Tatiana Melendez, Jesus Rosado, Kalkal Trivedi and Nicole Vega-Cotto; having all of you and being able to count on you during these years made all the difference; I could not have done it without all of you. Specially, Nicole Vega-Cotto for being the family away from mine and for making your home like my second home.

Last but not least, I want to thank God for every blessing, every opened door, and for always guiding me; everything that He allowed brought me to this point.

I dedicate this work to my loving parents. I am who I am because you believed in me. Your faith, guidance, love and support shaped the person I am today. I am thankful beyond words.

Table of Content

Introduction

Cancer cells by nature have a higher rate of proliferation than normal cells (Feitelson et al. 2015). That means that they are in a constant need of replicating their DNA and as such depend on several mechanisms to repair damages to it. Researchers have taken advantage of this to develop strategies to treat cancer. Keeping in mind that DNA damage repair is especially required in cells with high rate of proliferation, one way to cause death of the cancer cell is by targeting and disrupting the DNA repair pathway. The aim is to cause accumulation of toxic levels of DNA damage that will render the cell unable to repair and divide. As normal cells are not constantly dividing, this approach is presumed to have a larger effect in tumors compared to normal tissue. However, this is not always the case and the toxicity and adverse effects of treatments demands for the developing of better strategies. To be able to develop new treatments, it is imperative to keep exploring and gaining knowledge on the exact mechanism of the DNA damage response (DDR), which factors are recruited, what is their functional role in the process, and whether or not it represents a suitable target in the clinic.

Activation of the DDR signal involves an orchestrated set of cellular events that are required for the proper and efficient repair of the DNA damage. Similar to other pathways in the cell, the signaling pathway is driven by a number of protein modifications, known as post-translational modifications (PTM), that are necessary to signal the damage, recruit more DDR factors and amplify the signal. Some of these modifications are phosphorylation, methylation and ubiquitylation.

Modification of the protein can lead to its activation (or deactivation), or a change of its conformation to allow its localization to certain parts in the cell, or the creation of docking sites that help in protein-protein interaction. In response to DNA damage, different proteins undergo (and/or catalyze) many of these modifications which mediates their recruitment and function at the sites of DNA breaks. Similarly, modification of histones tails is important in the DDR signal as it modulates the chromatin structure. This results in the relaxation of the chromatin, making the breaks physically available for the repair machinery. Hence, protein modification is an integral part the DDR signaling cascade.

An important regulator of chromatin structure is the methyltransferase G9a. (Tachibana et al. 2001) A member of the Suv39 family of SET domain containing proteins, G9a is the main euchromatin histone methyltransferase responsible for the mono- and di-methylation of the lysine 9 in histone 3 (H3K9me2) (Tachibana et al. 2002). In addition, G9a has been implicated in the silencing of tumor suppressor genes, contributing to tumorigenesis and metastasis (Chaturvedi et al. 2012). Overexpression of G9a has been reported in a number of different types of cancer including hepatocellular carcinoma, neuroblastoma, lung cancer, aggressive ovarian cancer, and invasive breast cancer. G9a upregulation has been correlated to poor prognosis and patient survival (discussed in detail later). Even more, G9a was found to be a substrate of the DNA damage related ATM kinase, suggesting that it has role in the DNA damage response (Matsuoka et al. 2007).

Given its involvement in chromatin modulation and its implication in cancer development and progression, it is important to elucidate the potential role of G9a in response to DNA damage. Understanding its role in the pathway will lead to the development of new and better strategies to treat cancer.

In the following sections an overview of the DNA damage response is presented. It includes a description of the different mechanism of DNA repair, and important protein and histone modifications in the process. Also, an overview on G9a methyltransferase, in which its activity, its importance in the regulation of different cellular process and its implications in cancer, is discussed.

DNA Damage: an overview

Daily, thousands of DNA lesions are accumulated in the cell and the proper repair of those DNA damages is crucial to maintain genome integrity (Fig. 1 and (Abbotts & Wilson 2017). DNA damage can arise from different sources. For example, some endogenous sources are exposure to reactive oxygen species (ROS), which results from normal metabolic reactions inside the cell, and accumulation of replicative stress during DNA replication. Some exogenous ones are exposure to chemicals, UV light or ionizing radiation. Cells have several DNA repair pathways to respond to DNA insults. These processes are put in place to

Damage type	Lesion	Potential consequences if unrepaired	Rate (per cell per day)	Major repair enzyme
Depurination/depyrimidation (spontaneous, glycosylase-mediated)	Abasic site	Mutagenic bypass, replication fork stalling, conversion to DSB	~10000	APE1
Cytosine deamination	Uracil (U:G)	Mutagenic base mispairing (C→T)	400	UNG, SMUG1, TDG
5-Methylcytosine deamination	Thymine (T:G)	Mutagenic base mispairing (C→T)	30	TDG, MBD4
Methylation	7-methylguanine	Tolerance, abasic site formation, ring-opening to FaPy-G	4000	MPG
	3-methyladenine	Replication stalling, chromosomal instability	600	MPG
Nitrosamine alkylation	O^6-methylguanine	Mutagenic base mispairing (G→A)	~200	MGMT
ROS attack, abortive TOP1 activity, etc.	SSB	Replication fork collapse, conversion to DSB	~10000	SSBR
Base oxidation	8-oxo-G	Mutagenic base mispairing (G→T)	~1000	OGG1
	Thymine glycol	Mutagenic base mispairing (T→C)	~500	NTH1

Table 1. Different types of DNA lesion, their consequences and enzymes associated with their repair. Taken from Abbots, 2017.

help the repair of the damaged DNA and assure that the integrity of the genome is kept in the nascent cell.

In the event of unrepaired DNA damage, there are several cellular mechanisms that cells have in place to assure that the unhealthy, mutation-carrier cells do not survive. During this time the cell won't continue to division, unless the repair is done, and the repair signal is turned off. Different mechanism function in parallel and involved, not only DNA damage response (DDR) factors but also activation of checkpoint pathways. Extensive and/or unrepaired DNA damage can cause the cell to exit the cell cycle and undergo senescence (irreversible arrest of cell proliferation) or in some cases apoptosis (programmed cell death), preventing in this way the development of cancer. When one of these processes is altered, cells with (potentially oncogenic) mutations will survive as a result. This will trigger other cellular processes, like an immune response, to get rid of the damaged/mutated cell. This way, the system makes sure that only cells with genome integrity are allowed to survive. However, in some cases, there are cells with the precise mutations that confer them the ability to bypass those mechanism. Those cells will be at risk of developing into cancerous cells and eventually give rise to a tumor.

Given the importance to maintain genome integrity, it is essential to understand the mechanisms and the factors involved in the repair.

Different mechanisms of DNA repair

As the repair of DNA damage is such an important activity, organisms from bacteria to humans, have developed and conserved different mechanisms to maintain fidelity of the DNA. The great majority of DNA lesions involved single-strand DNA (ssDNA) breaks. Other types of damages involve single nucleotide mutations, like base modification or incorrect insertion (Fig 2). This type of DNA lesions are repaired by different pathways that have been described. Base excision repair (BER) was first suggested by Lindahl in 1993 (Lindahl 1993) as a mechanism to repair modified bases. A different pathway was suggested few years before by Modrich to repair bases that are mis-incorporated during the replication of the DNA (Mismatch repair, MMR) (Modrich 1991). Years later Sancar proposed the nucleotide excision repair (NER) which is used to remove bulky DNA adducts that have been induced by UV light (Petit & Sancar 1999). In general, DNA repair pathways involves sensing of the damaged DNA, initiation of a signaling cascade, recruitment of repair factors and processing of the breaks for repair.

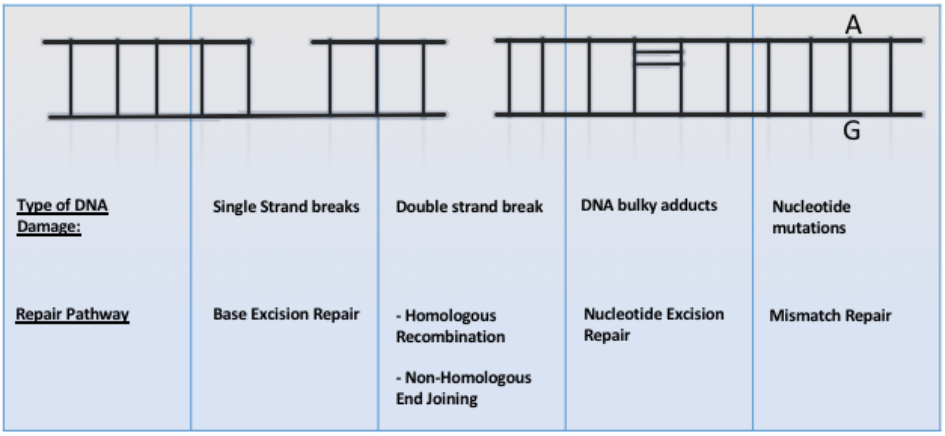

Figure 2. Different types of DNA damage and repair mechanism.
(Adapted from O'Connor 2016).

Base Excision Repair

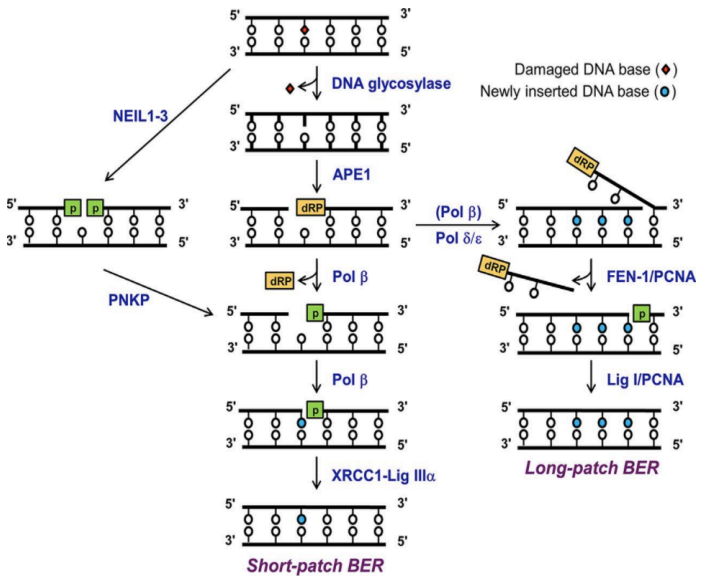

Figure 3. Base excision repair pathway and the different enzymes involved in the process. (Carter and Parson 2016).

The DNA can undergo spontaneous changes like hydrolysis, leading to apurinic/apyrimidinic (AP) sites; deamination of cytosine bases resulting in U:G or T:G; or oxidation of guanine due to intracellular ROS leading to G>T mutations. In the BER pathway, DNA glycosylases recognize the damaged base and excise it by cleavage of the glycosidic bond, generating an AP site. APE1 (AP endonuclease 1), recognizes the AP site and cleaves the DNA backbone, which results in a gap that is flanked in one side by a 3'-hydroxyl end and in the other side by 5'-deoxyribosephosphate (5'-dRP) end. The 3'hydroxyl end is a substrate for DNA polymerase β (Pol β), which removes 5'-dRP moieties and inserts the new corrected nucleotide. After this, DNA ligase IIIα and X-ray cross-complementing protein 1 (XRCC1) complete the process by sealing the remaining gap. If Pol β can't remove the 5'-dRP, then Pol δ/ε is recruited. This results in the generation of

a 5’ overhang by the addition of 2 to 8 nucleotides into the gap. This is recognized by flap endonuclease 1 (FEN1) and excised. DNA ligase I with PCNA completes the process and seals the nick. (Fig. 3 and Carter and Parsons 2016).

Nucleotide Excision Repair

NER is mostly used to repair DNA adducts that arise from exposure to UV light or chemicals. The damaged DNA is recognized by XPC (Xeroderma pigmentosum group C) which is in complex with RAD23b and centrin 2 (CENT2) with the help of UV DNA damage-binding protein (UV-DDB). Transcription initiation factor IIH (TFIIH) is recruited and its helicase activity unwinds the DNA. RPA loads the ssDNA and XPF-ERCC1 (excision repair cross-complementing 1) is recruited and creates an incision 5’ to the lesion. This is known as the “point of no return”. After this, the XPG subunit cuts the strand 3’ to the lesion. PCNA is recruited and it recruits DNA Pol δ, DNA Pol κ or DNA Pol ε for DNA synthesis. DNA ligase 1 or 3 completes the process by sealing the final nick (Marteijn et al. 2014). (Fig. 5).

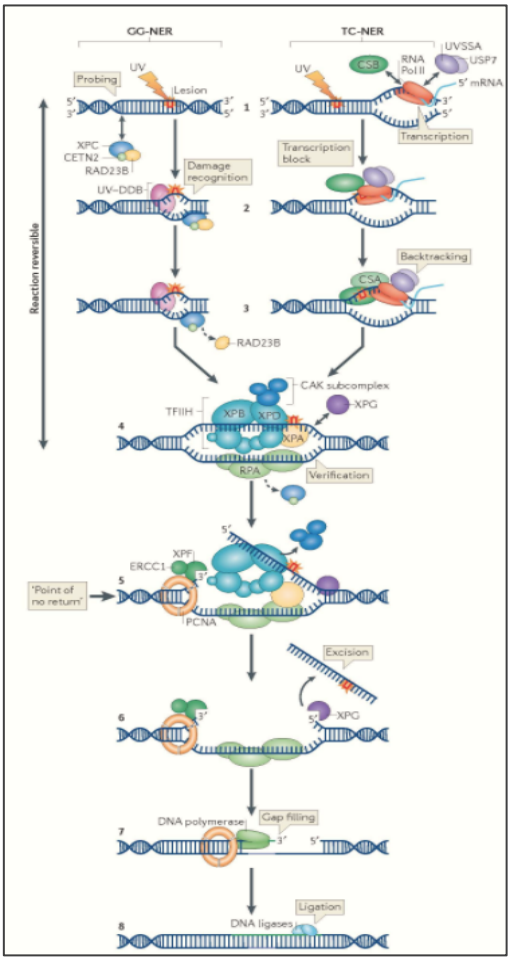

Figure 5. Nucleotide excision repair. (Martejin, 2015).

Mis-Match Repair

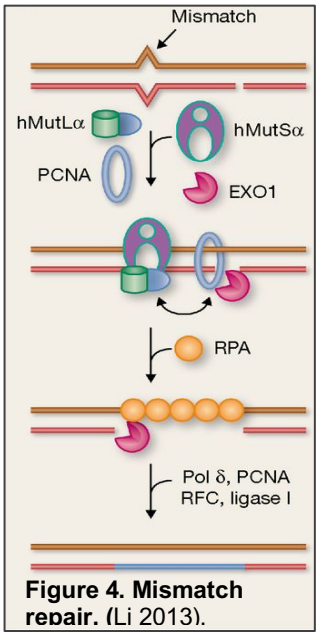

Figure 4. Mismatch repair. (Li 2013).

MMR is primarily used during replication and corrects the insertion of incorrect bases in the process. The repair starts with the recognition of the base-base mismatch by Mutator S (MutS) protein complex. This changes the conformation of the MutS protein complex which triggers recruitment of MutL. When the two are in complex, they exhibit endonuclease activity in a PCNA dependent manner, resulting in recognition and excision of the lagging strand from the mismatch. Exonuclease 1 (Exo1) is recruited and it performs nucleotide excision. Replication protein A (RPA) is loaded into the single stranded DNA to stabilize it. After this, DNA polymerase δ synthesize the corrected nucleotides and DNA ligase I ligate the remaining nick (Li 2013) (Fig. 4).

Double Strand Breaks

The most toxic form of DNA damage is double strand breaks (DSBs). Upon DNA DSB, several steps of post-translational modifications (PTM) are orchestrated to: signal the damage, recruit and accumulate the DNA repair factors, and process the breaks for repair. Several of the early steps of the repair signal are shared among the different types of repair mechanisms. However, one of the

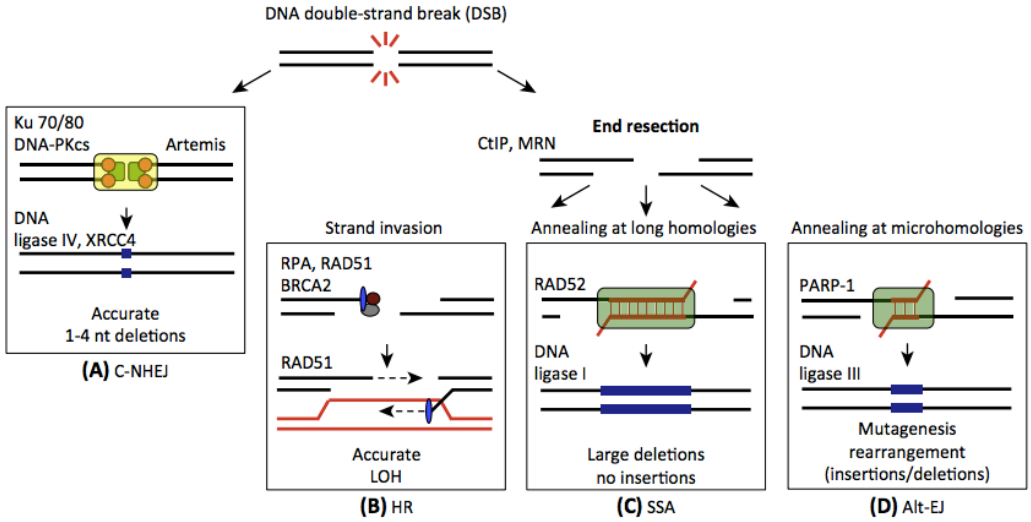

Figure 6. Different types of DNA DSB repair. (Ceccaldi et al. 2016)

steps that regulate which mechanism is used is the processing of the DNA ends. If the DNA ends undergo resection, then canonical non-homologous end joining (c-NHEJ) will be inhibited and the repair will be direct towards homologous recombination (HR), single strand annealing (SSA) or alternative NHEJ (alt-NHEJ). Nonetheless, there are other factors regulating DNA end resection.

Choice of DNA repair pathway

The choice of which mechanism to use will largely depend on the cell-cycle status. Canonical non-homologous end-joining (C-NHEJ) can occur any time during the cell cycle but it is more common during G0/G1 and G2 (Karanam et al. 2012). Homologous recombination is preferred during S and G2 phase, when there is a sister chromatid that can be used as a template for the repair. Importantly, the cell cycle will affect the ability of the cell to undergo end resection. Two proteins that are known to regulate this process are 53BP1 and BRCA1, and the stage of the cell cycle will influence their function via certain modifications. During S and

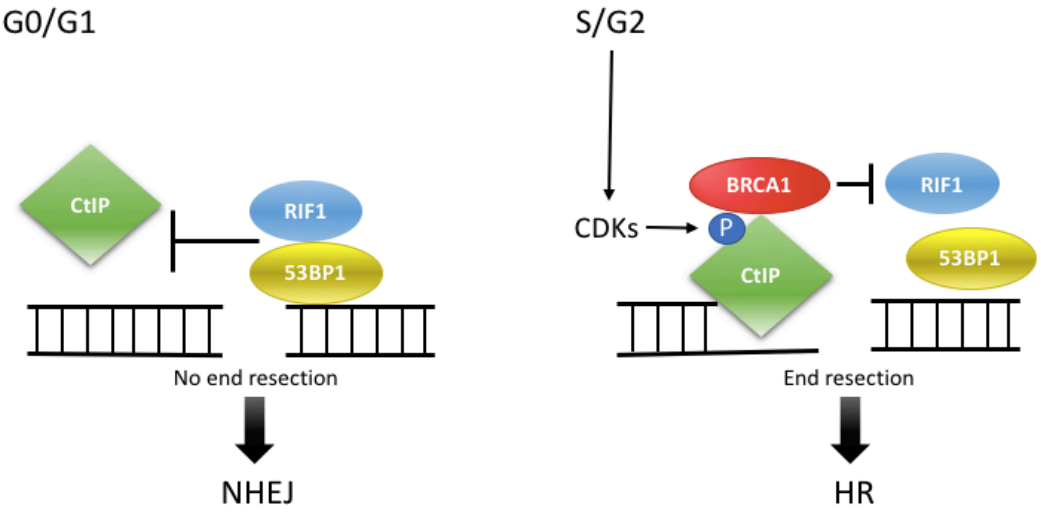

Figure 7. Regulation of DNA end resection through 53BP1/BRCA1 and cell cycle.

G2 phases cyclin-dependent kinases (CDKs) are upregulated and mediate the phosphorylation of several substrates including CtIP (CTBP-interacting protein) endonuclease (Huertas & Jackson 2009). This phosphorylation favors its recruitment by interacting with BRCA1 (breast cancer 1) which promotes DNA end resection (Yun & Hiom 2009); although, CtIP can also operate independently from BRCA1 (Polato et al. 2014). 53BP1 antagonizes this process and promotes repair through NHEJ by protecting the DNA ends at the break sites from being processed by CtIP. To do this, it collaborates with other factors like PAX transactivation domain interacting protein (PTIP) and RAP1-interacting factor 1 (RIF1), which is required for its end resection-limiting function (Chapman et al. 2013). In S and G2 phases, BRCA1 limits the RIF1 accumulation at the DNA break sites, removing the blockade from the DNA ends which enables end resection and repair through HR (Bunting et al. 2010; Escribano-Díaz et al. 2013) (Fig. 7).

Non-Homologous End Joining

During c-NHEJ, the heterodimer Ku, composed by Ku70 and Ku80 loads onto the DNA and protects the DNA ends from degradation. Ku recruits DNA-PK catalytic subunit (DNA-PKcs) by interacting with it through Ku80 carboxyl-terminal domain (CTD) (Falck et al. 2005). It is required that Ku is bound to the DNA for the activation of DNA-PKcs (Bennett et al. 2012). DNA-PKcs undergoes autophosphorylation and phosphorylates other NHEJ components. If the breaks are not blunt ends and/or DNA resection is needed, DNA-PKcs will recruit and phosphorylate Artemis nuclease. Subsequent recruitment of X-ray repair corss-complementing protein 4 (XRCC4), XCCR4-like factor (XLF) and paralog of XRCC4 and XLF (PAXX) will protect and align the DNA ends for further ligation by Ligase IV (Ochi et al. 2015; Mahaney et al. 2013).

Homologous recombination

Homologoues recombination (HR) is favored during S and G2 phases as it requires a sister chromatid as a template to process the repair. This process involves extensive resection, a sequence homology of >100bp, and strand invasion. CtIP nuclease and the MRN (Mre11-RAD50-NBS1) complex mediate DNA end resection to exposed 3' ssDNA overhangs. Replication protein A (RPA) binds to ssDNA to prevent formation of DNA hairpins (Chen et al. 2013). In addition it has been shown that RPA antagonizes microhomology-mediated repair by preventing spontaneous annealing of the exposed ssDNA between short sequences of homology (Deng et al. 2014). RPA is displaced by RAD51

recombinase resulting in nucleofilament formation that is stabilized by BRCA2 (breast cancer 2) (Esashi et al. 2007; Ayoub et al. 2009). BRCA1 recruits BRCA2 through its interaction with the bridging protein PALB2 (Partner and localizer of BRCA2) (Xia et al. 2006; Zhang et al. 2009). This interaction promotes strand invasion of the RAD51/ssDNA nucleoprotein filament into the sister chromatid in search of homology sequence, followed by annealing and synthesis of the new DNA.

Alternative NHEJ

Contrary to c-NHEJ, alternative NHEJ (alt-NHEJ) does not depend on Ku protein, it undergoes resection and requires few nucleotides of homology, referred to as microhomology (6 to 20bp), to repair the break. In fact, alt-NHEJ share more steps with HR than c-NHEJ. DNA ends resection is part of the alt-NHEJ mechanism, resecting up to 20nt in search of homology. Deletions at the final joints are evidence of the limited resection used in this mechanism. Also, it has been suggested that alt-NHEJ is an important contributor of chromosome translocations (Simsek & Jasin 2010). PARP1 has been identified as one of the proteins required for alt-NHEJ, as it mediates annealing of microhomologies (Wang et al. 2006). In addition, alt-NHEJ has been linked to XRCC1 and DNA ligase III (instead of XRCC4 and Ligase IV which are involved in C-NHEJ), and DNA polymerase θ has been identified to promote alt-NHEJ while inhibiting RAD-51 nucleoprotein filament formation in HR-deficient cells (Ceccaldi et al. 2015).

Single strand annealing

Single strand annealing (SSA), contrary to HR is a highly mutagenic pathway as, similar to alt-NHEJ, it involves resection of DNA ends, but different from alt-NHEJ, it needs longer sequences of DNA homology (>20bp), and thus it often requires more resection. After homology is found, RAD52 mediates annealing between the sequences. Xeroderma pigmentosum group F (XPF)-ERCC1 (excision repair cross-complementing 1) complex cuts and removes the 3' overhangs before the process is completed by ligating the DNA strands.

Signaling pathway

Each one of the repair pathways have proteins associated specifically to them. However, there is extensive overlapping and they share many of the steps. This is especially true in the early steps of the signaling pathway. The Mre11-RAD50-NBS1 (MRN) complex is involved in sensing the damage. It binds the DNA ends and recruits ATM (ataxia telangiectasia mutated) kinase. ATM mediates

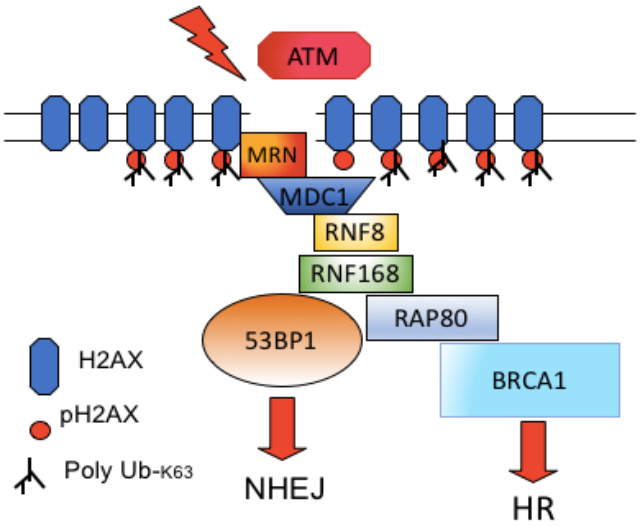

Figure 8. DNA damage response signaling pathway

phosphorylation of several substrates in the pathways. One of the first steps in the signaling pathway is the phosphorylation of the histone H2A variant H2AX to generate pH2AX. This phosphorylation creates binding sites for the recruitment of MDC1 (mediator of DNA-damage checkpoint 1). Phosphorylation of MDC1 by ATM promotes recruitment of the E3 ubiquitin ligase RNF8 (ring finger protein) and E2 conjugating enzyme UBC13 (Liu et al. 2012; Huen et al. 2007). Ubiquitylation of H1 promotes the recruitment of RNF168 (Thorslund et al. 2015) and further ubiquitylation of histone H2A promotes recruitment of 53BP1, RAP80 and subsequent BRCA1 (H. Kim et al. 2007; Sobhian et al. 2007); although more recent data suggests that RAP80 limits BRCA1 activity and that there is a RNF168/RAP80-indenpent pathway for BRCA1 recruitment (Goldstein & Kastan 2015). (Fig. 8).

Activation of ATM

Like many other cellular processes, the signaling pathway that is activated upon DNA damage is driven by a cascade of protein modifications. One of the proteins involved in the early steps of DNA damage signal is ATM kinase, that

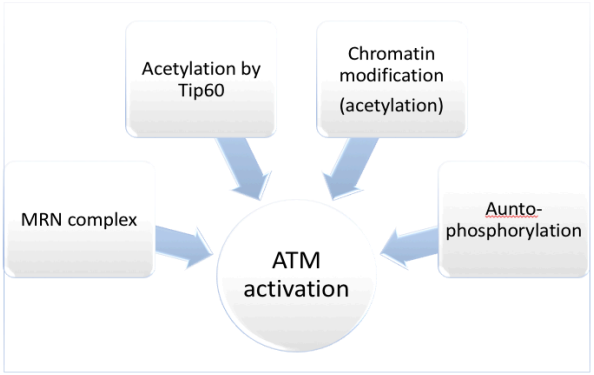

Figure 9. Different mechanism of ATM activation.

along with DNA PKcs and ATR are considered the apical kinase regulators of the DNA damage response.

ATM exist as an inactive nuclear homodimer that undergoes autophosphorylation at Ser1981 upon DNA damage (Bakkenist & Kastan 2003). This phosphorylation is thought to promote a transition between dimer-monomer status of ATM and promote its activation. However, this has been under debate since it was found that in mice, phosphorylation at Ser1987, which corresponds to Ser1981 in humans, is dispensable for ATM activation (Pellegrini et al. 2006). Despite this discrepancy, autophosphorylaion at Ser1981 is used as a marker for ATM activation. Even more, it was shown to be important for its retention at sites of DNA breaks and phosphorylation of its downstream substrates (So et al. 2009).

Other molecular events are also important for the full activation of ATM. Its direct interaction with NBS1, a component of the MRN complex, has been shown to be required for ATM activation in response to DNA damage (Uziel et al. 2003). This interaction is also required for its recruitment to sites of DSBs (Falck et al. 2005). In addition to this, modulation of the chromatin surrounding the breaks plays a role in ATM activation. It has been demonstrated that induction of chromatin acetylation through the use of HDAC inhibitors, results in activation of ATM (Bakkenist & Kastan 2003; Jang et al. 2010; Kaidi & Jackson 2013). Also, another important chromatin mark associated with ATM activation is tri-methyl lysine 9 of histone H3 (H3K9me3). Upon DNA damage-induced chromatin modulation, H3K9me3 is exposed and recognized by Tip60/Kat5 acetyltransferase, who

acetylates lysine 3016 and fully activates ATM (Kaidi & Jackson 2013; Sun et al. 2005; Sun et al. 2007).

Once it is recruited to sites of DNA breaks and activated, ATM mediates the phosphorylation of its downstream targets to expand the cellular response to DNA damage. This response is not limited to DNA repair pathways, but also triggers checkpoint pathways, apoptosis, senescence, and transcription (Shiloh & Ziv 2013). In the DNA repair pathway, ATM mediates the phosphorylation of several proteins including components of MRN complex, 53BP1, and H2AX (Harding et al. 2011; Lavin et al. 2015; Burma et al. 2001). The generation of pH2AX is especially important for further signaling cascade that will accumulate DDR factors for the repair of the DNA breaks.

pH2AX and signal amplification

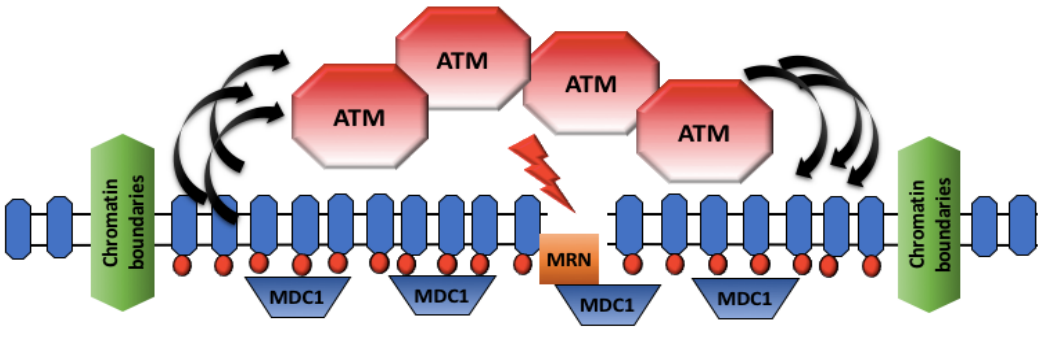

Figure 10. Amplification of the DDR signal through pH2AX/MDC1.

The histone variant H2AX was found to be phosphorylated at Ser139 in response to DSBs (Rogakou et al. 1998). Although H2AX is also a substrate for DNA-PKcs and ATR kinases, it was found that it is phosphorylated mainly by ATM

upon DSBs (Burma et al. 2001). MDC1 (mediator of DNA damage checkpoint) interacts with phosphorylated H2AX (pH2AX) through its tandem C-terminal BRCT repeats (Stucki et al. 2005). After its recruitment, MDC1 interacts with MRN complex and promotes retention and further activation of ATM (Lou et al. 2006). In this way, MDC1 contributes to the amplification of the DDR signal.

Phosphorylation of H2AX is important for the retention of DDR factors at sites of DNA breaks and amplification of the signal, although not required for the initial recognition of the DNA break (Celeste et al. 2003; Savic et al. 2009). It was found that upon DNA damage pH2AX domains extend for up to 2 megabases away from the breaks (J.-A. Kim et al. 2007). Studies using techniques that allows to follow chromatin modifications at specific loci of DSBs in the genome using ChIP, revealed that pH2AX domain (foci) are asymmetrically distributed around the breaks and that often, within those domains, continuous pH2AX stretches along the DNA strand are interrupted by segments with no pH2AX (Iacovoni et al. 2010; Massip et al. 2010). This means that there are segments of DNA that can be transcribed by their exclusion from pH2AX foci (Caron et al. 2012). It has been suggested that heterochromatin formation may suppress further spreading of pH2AX (J.-A. Kim et al. 2007) and more recently that cohesin protects actively transcribed genes from the effects of pH2AX (Caron et al. 2012). However, cohesin depletion only affects the spreading of pH2AX to a certain degree and not in every DNA break studied, suggesting that there is yet another mechanism that controls the extent of the pH2AX signal spreading (Caron et al. 2012).

Other chromatin modifications

Besides phosphorylation of H2AX, other histone modifications are an essential part of the DNA repair pathway. It serves various purposes. For instance, certain histones modifications are necessary to open the chromatin and make the break site available for the repair machinery. Also, histone modifications regulate the recruitment of important factors of the repair pathway. Additionally, transcriptional silencing of the chromatin surrounding the breaks may be important to assure effective DNA damage repair.

Several histone marks have been associated with DNA damage. Ubiquitylation of histone H2A by RNF8 serves for the recruitment of RNF168, and further ubiquitylation of histone H1 is important for subsequent recruitment of downstream factors in the repair pathway like 53BP1 and RAP80 (Thorslund et al. 2015; Nakada 2016). Histone acetylation plays an important role in relaxing the chromatin. This is because it neutralizes the positive charge of lysine in histones, therefore disrupting the interaction with the negatively charged DNA. This helps to de-condense the chromatin which makes it available for DNA repair machinery (Shahbazian & Grunstein 2007). Also, acetylation of lysine 16 in histone H4 (H4K16Ac) by MOF (males absent on the first) acetyltransferase has been suggested to be important for the activation of ATM upon DNA damage (Gupta et al. 2005). Another example is H3K56Ac, which has been shown to be reduced immediately after induction of DNA breaks by HDAC1/2 and this was important to promote repair through NHEJ (Miller et al. 2011).

Histone methylation is one of the most abundant histone modifications linked to DNA damage as well as other cellular processes. There are several histone lysine methylation marks associated with the DNA damage response. Perhaps the most studied one is lysine 9 of histone H3 (H3K9). Tri-methylation of H3K9 (H3K9me3), which is upregulated upon DNA damage, serves for the recruitment of Tip60 acetyltransferase, which is required for ATM acetylation and activation (Sun et al. 2009; Ayrapetov et al. 2014). Also, it was recently reported that BARD1 interacts with H3K9me2 at sites of DNA damage to promote HR repair (Wu et al. 2015). Another histone mark that has been reported to be upregulated upon DNA damage is H3K36me2 (Fnu et al. 2011). Metnase (also SETMAR) was identified as the methyltransferase responsible for this mark in response to DNA damage (Kim et al. 2015). Methylation of lysine 20 in histone H4 (H4K20), catalyzed by MMSET, was found to be important for 53BP1 recruitment (Pei et al. 2011; Hajdu et al. 2011).

It is clear that the histone code is an integral part of the DNA damage response modulation. Given the extensive histone modifications and the crosstalk among them, it is important to gain more insight on their dynamics and the mechanisms by which they influence the different repair pathways. This understanding can help in the identification of novel targets for the development of new drugs to achieve therapeutic goal through chromatin modulation. In this line, one new interesting target is the chromatin regulator G9a methyltransferase, which was found to be a substrate of ATM kinase and also upregulated in several types of cancer.

G9a methyltransferase

G9 methyltransferase is the main euchromatin histone methyltransferase responsible for the mono- and di-methylation of H3K9. As such, G9a is an important regulator of the epigenome. Epigenetic regulations, which affect histones and DNA alike, are post-translational modifications that modulate chromatin changes. These changes control gene expression and regulation throughout the cell cycle. Nonetheless, as already discussed in the previous sections, regulation of chromatin architecture is equally important during DNA damage repair. In response to DNA damage, expression of the genes that respond to the damage signal is altered, resulting in their expression or silencing, according to the need. In addition to this, chromatin changes at the sites of DNA breaks, are important to assure an adequate response which involves both recruitment of DNA damage repair (DDR) factors and the spreading of the damage signal. It is not surprising then, that several proteins involved in epigenetic changes are tightly regulated, and dysregulation of these and their function, can lead to genome instability and development of a number of diseases.

Initial discovery of G9a/GLP

G9a gene, also called BAT8 and Euchromatin histone methyltransferase 2 (EHMT2), was first discovered during the characterization of an unknown region of the major histocompatibility complex (MHC) class III cluster in chromosome 6 (Spies et al. 1989; Dunham et al. 1990). The product of the gene was not known yet but, given its localization, it was thought to be a gene involved in some aspect

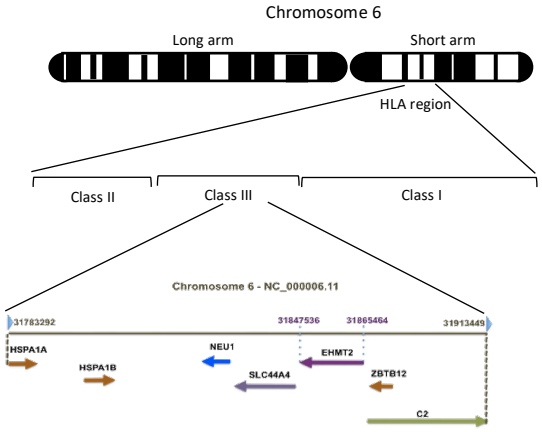

Figure 11. Genomic location of EHMT2 (G9a) gene in chromosome 6 in humans. It is part of the class III of the major histocompatibility complex (MHC) or human leukocyte antigen (HLA) cluster of genes.

© Atlas of Genetics and Cytogenetics in Oncology and Haematology

of the immune response (Fig. 11). After the first description of the gene, further efforts to characterize its function led to the discovery of a 1001 amino acid product (Milner & Duncan Campbell 1993). Later it was shown that G9a gene was expressed in the same transcript as NG36 gene, containing 28 exons, instead of 24 as originally thought, and resulting in a protein product of 1210 amino acid (Brown et al. 2001). There is a shorter form (isoform b) that lacks exon 10. G9a is also found in mice, in chromosome 17, and as in humans, the mouse homolog also has two splice variants, long (L) and short (S). The full-length variant (isoform L) lacks exon 1, while the isoform S lacks part of exon 2, resulting in a N-terminal resembling the human G9a (Fig. 12).

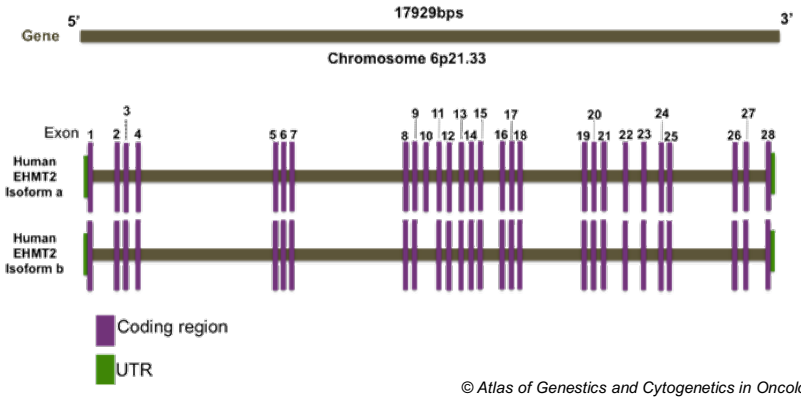

© Atlas of Genetics and Cytogenetics in Oncology and Haematology

Figure 12. Splice variants of G9a. They differ in exon 10 which is included in isoform a but spliced out in isoform b

G9a-like protein (GLP), a closely related G9a paralog, was first described as part of the E2F6 (E2 transcription factor 6) multimeric silencing complex, and found to exhibit methyltransferase activity and to share structural similarities with G9a (Ogawa et al. 2002). In fact, it was found that the two share many of their substrate specificities and even more, that they form heteromeric complexes via their SET domain which is the functional form *in vivo* (Tachibana et al. 2005; Weiss et al. 2010). Together, they exhibit methyltransferase activity for H3K9 (mono- di-methylation), H3K56, H1 and H3K27 (Tachibana et al. 2002; Weiss et al. 2010; Wu et al. 2011; Yu et al. 2012), being the main methyltransferase for mono- and di-methylation of H3K9 in euchromatin. It was found that genetic deletion of either protein severely reduced levels of H3K9me1 and H3K9me2. However, mutations of their catalytic domains showed that G9a activity is more important than that of GLP *in vivo* (Tachibana et al. 2008). The complex also binds the zinc finger protein Wiz, and it is thought that a complex of G9a-GLP-Wiz is the most stable and therefore dominant form inside the cell (Ueda et al. 2006).

G9a structure and activity

Figure 13. G9a methyltransferase. Shown are the different domains. SET catalytic domain, E-Glutamic acid rich region, Cys-Cysteine rich region, ANK- ANK (Ankyrin) repeats, NLS- Nuclear localization signal. Numbers represent amino acid position.

G9a methyltransferase is a member of the Su(var)39 (Suppressor of variegation 3-9) family of SET (Su(var) 3-9 Enhancer-of-zest and Trithorax)

domain containing proteins. Structurally, G9a contain a SET catalytic domain composed by Pre-SET, SET, and Post-SET, a domain of ANK (Ankyrin) repeats with 7 ANK repeats that mediates protein-protein interactions, and a nuclear localization signal. It was also identified a site for automethylation at lysine 185 (K239 in mouse), a Cysteine-rich region (12 Cys), and a E-rich domain containing 24 glutamic acid residues. The ANK domain has been shown to recognize and bind to mono- and di-methyl lysine, which gives G9a the ability to not only methylate histone tales but also to bind and serve as scaffold to recruit other factors to its targeting substrates in the chromatin (Collins et al. 2008).

Generally, G9a is associated with repression of active genes. Through catalysis of H3K9me2, G9a regulates a number of different genes that influence several cellular processes. G9a regulate differentiation and cell lineage commitment and also, other biological pathways like responses to cellular stress and drug addiction (Maze et al. 2010; Cedar H 2009). There is a minimum of 7 amino acid sequence with a consensus of RK/ARK that is required for G9a to recognize and methylate its substrates. Studies using histone H3 as the substrate, revealed that the heptapeptide sequence is 6-TARKSTG-12 and that the arginine in position 8 is required for the methyltransferase activity. G9a also has preference for hydrophilic amino acid in position 6 and 10 and hydrophobic amino acid in position 11. In addition to this, phosphorylation at Ser10 and Thr11 prevents methylation by G9a (Chin et al. 2005). Interestingly, methylated ARK in G9a, which does not affects its activity, resembles trimethyl-H3K9 peptide, and serves for heterochromatin protein 1 (HP1) association and consequently, spreading of

H3K9me2 and silencing of the chromatin (Chin et al. 2007). G9a transfers a methyl group from the co-factor S-Adenosyl-methionine (SAM) to the ε-amino group of its target substrates. SAM binds to the post-set domain, promoting a change in conformation of the protein (Patnaik et al. 2004). This folding prompt a close conformation that creates the substrate-binding pocket and allows for the transferring of the methyl group.

The two isoforms in humans and mouse as well, differ on exons included in the pre-mRNA. In humans, inclusion of exon 10 (E10) gives rise to the full length isoform a. Inclusion or exclusion of E10 does not affect the reading frame of the protein and thus, both isoforms a and b, have intact SET domains (Fiszbein et al. 2016). However, it has been shown that in different tissues and different stages of cell development one splice variant may be favored over the other. For example, in neuronal differentiation, isoform including E10 is upregulated and moreover, it was shown to be required in this process (Fiszbein et al. 2016). Thus, it has been proposed that alternative splicing is one way to modulate G9a function (Mauger et al. 2015).

Non-histone targets

Besides targeting histones, G9a has also been shown to exert its methyltransferase activity towards non-histone substrates. Methylation of non-histone targets is a field not largely explored. Nonetheless, it has been proved that G9a-mediated methylation of non-histone proteins represents another important function of G9a (Rathert et al. 2008). One example is methylation of the chromatin

remodeling factor, Reptin, at lysine 67. Methylated Reptin negatively modulates the response to hypoxia conditions by promoting HDAC1 recruitment to hypoxia-responsive genes which mediated transcriptional repression (Lee et al. 2010). In contrast, and under similar conditions, G9a also methylates Pontin which promotes recruitment of p300 to HIF1a (hypoxia-inducible factor 1-alpha)-target promoters resulting in transcriptional activation of hypoxia-responsive genes. Increased methylation of Pontin was associated to increased migration and invasiveness of the cells (Lee et al. 2011).

Another target of G9a is the tumor repressor p53. G9a methylates p53 at lysine 373, and this modification is associated with inactive status of the protein (Huang et al. 2010). This has been associated with tumorigenesis and aggressive cancer types. However, new evidence suggests that in certain tumors, in a cell line-specific manner, G9a can induce p53 activation in a methyltransferase-independent manner. In fact, they found that in a subset of patient tumors, expression of G9a and wildtype p53 correlated to better survival of the patients (Rada et al. 2016). MyoD, an important myogenic factor during muscle skeletal differentiation, was shown to be methylated at lysine 104 by G9a which resulted in inactive status, which inhibited the ability of the cells to differentiate (Ling et al. 2012). Several other targets of G9a have been reported recently, but little is known about the effects that this post-translational modification exerts on their function. For example, CDYL methylation at lysine135, affected its ability to bind H3K9me3 by altering its conformation. (Rathert et al. 2008). CDYL was recently found to possess a crotonyl-CoA-hydratase activity towards H3K9, which might be linked

Figure 14. Non-histone targets of G9a

to its corepressor function (S. Liu et al. 2017). Also, C/EBPβ, a transcription factor that regulates expression of genes involved in several cellular pathways, from adipogenesis to immune response, was found to be methylated by G9a, which inhibited its ability to activate expression of its targets genes. Other targets of G9a are G9a itself, Wiz, ACINUS, HDAC1, p21, CSB (cockayne syndrome group B), SIRT1 (sirtuin 1), KLF12 (kruppel-like factor 12) and mAM (mouse ATFa-associated modulator) (Rathert et al. 2008; Pless et al. 2008; Chin et al. 2007).

This suggests that G9a can modulate gene transcription not only by directly generating H3K9me2 on the promoter regions of its target genes, but also by activating and targeting other transcriptional factors to the chromatin. In addition, it shows that G9a expression and G9a-mediated modulation of other protein functions, is cell line and cellular stage-specific and highlights the importance of maintaining G9a homeostasis inside the cell.

Coactivator and Corepressor functions of G9a

Challenging the general perception that G9a only acts as a corepressor, there is more recent evidence showing that G9a can also act as a coactivator in a methyltransferase-independent manner. This crosstalk between repressor and

activator functions of G9a seems to be gene-specific and in some cases, cell stage-specific. G9a can interact with several transcriptional co-activator complexes to promote transcription of target genes independent of its catalytic activity. For example, G9a association with glucocorticoid receptor (GR) leads to recruitment of Coactivator Arginine Methyltransferase (CARM1) and the acetyltransferase p300 to GR target genes, resulting in activation of gene expression. However, it was found that in a subset of genes, expression is reduced in this setting (Bittencourt et al. 2012) , providing more evidence for the bivalent role of G9a in regulating gene transcription. Another example of such contradictory functions, is Runx2 association with G9a. In a methyltransferase-dependent manner, G9a reduced expression of Runx2-target genes, whereas it promotes their expression independently of its histone methyltransferase (HMT) activity (Purcell et al. 2012). Additionally, G9a has been found to regulate p21 expression by interacting with CDP/cut and UHRF1, which leads to silencing of the gene (Kim et al. 2009; Nishio & Walsh 2004). However, it was found that in certain conditions G9a interaction with PCAF (p300/CBP-associated factor) at p21 promoter induces transcription in a HMT-independent way (Oh et al. 2014; Rao et al. 2016). In the case of myogenesis, G9a interacts with Sharp1 transcription factor, and inhibits transcription of the myogenesis-related genes (Ling et al. 2012). G9a is also important to inhibit leukemogenesis, by interacting with YY1 protein, and inhibiting expression of JAK2.

These studies demonstrate the double functionality of G9a activity (catalytic or as a scaffold) in regulating gene expression. Nevertheless, its catalytic activity

on the chromatin results in silencing of the targeted genes. There is however, one case where G9a epigenetically enhanced gene expression by maintaining mono-methylated levels of H3K9 (Ding et al. 2013). It seems that the general consensus is that G9a functions as a corepressor in a histone methyltransferase (HMT)-dependent way, and as a coactivator independently of its HMT activity. However, as discussed previously, G9a-mediated methylation of non-histone targets can result in either function.

Other biological function

Epigenetic activity of G9a almost always results in gene repression. That is because di-methylation of H3K9 interacts with HP1 (heterochromatin protein 1) to promote recruitment of other factors and repress gene transcription. Since G9a-GLP is the main methyltransferase of H3K9 and it is specifically associated with euchromatin thus, it is generally involved in the transcriptional silencing of active genes. Given its function and its ubiquitous expression, G9a is linked with several biological functions.

G9a has been shown to be important during embryonic development and cell differentiation by repressing pluripotency of the cells. For example, treatment of hematopoietic stem and progenitor cell (HSPC) with UNC0638 resulted in a retention of stem cell-like phenotype and function and delay of lineage commitment due to reduced de novo formed H3K9me2 patterning (Chen et al. 2012).

In contrast with these studies, overexpression of G9a negatively regulates differentiation of skeletal muscle precursors, which correlated with elevated levels

of H3K9me2 in muscle promoters (Ling et al. 2012). In *G9a-knockout* mice, a lethal phenotype is observed between embryonic days 9.5 (E9.5) and E12.5. Interestingly, it was found that embryos at E9.5 presented growth retardation and though they looked morphologically normal, they resembled embryos between days E.8 and E8.5. This suggested that G9a is involved in mouse embryonic development. In fact, G9a was found to be important for the silencing of pluripotency associated genes Oct-3/4, Nanog and DNMT3L. These genes are required to maintain pluripotency, thus Ga9 is required in this setting for cell commitment and differentiation (Feldman et al. 2006). Also, germ line specific G9a-/- resulted in failure to complete meiosis (Tachibana et al. 2007).

G9a also regulates B-cell differentiation to some extent. In V(D)J recombination, G9a inhibits recombination of chromosomal gene segments by promoting local DNA methylation (Osipovich et al. 2004). In T-cell, G9a regulates differentiation and homeostasis, and in T-cell specific G9a-/- expression of IL-4, IL-5 and IL-13 is impaired. Also, lack of G9a inhibits T-cell differentiation into Th2 cells leading to impaired cytokine production. (Lehnertz et al. 2010; Antignano et al. 2014).

G9a has been shown to repress neuronal genes in tissues outside the nervous system. Dysregulation of this led to brain impairment. For example, in mice a conditional ablation of G9a/GLP resulted in mental retardation-like syndrome due to the expression of early neuronal progenitor genes. This phenotype resembles Kleefstra syndrome in humans in which part of GLP gene is deleted. Also, continuous use of cocaine leads to suppression of G9a and thus

H3K9me2 in nucleous accumbens (NAc) neurons, which mediates cocaine addiction. This shows that G9a plays a role in cocaine-induced structural and behavioral plasticity. In contrast to this, different regions of the brain have the opposite effect in differentiation, and overexpression of G9a impairs the process. This demonstrates that G9a homeostasis is important to maintain controlled differentiation and cell line commitment.

Cellular Senescence and proliferation

G9a has been shown to be involved in senescence, quiescence, and proliferation. Recruitment of G9a to p21 promoter results in gene silencing, which inhibits the cell from exiting cell cycle (Oh et al. 2014; Rao et al. 2016). Similarly, it has been reported that G9a is in a complex with E2F6 transcription factor which results in silencing of E2F responsive genes, showing that G9a has a role in gene silencing in quiescent cells (Ogawa et al. 2002). Given its role in the regulation of these processes, it is not surprising that dysregulation of G9a function results in tumor cell proliferation and survival.

G9a in cancer

Dysregulation of the epigenome (DNA and histone modifications) plays an important role in cancer development. Silencing of tumor repressor genes, or upregulation of oncogenes can lead to different pathologies and the inability of the cell to undergo apoptosis or autophagy results in increased cell proliferation and tumor cell survival. G9a has been shown to be overexpressed in a number of

different types of cancer, which was correlated to poor prognosis, aggressiveness of the disease, metastasis and decreased patient survival (Ke et al. 2014a).

In lung cancer for example, it has been shown that G9a overexpression led to increased H3K9me2 levels at the promoter region of Ep-CAM (Chen et al. 2010a). In this case, depletion of G9a led to decrease recruitment of repressive factors like HP1, HDAC1 and DNMT1 to promoter region of Ep-CAM, resulting in inhibition of cell migration and invasion. More recently, it was reported that G9a silenced CASP1 gene in NSCLC which resulted in tumor cell growth and invasion (Huang et al. 2017). Another recent study found that G9a expression levels is squamous cell cancer is higher than in normal cells, and treatment with the G9a inhibitor BIX01294 led to decreased proliferation and cell death (Kim & Park 2017).

In breast cancer it was found that G9a promotes expression of epithelial-mesenchymal transition (EMT) markers by silencing expression of E-cadherin in Caludin-low breast cancer (CLBC) model through recruitment of HP1 and DNMTs to promoter region of E-cadherin (Dong et al. 2012). Knockdown of G9a restored

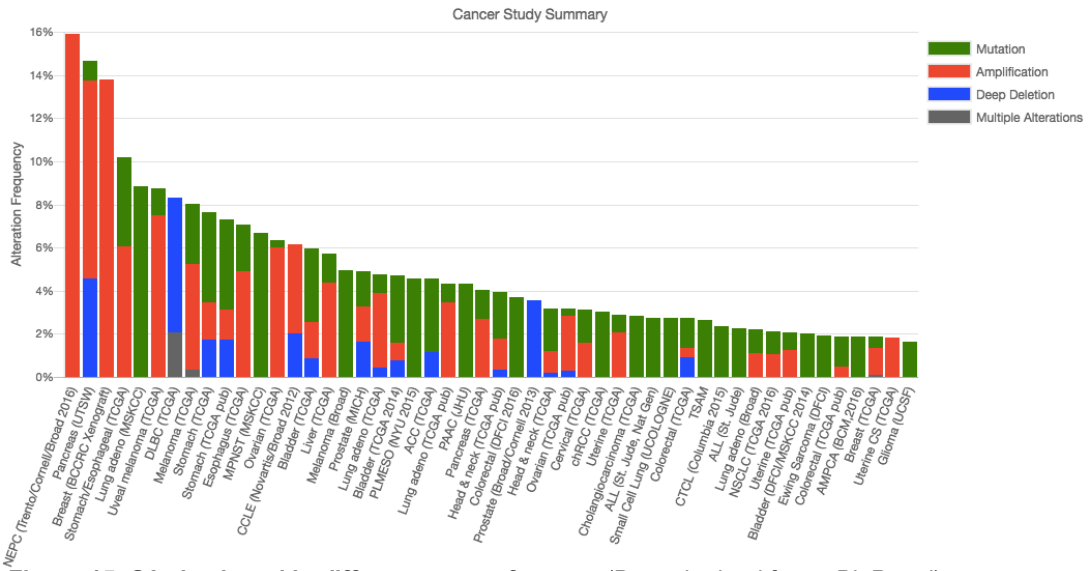

Figure 15. G9a is altered in different types of cancer (Data obtained from cBioPortal)

expression of E-cadherin and resulted in inhibition of cell invasion and migration and suppressed tumor growth and metastasis. In pancreatic cancer cells, treatment with G9a inhibitor BRD4770 led to senescence and inhibited cell proliferation (Yuan et al. 2012). G9a was reported to suppress Runx3 in gastric cancer, β-catenin-inhibitory genes in neuroendocrine tumors, and SIAH1 in bladder carcinoma (Cho et al. 2011; Kim et al. 2013; Lee et al. 2008). In all cases either downregulation of G9a or its inhibition resulted in restored gene expression and suppression of cell proliferation.

Development of G9a inhibitors

Given the elevated expression levels of G9a in several types of cancer and the growing evidence for its implication in tumorigenesis, metastasis, and cancer progression, many efforts have been placed in the development of pharmacological inhibitors for G9a that can be used in the clinic. One of the first inhibitors to be developed was BIX01294 (Kubicek et al. 2007). This was selected from a chemical library of 125,000 compounds, as the one that did not compete with G9a substrate but with its cofactor, S-Adenosyl-methionine (SAM) (Kubicek et al. 2007). Even though BIX01294 has been used in several studies, showing suppression of cell proliferation, it also exhibits cellular toxicity that was not due to inhibitory effects on G9a. Thus, further modifications were done which led to the development of the optimized inhibitor UNC0638 (Vedadi, Barsyte-Lovejoy, Liu, Rival-Gervier, Allali-Hassani, Labrie, Wigle, DiMaggio, et al. 2011). This showed selectivity for G9a and presented less toxicity for the cells and enhanced cell

permeability due to higher lipophilic characteristics. UNC0638 is widely used in cell assays and *in vitro* studies with G9a. It has proven to suppress cell proliferation in various cancer cell lines. However, UNC0638 presented poor pharmacokinetics which affects efficient use for *in vivo* experiments. This led to the development of UNC0642 which is more suitable for animal studies (Liu et al. 2013). Other inhibitors that have also been developed are BRD4770 and A366 (Sweis et al. 2014; Yuan et al. 2012).

More recent studies have shown that inhibition of G9a sensitizes cells to radiation and other DNA damaging agents (Nakajima et al. 2017; Agarwal & Jackson 2016). However, the underlying mechanism for these effects is not well understood. Given the implication of G9a in cancer development and progression and the observations that it might be involved in DNA damage response, understanding its functional role in this process can be of great help for the development of new strategies to treat cancer. In this study we aimed to elucidate the role of G9a in the DNA repair pathway. For this we studied the potential effects of G9a inhibition in the recruitment of DDR factors and in chromatin architecture, and also studied G9a interacting partners in response to DNA damage.

Chapter I: G9a methyltransferase promotes the DNA damage response.

Introduction

Dynamic chromatin architecture plays an important role in the regulation of many biological processes. Post-translational modification that affect histones, chromatin associated proteins and modifications to DNA as well, can take place to regulate regions of chromatin. These modifications, known as epigenetic marks, can directly affect protein function or facilitate protein-protein or protein-DNA physical associations. Processes like gene transcription, replication and DNA repair alike are affected by these changes.

In the case of DNA repair, histones modifications are at the center of the signaling pathway. Histones post-translational modifications like phosphorylation, methylation, acetylation or ubiquitination have been linked to the DNA damage response (DDR) pathway, and serve to regulate DNA damage recognition, protein recruitment to sites of DNA damage, and DDR signal amplification. These histone modifications can also regulate local transcriptional activity. For example, methylation of lysine in position 4 and 36 of Histone H3 has been associated with activation while methylation of lysine 9 and 27 of H3 is usually linked with transcriptional repression. One methyltransferase protein responsible for H3K9 methylation is G9a, also known as Euchromatin Histone Methyl Transferase 2 (EHMT2). G9a methyltransferase is a member of the Su(var)39 (Suppressor of variegation 3-9) family of SET (Su(var) 3-9 Enhancer-of-zest and Trithorax) domain containing proteins. It is the main euchromatic histone methyltransferase responsible for the mono- and di-methylation of the lysine 9 in histone 3 (H3K9me1/H3K9me2). It has been shown to also methylate lysine 56 and lysine

27 of histone 3 (H3K56 and H3K27) (Yu et al. 2012; Tachibana et al. 2001). G9a transfers a methyl group from its enzymatic co-factor S-Adenosyl-methionine (SAM) to the amino group of the targeted lysine on histones and other non-histones substrates.

In addition to histone substrate, G9a has multiple non-histone protein substrates including G9a itself, Wiz, ACINUS, Reptin, CDYL and HDAC1 (Chin et al. 2007; Rathert et al. 2008). Moreover, G9a has been reported to be dysregulated in cancer and implicated in the silencing of tumor suppressor genes contributing in this way to tumorigenesis. Overexpression of G9a has been reported in hepatocellular carcinoma, neuroblastoma, lung cancer, aggressive ovarian cancer, and invasive breast cancer, among others, where it has been correlated to poor prognosis and survival (Wu et al. 2013; Ke et al. 2014b; Chen et al. 2010b; Hua et al. 2014; Dong et al. 2012).

Recent studies have shown that catalytic inhibition of G9a potentiates the effects of DNA damaging agents, suggesting that it is involved in the DNA repair pathway (Agarwal & Jackson 2016). However, the underline mechanism of this effect has not been profoundly studied. Here we present data that shows that G9a localizes to sites of DNA damage in an ATM-dependent fashion. We also show that G9a catalytic inhibition, using the G9a specific small molecule inhibitor UNC0638, affects the early recruitment of 53BP1 and BRCA1 which results in decreased DNA repair efficiency through both HR and NHEJ. This new data brings more light into the underline mechanism by which G9a promotes DNA repair and establishes G9a as a potential pharmacological target in the clinic.

Results

G9a and GLP1 are recruited to DNA damage sites.

Several studies have reported that inhibition of G9a potentiates the effects of DNA damaging drugs on tumor growth and progression. This suggests that G9a has a role in the DNA damage response pathway. To investigate this, we first wanted to determine G9a cellular localization after DNA damage. U2OS cells, pre-sensitized with an overnight incubation with IDU (5-iodo-2-deoxyuridine), were subjected to localized, UV laser scissors- induced DNA breaks (Rogakou et al. 1999) followed by immunofluorescence using antibodies against endogenous G9a and GLP1. Interestingly, we found that both G9a and GLP1 were rapidly recruited to sites of DNA damage, as seen by colocalization with pH2AX. They were detectable within 2 minutes and remain at DNA breaks for up to 24 hours (Fig. 1A). To confirm this, we also transfected USOS cells with a vector encoding GFP-tagged human G9a.

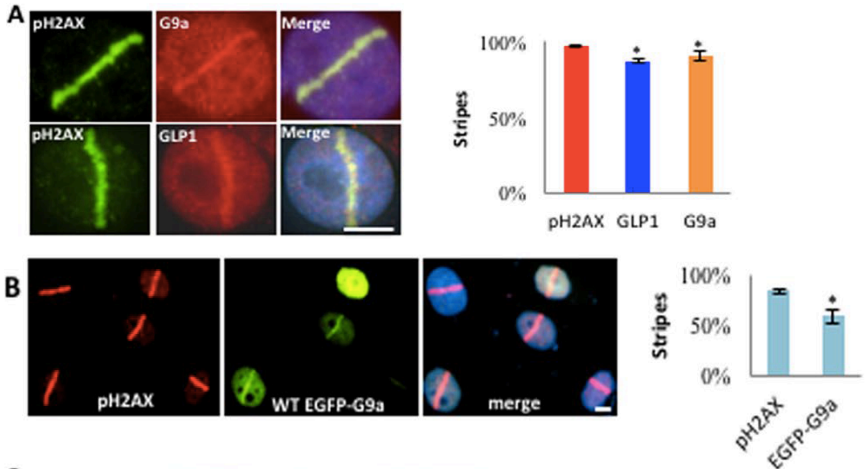

Figure 1. G9a and GLP1 localize to DNA damage sites. A) U2OS cells were micro-irradiated and processed for IF staining after 10 min recovery using indicated antibodies. B) U2OS cells were transfected with GFP-G9a and subjected to laser-microradiation followed by IF. pH2AX staining and GFP signal are shown.

DNA damage was induced with laser scissors, and IF was performed. Similarly, we observed that exogenous GFP-tagged G9a showed rapid recruitment to sites of DNA breaks (Fig. 1B).

It is known that G9a forms a heterodimer with GLP1 through the interaction of their SET domains (Tachibana et al. 2005). To further understand the dynamics of their recruitment to DNA breaks, we used shRNA specific for either G9a or GLP1. Cells treated with either control, G9a or GLP1 shRNA were subjected to laser scissors-induced DNA damage and localization of G9a and GLP1 was visualized by IF. We found that G9a knockdown resulted in loss of GLP1 recruitment to DNA breaks while GLP1 knockdown had no effect on G9a recruitment (Fig. 2A and B). This data shows that G9a and GLP1 are recruited to sites of DNA breaks and that while GLP1 recruitment is dependent in part on G9a, G9a does not require GLP1 for recruitment to DNA breaks. Also, loss of GLP1 localization can be in part due to the effects of G9a knockdown as this affected GLP1 protein levels to some extent (Fig. 2C).

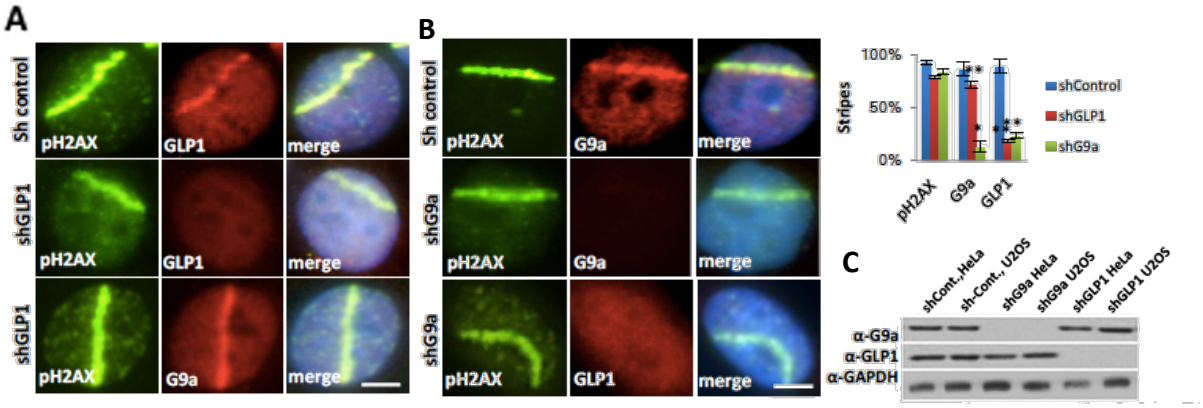

Figure 2. G9a is required for GLP1 localization to DNA breaks. A and B) U2OS expressing control shRNA, GLP1 shRNA or G9a shRNA were subjected to laser-induced DNA damage followed by IF staining using indicated antibodies. C) Western blots of cells showing knockdown efficiency.

G9a localization to sites of DNA damage is dependent on ATM activation.

G9a has been reported to have an ATM/ATR phosphorylation site at ser569 (Matsuoka et al. 2007). Given that G9a phosphorylation was induced by DNA damage, we set out to determine if ATM activation had a role in the recruitment of G9a to damage sites. U2OS cells were treated with either ATMi (KU55933), ATRi (VE-821) or vehicle and subjected to laser microirradiation. Recruitment of G9a to DNA damage sites was analyzed by immunofluorescence. Treatment with ATMi but not ATRi reduced both G9a and GLP1 recruitment to laser scissors-induced DNA breaks (Fig. 3). Consistent with this, recruitment of G9a to damage sites in ATM -/- human fibroblasts was also greatly reduced. Intriguingly, recruitment of G9a in H2AX -/- and MDC1 -/- fibroblasts was not affected. This data suggests that G9a/GLP1 recruitment to sites of DNA breaks is dependent of ATM activity but not on H2AX or MDC1 presence.

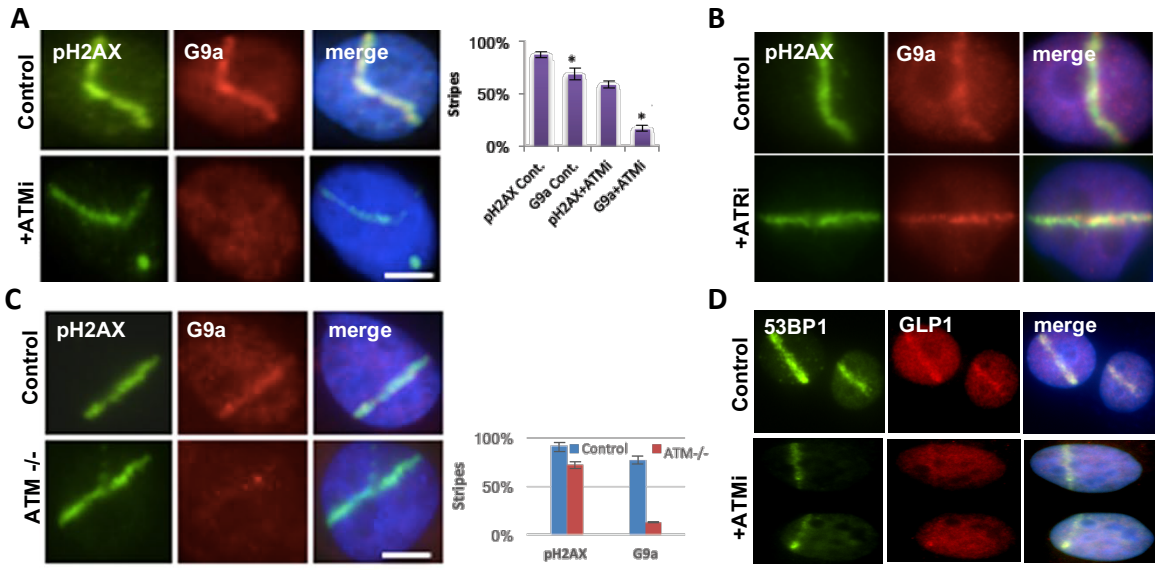

Figure 3. G9a localization is dependent on ATM activation. A) U2OS cells treated with ATMi (0.5uM, overnight), ATRi (VE-821, 3uM) or vehicle (A and B and D) and ATM -/- or ATM+/+ human fibroblasts (C) were subjected to laser micro-irradiation followd by IF staining using the indicated antibodies. Data is quantified and expressed as the mean ± SEM of at least 3 experiments. **P<0.001, *P<0.05.

Phosphorylation of G9a on S569 is required for its recruitment to DNA breaks.

To investigate the role that G9a phosphorylation has in its recruitment, affinity-purified phospho-specific antibody to G9a phosphorylated on S569 was developed. DNA damage was induced by Neocarznostatin (NCS) and proteins were collected and analyzed by western blot. In cells treated with NCS, but not in control cells, this antibody recognized a band of a size consistent with G9a (Fig. 4A). We failed to see the band in cells treated with shRNA for G9a, but shRNA for GLP1 had no effect, showing the specificity of the antibody for phosphorylated G9a. Furthermore, this antibody was able to recognize wt-G9a-GFP but failed to

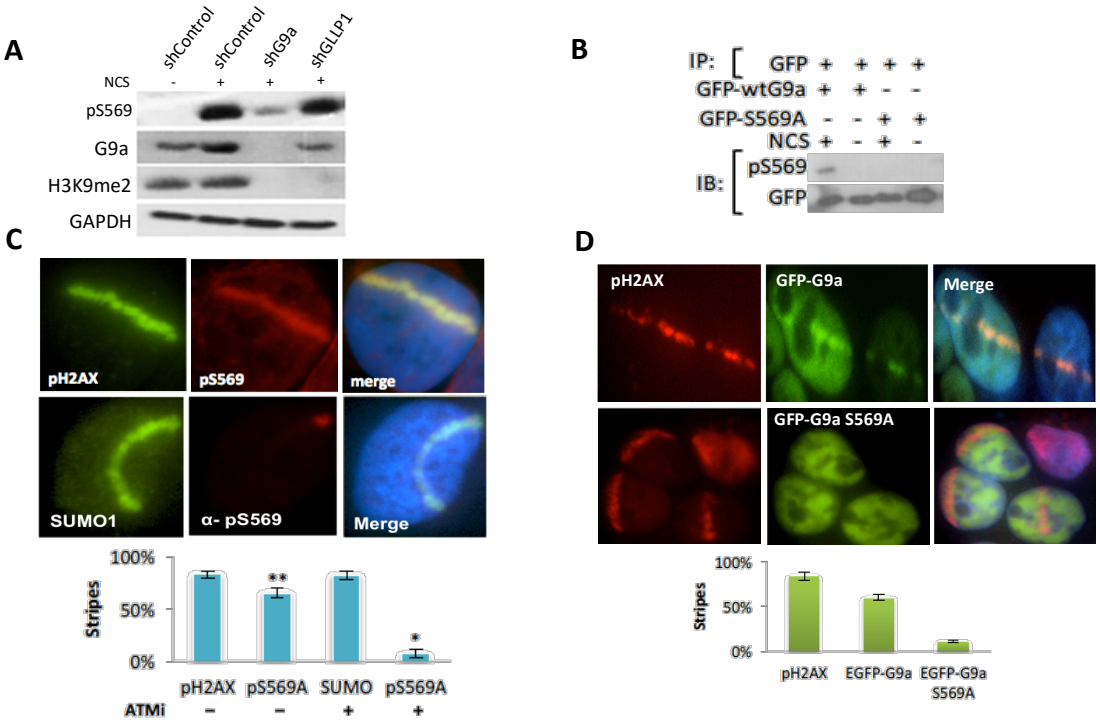

Figure 4. Phosphorylation of G9a is required for its recruitment to DNA breaks. A) Wester blots of U2OS cells expressing indicated shRNA and treated with NCS or vehicle and probed with indicated antibodies. B) Western blot of U2OS cells expressing indicated constructs and treated with NCS or vehicle, subjected to immunoprecipitation using GFP antibody, and probed with indicated antibodies. Normal U2OS cells (C) or cells expressing either wtGFP-G9a or mutant GFP-G9a S569A were subjected to laser micro-irradiation and processed for IF staining with indicated antibodies. Quantification is expressed as mean ± SEM of at least 3 experiments.

recognize the phospho-mutant S569A G9a-GFP after treatment with NCS, demonstrating that the antibody is specific for G9a phosphorylated at S569 (Fig. 4B). IF experiments using this antibody demonstrated that pS569-G9a is rapidly recruited to sites of DNA damage but treatment with ATM inhibitor abolishes this (Fig. 4C). To further evaluate the role of phosphorylated S569, recruitment of phospho-mutant S569A G9a-GFP to sites of DNA breaks was evaluated. Hela cells expressing wild type or phospho-mutant G9a were subjected to microirradiation followed by IF. As expected, and unlike wtG9a, phospho-mutant G9a failed to recruit to sites of laser induced DNA breaks (Fig. 4D). This data demonstrates that G9a is phosphorylated on Ser569 in an ATM-dependent manner and that this phosphorylation is required for its recruitment to DNA damage sites.

G9a is required for early recruitment of 53BP1 and BRCA1 to DNA breaks.

Given that G9a was recruited to sites of DNA damage in an ATM-dependent manner, we set out to elucidate its role in this process. To do this, we investigated the effects of G9a knockdown and catalytic inhibition on recruitment of DNA repair factors to laser scissor-induced DNA breaks. U2OS cells were stably transfected with G9a shRNA and induction of DNA damage was done by UV laser scissors followed by IF using antibodies recognizing the endogenous proteins. Notably, G9a knockdown abrogated early recruitment of 53BP1 normally seen at 10 minutes. To evaluate the role of the catalytic activity of G9a, cells were transfected with an shRNA-resistant cDNA expressing wtG9a or G9a-SET domain mutant.

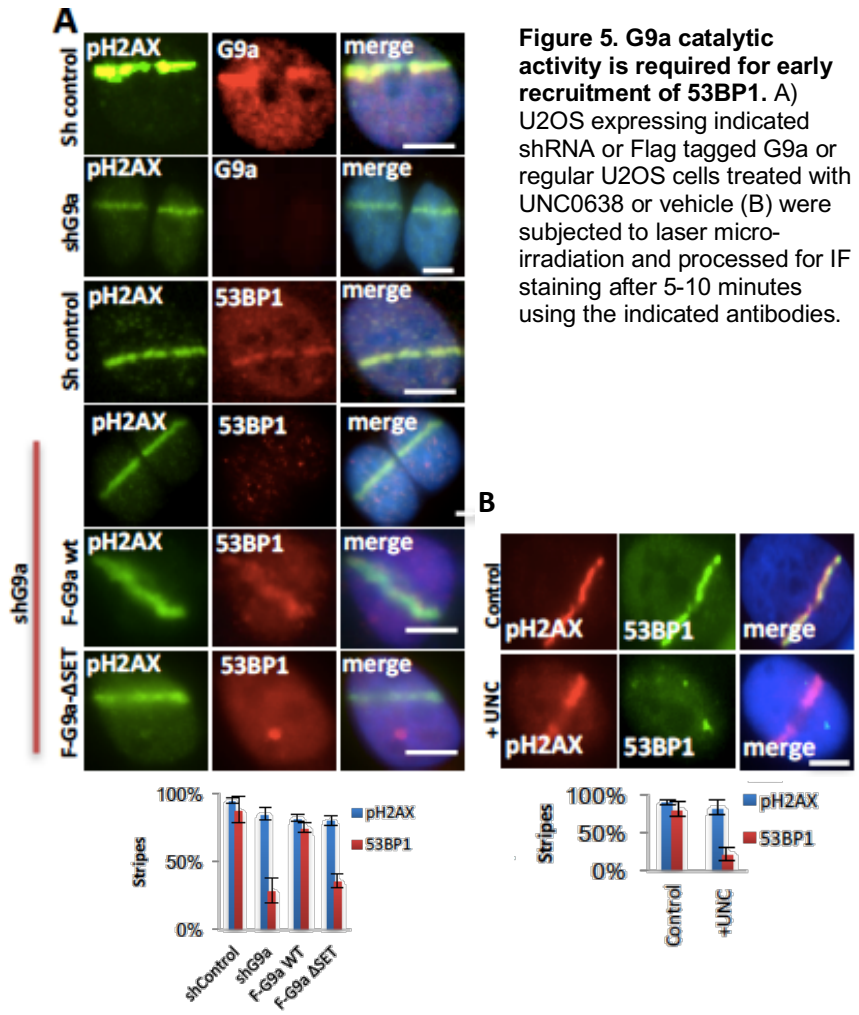

Figure 5. G9a catalytic activity is required for early recruitment of 53BP1. A) U2OS expressing indicated shRNA or Flag tagged G9a or regular U2OS cells treated with UNC0638 or vehicle (B) were subjected to laser micro-irradiation and processed for IF staining after 5-10 minutes using the indicated antibodies.

wtG9a but not the G9a-SET domain mutant, was able to rescue 53BP1 recruitment. To further confirm that catalytic activity was important in this process we treated the cells G9a specific small molecule inhibitor UNC0638. Catalytic inhibition of G9a activity caused similar effects, resulting in abrogation of the early recruitment of 53BP1 10 minutes after induction of DNA breaks (Fig. 5B).

To gain more insight into the underline mechanism, we analyzed factors that are required for 53BP1 in this setting. 53BP1 recruitment is known to be dependent on RNF168-mediated polyubiquitination (Stewart et al. 2009). Consistent with this, G9a knock down, and also catalytic inhibition, led to decreased recruitment of both RNF8 and RNF168 to laser scissors-induced breaks (Fig. 6A). As expected, polyubiquitination signal was also lost at sites of DNA breaks (Fig. 6B). This data suggests that the catalytic activity of G9a is necessary

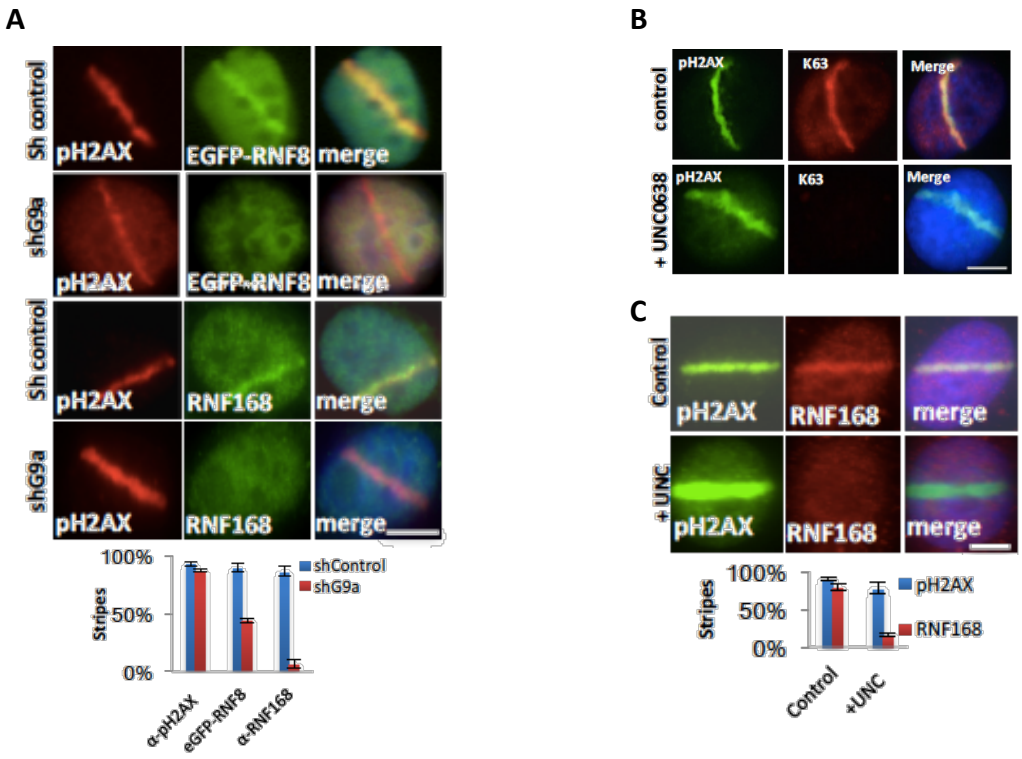

Figure 6. G9a catalytic activity is required for early recruitment of RNF188. A) U2OS expressing indicated shRNA or regular U2OS cells treated with UNC0638 or vehicle (B and C) were subjected to laser micro-irradiation and processed for IF staining after 5-10 minutes using the indicated antibodies.

for proper localization of RNF168 and hence 53BP1. Similar results were observed for BRCA1 recruitment in cells treated with UNC0638 (Fig. 7), although some differences were observed due to the normal slower dynamics of BRCA1 recruitment compared to 53BP1.

It has been shown that early and late recruitment of DNA repair factors follow different dynamics and may be regulated by different pathways. The experiments described so far evaluated recruitment of DNA factors at early stages of the response, around 5-10min after induction of DNA breaks. To study the role of G9a in the dynamics of DNA factors recruitment, we looked at recruitment of these over a time course of 4hrs. Cells stably expressing G9a shRNA or treated

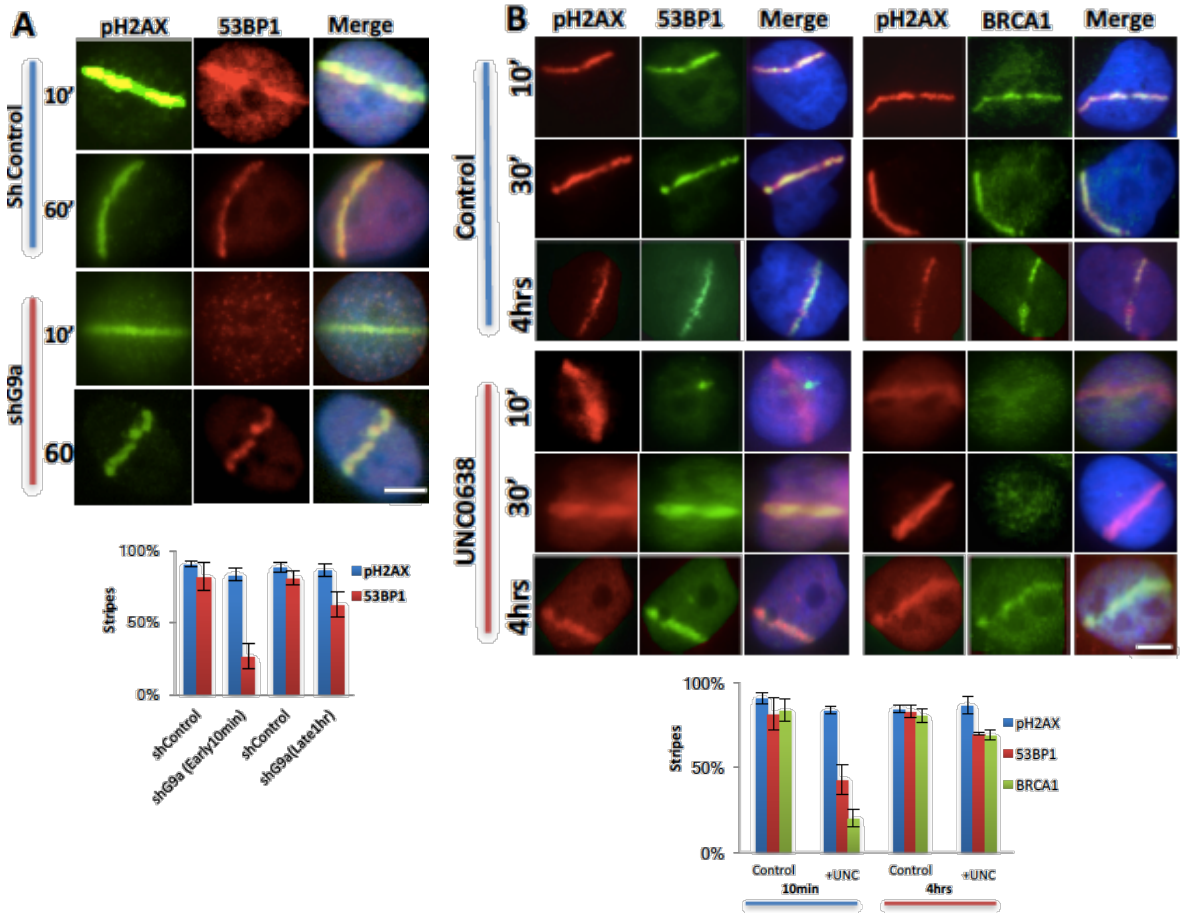

Figure 7. G9a is not required for late recruitment of 53BP1. U2OS cells expressing indicated shRNA (A) or treated with G9a catalytic inhibitor UNC0638 (B) were subjected to lase micro-irradiation and after indicated time points processed for IF staining. Quantifications are shown as the mean ± SEM of at least 3 experiments.

with UNC0638 were subjected to laser micro-iradiation followed by IF. Interestingly, late recruitment of these factors was not affected by catalytic inhibition of G9a. Late recruitment of 53BP1 (30min) and BRCA1 (4hrs) appeared normal in these conditions (Fig. 9). This data suggests that G9a activity is required for early recruitment for both 53BP1 and BRCA1 but dispensable for their late recruitment and retention at sites of DNA damage.

G9a promotes HR and NHEJ repair.

To further investigate the role of G9a during DNA repair response, we investigated the effects of G9a catalytic inhibition or knockdown on HR- and NHEJ-mediated repair. U2OS-DR/U2OS280 or U2OS EJ5-GFP cell lines that contain a GFP-based reporter system (K. Nakanishi et al. 2005; Mao et al. 2008; Andrew J. Pierce et al. 1999) were treated with G9a shRNA or UNC0638, and DNA repair efficiency was measured by percentage of GFP positive cells. G9a catalytic inhibition and knockdown resulted in a decrease of both HR and NHEJ mediated DNA repair. This effect was partially rescued by ectopic expression wtG9a. These findings demonstrate that G9a promote DNA damage response and is an important factor of it.

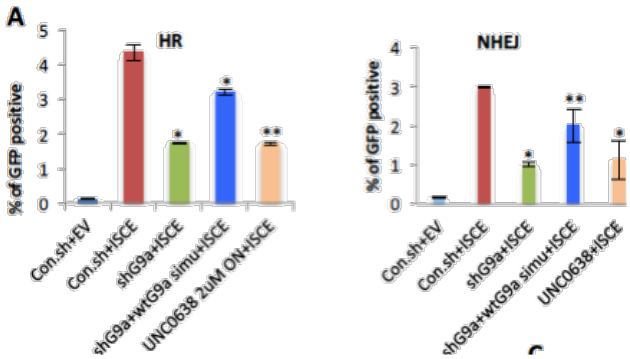

Figure 8. G9a promotes HR and NHEJ. U2OS cells with a GFP-based reporter were transfected or treated with G9a catalytic inhibitor, UC0638 and repair efficiency by HR and NHEJ was measured by percentage of GFP positive cells.

Discussion

G9a methyltransferase is well known for its role in repressive complexes and maintenance of heterochromatic status in euchromatin regions (Tachibana et al. 2002). Recent studies have suggested that G9a may play a role in the DNA repair process. It was identified as a substrate of ATM/ATR in response to DNA damage and it was shown to induce activation of DDR factors and promoting repair after DNA damage (Matsuoka et al. 2007; Agarwal & Jackson 2016; Zhang et al. 2015). However, the exact mechanism that underlies these effects is not well understood. Here we provided new information that demonstrates a direct role of G9a in the DNA repair pathway.

The observation that G9a localizes to sites of DNA damage was the first indication that it plays a role in the repair pathway. Even though G9a is well known for its histone methyltransferase activity it has also been found to have several non-histones substrates. This brings the possibility that the functional role of G9a could be related to changes in the chromatin landscape surrounding the damaged DNA. This G9a-induced local changes might help with recruitment/accessibility for DNA repair factors, promoting in this way the repair of the damaged DNA. Also, G9a is responsible for H3K9me2, which maintain silenced euchromatic status. It has been shown that local transcriptional silencing is induced after DNA damage to promote repair. G9a could be involved in this process by generating silence marks locally. Further investigation is needed to determine if G9a has, indeed, a role in this process. In the other hand, G9a may also act by methylating novel

substrates which have a direct role in the DNA repair pathway. There is evidence that shows that p53 methylation by G9a renders it inactive (Huang et al. 2010), showing how methylation of non-histones substrates by G9a might have an important role during DNA damage response. The dynamics of protein methylation/demethylation have been shown to play an important role in DNA repair. One example is MDC1 demethylation by JMJD1C at K45 which promotes MDC1-RNF8 interaction, RNF8-dependent ubiquitination of MDC1, and recruitment of RAP80-BRCA1 (Watanabe et al. 2013). More investigation is needed to establish a functional relation between G9a activity and these proteins in response to DNA damage. There is the possibility that G9a might be involved in the repair process not only by altering the chromatin landscape but also by mediating recruitment and regulation of non-histones substrates at DNA breaks in methyltransferase-dependent manner. It is also possible that it is present as a mediator protein, as it has been shown that G9a has methyltransferase-independent roles. However, the fact that inhibition of its activity causes a deficiency in DNA repair, makes this less likely. It is possible that the role of G9a involves both its methyltransferase activity and its molecular scaffolding properties.

We have also shown that recruitment of G9a is independent of GLP1. Although the two exist as a heterodimer and in association with other proteins like Wiz, we found that G9a is still recruited even after shRNA-mediated GLP1 knockdown. This suggests that in the setting of DNA damage, G9a has a major role than that of GLP1. This idea would be consistent with the observation that, although both G9a and GLP1 act together in the methylation of H3K9me2, G9a

plays a major in this process. Nonetheless, there are studies that show GLP1 has major roles than G9a in certain settings. For example, Kleefstra Syndrome has been associated with loss of GLP1 but not G9a (Willemsen et al. 2012), showing that G9a and GLP1 have some non-redundant roles in vivo and can act independently in certain cases. This further supports the idea that, although GLP1 is also recruited to sites of DNA breaks, G9a has a bigger role in the repair process.

An SQ site in G9a was identified as a target for phosphorylation by ATM/ATR. Here we demonstrated that ATM activity has an impact in the recruitment of G9a, as seen by failure of G9a to localize to damaged DNA upon ATM inhibition but not after ATR inhibition. More importantly, and although other sites have been identified to be phosphorylated (Zhou et al. 2012) here we provided evidence that G9a phosphorylation at ser569 is required for its recruitment in response to DNA damage. This does not rule out that phosphorylation at other sites might also be important for its role during DNA repair. G9a itself does not contain a domain to mediate binding to the DNA. This means that its recruitment could also depends on other factors that are either forming part of the complex with G9a or already present at the DNA breaks.

We have shown that inhibition of G9a catalytic activity abolishes early recruitment of RNF168, 53BP1 and BRCA1 to sites of DNA breaks. Given that ubiquitylation signal is required for the recruitment of both 53BP1 and BRCA1, our data suggests that G9a functions upstream of RNF168. In fact, and consistent with this observation, poly-ubiquitylation signal was not detectable at DNA damage sites following inhibition of G9a catalytic activity. However, recruitment of these

factors at later time points was restored. Intriguingly, it has been shown that early recruitment of DNA repair factors does not require pH2AX. Nevertheless, phosphorylated H2AX is important for their late recruitment and retention at DNA damage sites (Celeste et al. 2003). The mechanism underline H2AX-independet recruitment is still not well understood. Taken together, our data suggests that G9a might be important to mediate the early recruitment of these factors to DNA breaks, while H2AX is essential for late recruitment. The fact that G9a recruitment itself was independent of H2AX further supports this idea.

As expected, catalytic inhibition of G9a activity resulted in deficiency of both HR- and NHEJ-mediated DNA repair, further supporting the idea that G9a activity promotes the DNA damage response signal. The implications that this data has in the clinic are great. First, not only we provided evidence that G9a is directly involved in the DNA repair pathway, but also provided data that will advance our knowledge on the mechanism by which G9a promotes cell survival and resistance to DNA damaging agents. The observation that G9a is required for early recruitment of DDR factors suggests that use of G9a inhibitors might be especially useful in tumors harboring a repair defect in late steps of the repair pathway.

Methods

Cell Culture, reagents and treatments

U2OS, HeLa, and HEK293T cells were obtained from the ATCC (American Type Culture Collection; Rockville, MD) and grown on regular DMEM (Dulbecco's modified Eagle's Medium; Invitrogen) that was supplemented with 10% fetal bovine serum (FBS; HyClone) and 1% antimycotic/antibacaterial. $ATM^{+/+}$ (GM00200) and $ATM^{-/-}$ (GM09607) human fibroblast cells were obtained from Coriell Institute and grown in regular DMEM supplemented with 15% FBS. $H2AX^{+/+}$ and $H2AX^{-/-}$ MEFs were a gift from Andre Nussenzweig, and $MDC1^{-/-}$ MEFs were a gift from Zhenkun. Cells were kept in a humidified incubator at 37°C with 5% CO_2.

Whenever indicated cells were treated with G9a small molecule inhibitor UNC0638 (Sigma-Aldrich, 1μM for 16-24 hour); ATM inhibitor KU-55933 (Astra-Zeneca/Kudos Pharmaceuticals (Cambridge, UK), 0.5 μM overnight); Neocarzinostatin (NCS, Sigma-Aldrish, 200 ng/mL), and ATR inhibitor (VE-821, Cayman Chemical, 3uM). The antibodies (with concentrations) used were: rabbit anti-G9a (Bethyl Laboratories, 1:1000 for western blot), rabbit anti-G9a (Cell Signaling, 1:50 for immunofluorescence), rabbit anti-GLP1 (Bethyl Laboratories, 1:1000 western blot, 1:100 immunofluorescence), mouse anti-pH2AX (Ser139) (Millipore®,1:4000 for western blot and 1:300 for IF), rabbit anti-pH2AX (Ser139) (Cell Signaling, 1:4000 for western blot and 1:300 for IF), anti-GFP (Abcam, 1:300 for immunofluorescence), anti-Flag (Sigma-Aldrish, 1:300), anti-K63 ubiquitin

(EMD Millipore, 1:200 for immunofluorescence), anti-SUMO (Santa Cruz Biotechnology, 1:300), rabbit anti-53BP1 (Bethyl Laboratories, 1:1000 for IF), anti-BRCA1 (Gift from Bing Xia), anti-RNF168 (Cell Signaling, 1:300 for IF), mouse anti-H3K9me2 (Cell Signaling, 1:4000), rabbit and mouse anti-H3 (Cell Signaling), and anti-GAPDH (Abcam, 1:10000 for western blot). For immunofluorescence experiments, secondary antibodies used were: anti-mouse (115-035-068, 1:200) and anti-rabbit (711-035-152, 1:200) from Jackson ImmunoResearch Labs.

Plasmids construction of full-length human G9a plasmid encoding enhanced GFP and point mutations

Flag tagged full length human G9a and deletion constructs are gift from Eiji Hara, EGFP-G9a, phospho-mutant EGFP-G9a S569A and G9a silent-mutant were generated as bellow. The pcDNA3 Flag tagged full-length human G9a cDNA was modified by insertion of an eGFP cassette into the KpnI site using following primers: KpnI5GFP 5'-GAG GTA CCA TGG TGA GCA AGG GCG AG-3' and KpnI3GFP 5'-GAG GTA CCC TTG TAC AGC TCG TCC-3'. The phosphorylation mutation (S569A) was generated using QuikChange site-directed mutagenesis kit (Agilent Technologies) using these primers (forward primer 5'-ATT CTG CAG TCG ACG GTA CCA TGG CCG CCG CCG AT-3' and reverse primer 5'-ATT CTG CAG TCG ACG GTA CCA TGG CTG CCG ATG AAG GC-3'). Similar methods were used to generate shRNA-resistant silent mutations in full-length flag-tagged human G9a cDNA using following primers: Sense: 5'-cagaggagccaccgaaagggttcatgggtctttggggga-3' and antisense: 5'-

tcccccaaagacccatgaacccttttcggtggctcctctg-3'. All constructs were sequence verified. GFP-RNF8 and RNF168 constructs are gift from Jiri Lukas, and shRNA constructs for G9a (TRCN0000036054) and shGLP1 (TRCN0000115670) were purchased from Sigma Aldrich.

Generation of G9a phospo-specific antibody: Rabbit polyclonal antibodies that recognize the S569-phosphorylated G9a were generated by Genscript (Piscataway, NJ) against keyhole limpet hemocyanin (KLH)- conjugated G9a phospho-peptide (CTAAPAPPPL{pSER}QDVP) and double affinity purified.

Protein extraction and western blotting.

RIPA buffer (50 mM TrisHCl pH 8, 150 mM NaCl, 1% NP40, 0.5 M Sodium Deoxycholate, 0.1% SDS, 25 mM NaF, 1 mM Na_3VO_4, and complete protease inhibitor cocktail (Roche®) was used to lyse the cells. After 30 minutes incubation on ice, protein was collected following centrifugation of the samples. To measure the protein concentration a Bio-Rad® colorimetric protein assay was used. Denaturing of the protein lysates (20-40 µg) were was achieved by using Laemmli loading buffer, and proteins were resolved by gradient SDS-PAGE (pre-cast, 4-15% gradient gels, Bio-Rad) and transferred to PVDF membranes. Western blot was as follow: primary antibodies were incubated in 2.5% milk in TBST overnight at 4^{o}C with constant shaking and secondary antibodies were incubated in TBST for 1 hour at room temperature. Detection of antigens was performed with standard chemiluminescence (ECL Pico, Bio-Rad) and visualized using a Chemi-Doc (Bio-

Rad) instrument. Secondary antibodies used were HRP conjugated goat anti-mouse or anti-rabbit (Bio-Rad).

Laser microirradiation

A total of 60,000 cells per well were seeded in a 4 well chamber slide (Lab-Tek, Nalge ® Nunc™ International) 2 days before microirradiation and pre-sensitized with 5-iodo-2-hydroxyuridine (IDU, Sigma-Aldrish) 24 hours before. Laser microirradiation was performed as before using a PALM (Photo-activated Localization Microscopy) UV-A pulsed laser (100 Hz, l 1⁄4 355 nm; P.A.L.M. Microlaser) integrated to a Zeiss Axiovert 200 microscope (Carl Zeiss AG). Targeted nuclei were selected using PALM Robo software (Zeiss) and generation of subnuclear DNA damage was achieved by focusing the laser through LD 40x objective to yield a spot size of ~1μm with laser output set to 50% which was the lowest power necessary to cause a detectable nuclear pH2AX stripe with minimal cellular toxicity. In average, at least 50 cells per well were irradiated within 5 minutes. Unless otherwise stated, cells were fixed with 4% paraformaldehyde (PFA) for 10 minutes after of recovery for indicated time points.

Ionizing radiation

Cells were seeded in triplicate chamber slides and irradiated with a ^{137}Cs γ-ray source (Best® Theratronics Gamma Cell 40-Exactor) with a dose rate of 1.08 Gy min^{-1} at room temperature. Cells were treated with mean irradiation doses from 0 to 10 Gy following incubation prior to fixation or harboring.

Immunofluorescence

To analyze DNA damage response factors, cells were permeabilized with 0.5% Triton X-100 in PBS for 10 minutes after the 10 minutes fixation with 4% PFA. Cells were then incubated for 1 hour at room temperature with indicated antibodies diluted in 5% goat serum in PBS. After incubation with primary antibodies, cells were washed 4 times with PBS. Alexa Fluor™'s 490 or 595 nm anti-mouse or rabbit (Thermofisher) diluted 1:500 in 5% goat serum in PBS were used as secondary antibodies and incubated for 1 hour at room temperature. Cells were washed 4 times with PBS and let dry for 10 min before mounted with Vectashield DAPI mounting media (Vector Laboratories). Images were taken with Nikon Eclipse 80i Microscope and fluorescence intensity was measured using ImageJ software.

DNA double strand break repair (DBSR) assays

Homologous recombination (HR) and non-homologous end joining (NHEJ) repair efficiency, was measured by stably selecting cells after lentiviral particle infections (shG9a or shGLP1) or drug treatment along with specific controls. HR assay was performed as described previously (Koji Nakanishi et al. 2005; A J Pierce et al. 1999) using U2OS/DR-GFP reporter cell line, whereas NHEJ assay was performed using U2OS EJ5-GFP cells (Bennardo et al. 2008). Cells seeded at 2 $x10^5$ cells per well in 6-well plates were transfected the next day with indicated plasmids mixed with 3.6 µl of Lipofectamine 2000 (Invitrogen) in a 1-ml culture medium without antibiotics. Transfected plasmids were as follow: 0.8 µg of pCBASce (I-SceI expression vector); and either 0.4 µg or 1 µg of pcDNA3.1 empty vector (expression vector for G9a silent-mutant (simut) or for wild-type G9a

(wtG9a)). The media was changed four hours after transfection and the percentage of GFP-positive cells was quantified 3 days after transfection, using the Cytomics FC 500 Series flow cytometer (Beckman Coulter). CXP software (Beckman Coulter) was used to analyzed data.

shRNA knockdowns

Sigma MISSION shRNA targeting, and non-targeting control plasmids were used according to manufacturer's instructions. Lentiviral particles were prepared using cationic lipid-mediated transfection (Invitrogen™ Lipofectamine® 2000) of sub-confluent HEK293T cells cultured in DMEM plus 10% FBS. For a 10-cm dish, lentiviral vector (10 µg) was co-transfected with the lentiviral packaging vector (psPAX2, Addgene, 12260) and the amphotropic envelope (pMD2.G, Addgene, 12259). 24 hr post transfection media containing viral-particles were filtered (Millipore Steriflip-GP Filter, 0.45 um Durapore PVDF) and tittered (Takara Clontech Lenti- X™GoStix™). Transduction of viral particles was conducted by adding viral particles to the target cells containing 8 µg/mL polybrene and spinoculation was performed by centrifugation for 2 hr at 1000g and plates were left at 37°C, 5% CO2 incubator. As the viral particles contain puromycin-resistance gene, determination of functional viral titer was performed by drug-resistance colony assay as described (Tonini et al. 2004). Three days post-transduction, cells were pelleted and re-suspended in fresh complete medium containing 2 µg/mL puromycin. Along with the transduced cultures, a non-transduced culture was also selected in puromycin-containing medium to serve as a control for judging when the transduced cells emerged from selection.

Chapter 2: G9a regulates ATM-dependent DNA damage response signal.

Introduction

G9a methyltransferase has been found to be overexpressed in a number of tumors, where it contributes to tumorigenesis and metastasis by silencing tumor suppressor genes and important genes for cell adherence like Ep-CAM and E-cadherin (Chen et al. 2010a; Dong et al. 2012). These data suggest that G9a overexpression is a marker for poor prognosis and metastasis (Hua et al. 2014). Recent studies have shown that the use of G9a catalytic inhibitors have a negative effect on tumor growth and progression. Treatment of cells with small molecule inhibitors of G9a catalytic activity can restore the normal expression profile in the G9a overexpressing cells, and can result in checkpoint activation, cell death, and/or restoration of senescence, or autophagy (Ke et al. 2014a; Casciello et al. 2015); all of which contributes to stopping the progression or even reversing the disease. It has also been shown that treatment with G9a inhibitors sensitize cells to DNA damaging agents and drugs.

Use of DNA damaging drugs like cisplatin, demonstrated to have a greater effect when used along with G9a inhibitor in squamous cell carcinoma (C. Liu et al. 2017). It is speculated that inhibition of G9a, which leads to decreased global histone methylation levels, results in a more relaxed chromatin allowing DNA damaging drugs to get easier access to the DNA. However, the exact mechanism through which G9a activity influences the efficacy of DNA damaging agents is unknown. Previous work in our laboratory demonstrated for the first time that G9a is directly involved in the DNA repair pathway, being rapidly recruited to sites of DNA damage in an ATM-dependent fashion (chapter I). Moreover, its inhibition

affected the early recruitment of some DNA damage repair factors like 53BP1, RNF168, and BRCA1 to sites of DNA breaks. These data demonstrate that G9a has a role in the DNA damage response signal and that this could contribute to the effects of G9a inhibition in sensitizing the cells to DNA damaging drugs. In other words, beyond the effect that we see on histone methylation and chromatin relaxation, catalytic inhibition of G9a may be having a direct impact on the DNA repair pathway that still remains to be elucidated.

Here we further investigate the role of G9a in the DNA damage signaling pathway. We show that G9a catalytic activity is important for the regulation of the ATM-dependent DNA damage response signal, and that its inhibition causes a disruption of the normal signal spreading in the nucleus. Our finding suggests that G9a may be limiting ATM activation through the methylation and activation of HDAC1, which can then then de-acetylate ATM and reduce its activation.

Results

G9a inhibition causes altered spreading of pH2AX after DNA damage.

We have previously shown that G9a methyltransferase is recruited to sites of DNA damage in an ATM-dependent fashion where inhibition of its catalytic activity affects the early recruitment of DNA damage repair (DDR) factors (Chapter I and Ginjala et al. 2017). In order to further understand how the catalytic activity of G9a affects the DNA damage response, we sought to identify the effects of G9a inhibition by using the commercially available G9a specific small molecule inhibitor UNC0638. This is a highly selective inhibitor that binds to the substrate-binding pocket of G9a/GLp and therefore competes with the peptide and not with S-adenosyl-methionine (Vedadi, Barsyte-Lovejoy, Liu, Rival-Gervier, Allali-Hassani, Labrie, Wigle, Dimaggio, et al. 2011). U2OS cells, treated or untreated with 1 uM

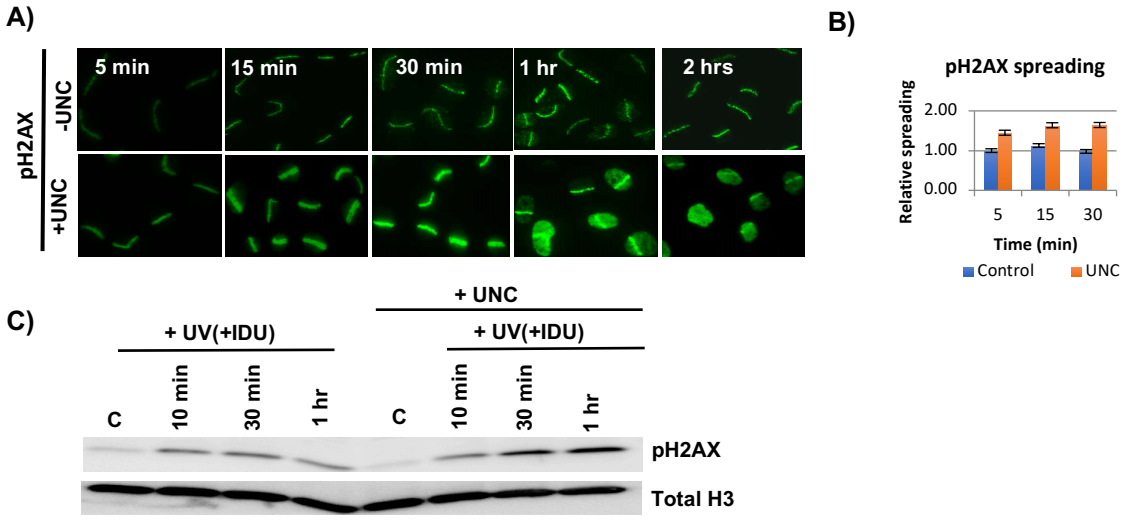

Figure 1. G9a catalytic inhibition causes altered spreading of pH2AX. A) U2OS cells were subjected to localized, UV laser-induced DNA damage followed by immunofluorescence using endogenous antibody for pH2AX. Shown is pHA2X signal spreading over time compared to control. B) Quantification of pH2AX signal spreading up to 30 min compared to normal spreading. C) Western blot showing increased pH2AX signal in cells treated with UNC0638 (1uM, overnight) and after UV(+IDU) damage, compared to UV damage alone.

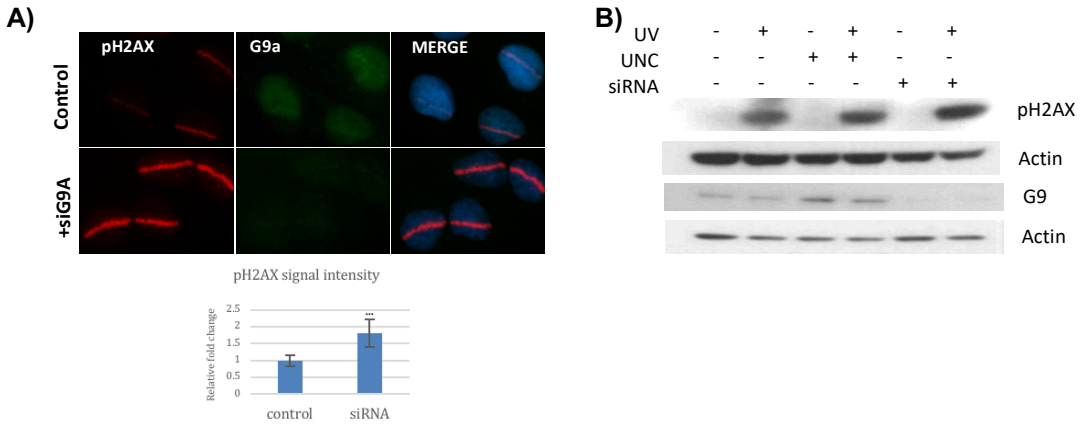

Figure 2. G9a knockdown also causes an increased in pH2AX signal. USOS cells were subjected to UV laser- (A) or UV(+IDU)-induced (B) DNA damage. Shown is increased pH2AX signal upon DNA damage along with UNC0638 treatment (1uM, overnight) compared to DNA damage alone.

UNC0638 overnight, were subjected to localized, UV laser-induced DNA damage. Interestingly, we noticed a striking difference on the induction of phosphorylated H2AX in cells treated with G9a inhibitor when compared to control cells (Fig. 1B and C). G9a catalytic inhibition caused an increase in pH2AX signal intensity as seen by IF and western blot (Fig. 1B and C). Moreover, the region of H2AX phosphorylation dramatically spread over time, eventually extending throughout the whole nucleus after 1 hour in a subset of cells (Fig. 1B). In order to confirm that this effect was due to the inhibition of G9a and not due to off target effects of the inhibitor, we reduced G9a expression using Sigma MISSION esiRNA. Treatment with siRNA also resulted in an increased pH2AX signal intensity and spreading, although to a lesser extent than G9a catalytic inhibition (Fig. 2).

Given that UV laser-scissors can create different types of DNA damage, we also looked at pH2AX foci formation in DiVa cells, a cell model in which one can specifically induce enzymatic DNA double stranded breaks (DSBs) at defined genomic loci. DiVa are U2OS cells that contain *Asi*SI restriction enzyme fused to

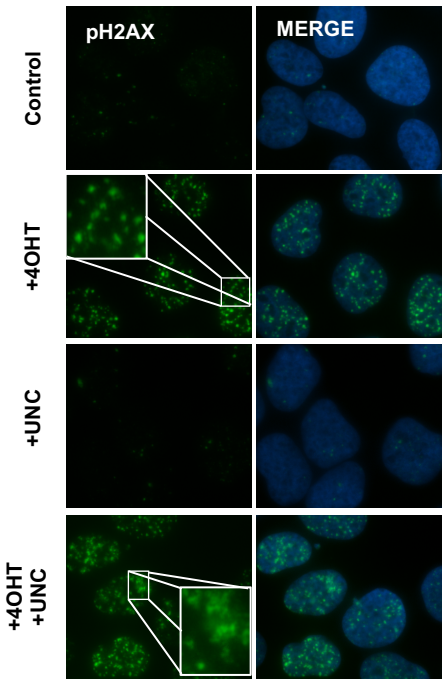

Figure 3. pH2AX spreading in DiVA cells after UNC0638 treatment. Double strand breaks were induced in DiVa cells by adding 4OH-Tamoxifen (300nM, 4 hours). After treatment cells were fix and processed for IF staining using the indicated antibodies. White squares a to enhance appearance of pH2AX foci.

a modified estrogen receptor which binds 4-hydroxytamoxifen (4OHT). Upon 4OHT treatment the enzyme, that recognizes an 8bp sequence in the human genome, localizes to the nucleus generating approximately 200 double stranded breaks (DSBs) at specific loci (Iacovoni et al. 2010). Exposure of DiVa cells to 4OH-T led to induction of pH2AX foci that likely reflect response to induced DNA breaks. Formation of pH2AX foci on cells treated with both UNC0638 and 4OH-Tamoxifen were broader and more diffused than pH2AX foci in cells treated with 4OHT alone. Furthermore, treatment with UNC0638 alone did not increase pH2AX signal, suggesting that it did not cause DNA damage by its own (Fig. 3).

Taken together this suggests that G9a activity is required for the regulation of the extent of H2AX phosphorylation and DDR signal amplification after DNA damage. Phosphorylation of the histone variant H2AX is one of the first steps in the DNA damage response signal. It gets phosphorylated up to 2 megabases away from the DNA break (Pilch et al. 2003). However, what controls the extent of H2AX

phosphorylation spreading away from DNA break sites is currently not well understood. This data suggests a possible role for G9a methyltransferase activity in this process.

ATM is required for the altered spreading of pH2AX.

To have a better understanding of the mechanism by which G9a controls the γH2AX signal spreading we aimed to determine what other factors are necessary for the altered spreading to occur. Given that ATM is one of the kinases responsible for the phosphorylation of H2AX in response to DNA damage we set out to determine its role in pH2AX altered spreading caused by G9a catalytic inhibition. U2OS cells were treated with either UNC0638, ATMi KU55 933 or both and subjected to UV-laser scissors to induced DNA damage. As expected, pH2AX

A)

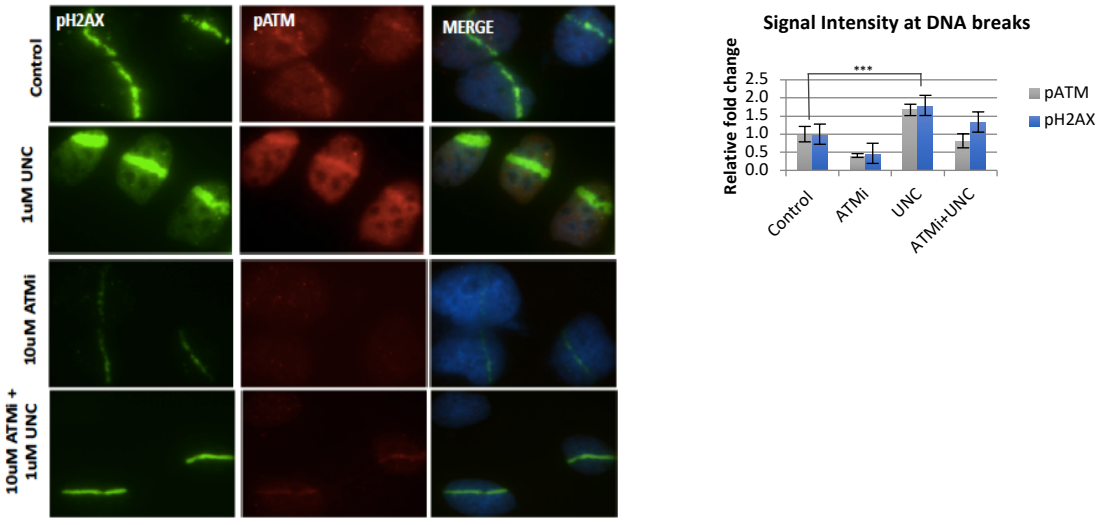

Figure 4. ATM is required for pH2AX altered spreading caused by G9a inhibition. U2OS cells were subjected to UV laser-induced DNA damage followed by IF using indicated antibodies after 10 min recovery. Altered spreading of pH2AX caused by UNC0638 treatment is recued to normal levels when ATM was inhibited at the same time. Quantification of signal intensities at DNA breaks is shown and expressed as the mean ± SD.

signal was greatly reduced in cells treated with ATMi alone. However, when cells were treated with both UNC0638 and ATMi, levels of pH2AX were rescued, showing a spreading similar to that in control cells (Fig. 4A).

ATM is hyper-phosphorylated upon G9a inhibition after DNA damage

Consistent with the increased phosphorylation of H2AX, we found that ATM was hyper-phosphorylated (Ser1981) in cells treated with G9a inhibitor (Fig. 4A), suggesting hyper-activation of ATM under these conditions. Treatment with both G9a and ATM inhibitors rescued the levels of ATM phosphorylation after DNA damage as seen by IF (Fig. 4A). Both pATM and pH2AX signal intensities behaved in similar ways (Fig. 4B). In order to confirm this, we used ATM deficient human fibroblasts and treated them with UNC0638. Although in this setting other kinases able to phosphorylate H2AX are present, we failed to see an increased signal for

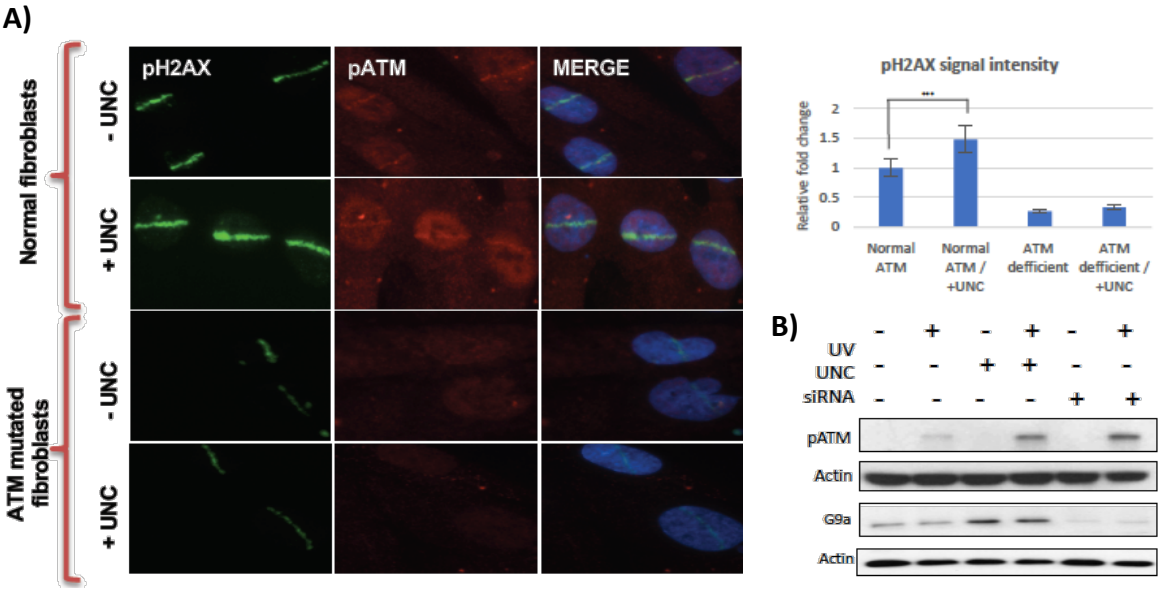

Figure 5. ATM is hyperphosphorylated and required for pH2AX altered spreading caused by UNC0638. A) ATM mutated fibroblasts were treated with UNC0638 (1uM, overnight) and subjected to UV laser-induced DNA damage followed by IF staining using indicated antibodies. B) U2OS cells were treated with UNC0638 or siRNA targeting G9a and UV(+IDU) irradiated, or control followed by protein extraction and western blot analysis using indicated antibodies. Quantification of pH2AX signal intensity at DNA breaks is shown and expressed as the mean ± SD of three independent experiments.

pH2AX when compared to control cells. Moreover, we were able to see an increased signal for pATM (Ser1981) in control fibroblast cells (Fig. 4A), showing that G9a inhibition has the same effect on ATM activation throughout different cell lines. We also looked for the effects of G9a knockdown on ATM activation and found that siRNA treatment also resulted on an increased phosphorylation of ATM as seen by western blot (Fig. 5B). This data shows that the effect of G9a catalytic inhibition on pH2AX signal spreading is dependent on ATM catalytic activity.

G9a catalytic inhibition causes altered spreading of MDC1

Phosphorylation of H2AX in chromatin near a DNA break is an important signal to promote the accumulation of the DDR proteins. Given the abnormal spreading of pH2AX signal in G9a inhibited conditions, we sought out to determine how further recruitment of downstream factors was affected. We already showed that G9a catalytic inhibition by UNC0638 as well as G9a knockdown, abrogated early recruitment of RNF8, RNF168 and 53BP1 to sites of DNA damage (Ginjala et al. 2017). This contrasting observation with ATM and H2AX increased phosphorylation observed in the

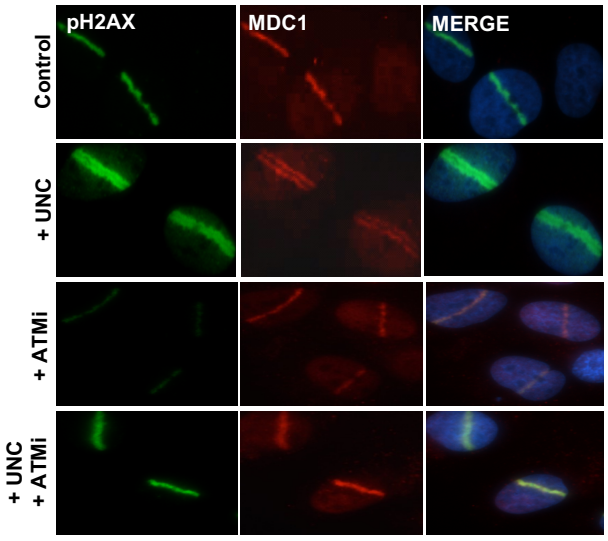

Figure 6. G9a inhibition affects MDC1 recruitment but does not abolishes it. U2OS cells were treated with UNC0638, ATMi or both and subjected to UV laser micro-irradiation followed by IF staining using the indicated antibodies. MDC1 recruitment shows an altered spreading in cells treated with UNC0638, which is rescued by simultaneous inhibition of ATM.

present study, prompted us to further investigate the effects of G9a inhibition on other factors in the pathway. Intriguingly, and though recruitment of RNF8 and other downstream factors was affected, we observed that MDC1 was still recruited in response to UV-laser-induced DNA damage upon G9a catalytic inhibition. However, recruitment pattern of MDC1 was altered and followed the same spreading pattern of pH2AX (Fig. 6). Furthermore, we found that, similar to pH2AX, treatment with ATMi decreased the UNC0638-induced abnormal spreading of MDC1, showing that ATM activity is necessary for the altered signal spreading observed under these conditions. MDC1 is recruited to regions of phosphorylated H2AX, promoting further recruitment of ATM and thus amplification of the DDR signal. Taken together, this data suggests that G9a activity is important for the proper localization of MDC1 and signal amplification as well as for the assembly of the response factors.

As we already showed, G9a recruitment to sites of DNA damage is dependent on its phosphorylation by ATM (Chapter I and Ginjala et al. 2017). We

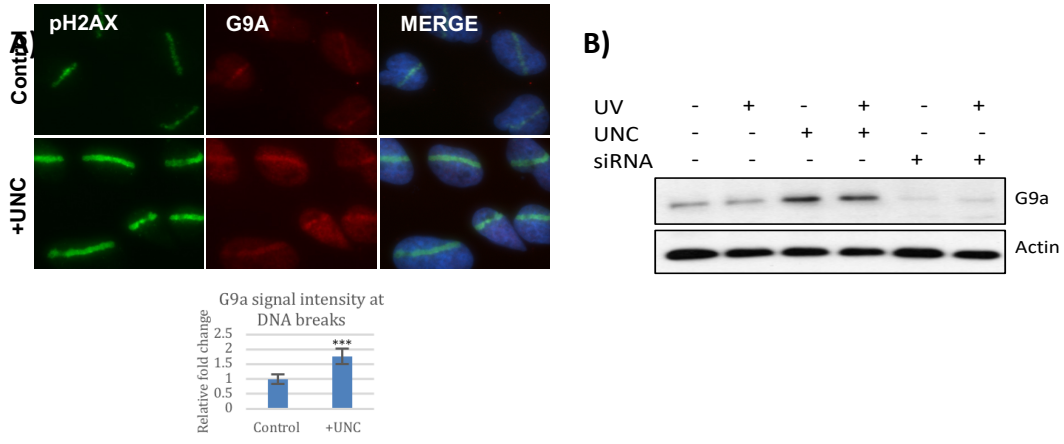

Figure 7. G9a catalytic inhibition increases its recruitment to sites of DNA breaks. U2OS cells were treated with UNC0638 and DNA damage was induced either by UV laser (A) or UV(+IDU) radiation (B). G9a recruitment to sites of DNA breaks was studied by IF staining using indicated antibodies (A) or protein levels were analyzed by western blot (B). Quantification of G9a signal intensity at DNA breaks is shown and expressed as the mean ± SD.

thus wondered if G9a recruitment itself was affected upon its catalytic inhibition by UNC0638. Notably, G9a recruitment to UV-laser induced DNA breaks was increased after its catalytic inhibition (Fig. 7A). Interestingly, we also observed that upon its inhibition, global levels of G9a were increased as seen by western blot (Fig. 7B).

G9a interacts with HDAC1/ 2

Previous studies have focused on identifying G9a interacting partners, mostly relevant to regulation of gene expression (Maier et al. 2015; Chaturvedi et al. 2012; Shankar et al. 2013). To gain more insight on the role of G9a during the DNA repair process we set out to identify G9a catalytic activity-dependent protein interactions during DNA damage. HeLa cells treated with UNC0638 or control and either mock treated or incubated with IDU and exposed to 100kJ UV were subjected to immunoprecipitation using an antibody against endogenous G9a. Immunoprecipitates were analyzed by LC-MS/MS and several interacting proteins were identified. Consistent with known G9a interacting partners, GLP1 and Wiz were identified as the most abundant peptides present in every sample group. Among the interacting

Proteins	No ab	C	UV	UNC	UV + UNC
G9a	0	167	160	322	153
GLP1	0	148	151	291	166
Wiz	0	189	185	353	188
CDYL	0	82	84	19	12
PRMT5	0	23	22	41	32
HDAC2	0	24	26	8	4
HDAC1	0	9	9	0	1
RUVBL2	0	3	1	9	4
RUVBL1	0	2	2	2	2

Figure 8. G9a interacting partners. Hela cells were treated with UNC0638 or control and subjected to immunoprecipitation using endogenous antibodies for G9a. Immunoprecipitates were analyzed by LC-MS/MS. Shown are G9a interacting partners of interest during DNA damage repose that were affected by G9a catalytic inhibition.

peptides whose interaction was affected upon G9a inhibition we identified HDAC1, HDAC2, PRMT5, RUVBL2 and CDYL (Fig. 8).

UNC0638 treatment resulted in a reduction of HDAC1/2 peptides interacting with G9a. It has been shown that HDAC1 is in a repressive complex with G9a involved in the silencing of hypoxia-responsive genes and adhesion molecules (Lee et al. 2010; Chen et al. 2010a). Since we found HDAC1/2 to be in a complex with G9a under DNA damage conditions (which was dependent on G9a catalytic activity), we wondered if HDAC1/2 activity was affected by inhibition of G9a activity. To evaluate this, we first looked for G9a-dependent methylation of HDAC1/2 during DNA damage.

HeLa cells were treated as before and subjected to immunoprecipitation using an antibody against methylated-lysine. Immunoprecipitates were analyzed by western blot using indicated antibodies. HDAC1 methylation was observed to be increased after DNA damage; this induction of HDAC1 methylation was inhibited by treatment with G9a inhibitor (Fig. 9), suggesting that G9a catalytic activity is important for HDAC1 methylation in response to DNA damage. This is not surprising as it has been previously shown that HDAC1 is a substrate of G9a (Rathert et al. 2008).

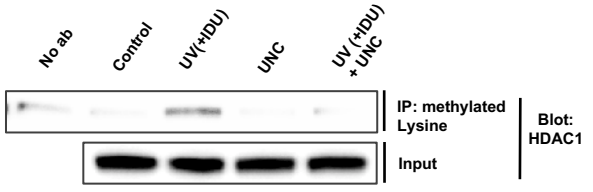

Figure 9. G9a promotes HDAC1 methylation in response to DNA damage. 293T cells treated with either UNC0638 (1uM, overnight), UV(+IDU) radiation or both were subjected to immunoprecipitation using an antibody for methylated lysine and blotted for HDAC1. Increased in HDAC1 methylation was induced by DNA damage but this was abolished by treatment with G9a inhibitor.

H3K56Ac levels are increased after G9a catalytic inhibition.

HDAC1/2 were identified to be responsible for regulating acetylation levels of lysine 53 in histone 3 (H3K56Ac) in response to DNA damage (Miller et al. 2011). To investigate the effects of G9a-mediated methylation on HDAC1/2 catalytic activity, we looked for acetylation levels of H3K56Ac in the presence of G9a inhibitor. U2OS cells were treated or not with UNC0638 and irradiated with 100KJ UV (+IDU). Proteins were extracted, and histone acetylation levels were evaluated by western blot. We found that G9a catalytic inhibition caused an increase on global levels of H3K56Ac when compared to control cells, suggesting lack of HDAC1/2 activity. Taken together this suggests that G9a-mediated methylation of HDAC1/2 is important for its deacetylase activity upon DNA damage.

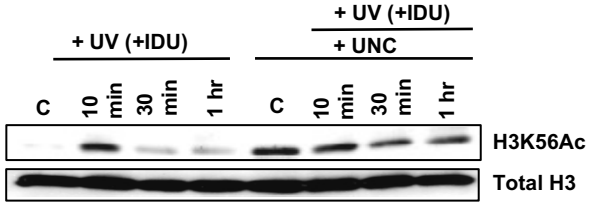

Figure 10. Acetylation levels of H3K56 increases after G9a catalytic inhibition. U2OS cells were treated with UNC0638 or control and DNA damage was induced using UV-radiation. Protein was extracted and acetylation levels of H3K56 was assessed by western blot analysis.

G9a catalytic inhibition results in increased ATM acetylation in response to DNA damage

Interestingly, previous works have shown that treatment with HDAC inhibitors induce ATM acetylation and autophosphorylation, leading to activation of ATM (Kaidi & Jackson 2013). Since HDAC1/2 was found in a complex with G9a under DNA damage conditions, and given that G9a inhibition resulted in decreased HDAC1/2 deacetylase activity, we decided to investigate if ATM acetylation levels

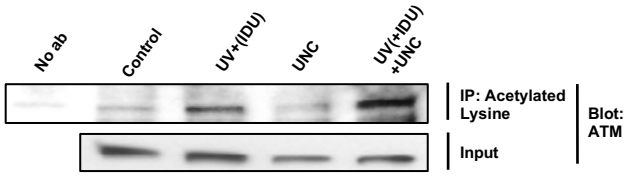

Figure 11. G9a catalytic inhibition resulted in increased acetylation of ATM. 293T cells were treated as before and subjected to immunoprecipitation using an antibody for acetylated lysine and blotted for total ATM. Acetylation levels of ATM increased after DNA damage in those cells treated with UNC0638 compared to DNA damage alone.

were also affected by G9a inhibition. 293T cells were treated with or without UNC0638 and 100kJ UV (+IDU) radiation and subjected to immunoprecipitation using an antibody recognizing acetylated lysines. We observed that ATM acetylation levels were notably increased in response to DNA damage in cells treated with G9a inhibitor compared to DNA damage alone. This data further suggests that G9a has a role in limiting ATM activation during the DNA damage repair process in part by regulating its acetylation levels.

G9a catalytic inhibition causes ATM hyperactivity

Catalytically inactive ATM homodimers are activated through its trans auto-phosphorylation and monomerization in response to DNA damage. Nonetheless, the fully activated form of ATM also depends on Tip60/Kat5 acetylation on K3016 (Sun et al. 2005). To further study the activation status of ATM, we looked for phosphorylation levels of the known ATM substrates, CHK2 and KAP1. U2OS cells were UNC0638 treated, UV(+IDU)-irradiated or both followed by protein extraction at indicated time points and western blot analysis. Notably, the phosphorylation levels of ATM, KAP1 and ChK2 were higher in cells treated with UNC0638 and UV(+IDU)-irradiated than in either UV(+IDU)-irradiated or UNC0638 treated cells

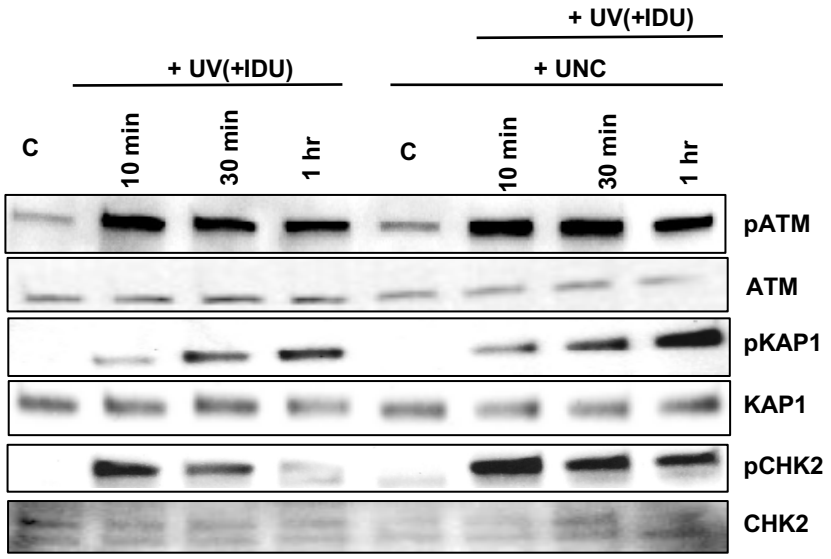

Figure 12. ATM is hyperactive after UNC0638 treatment in response to DNA damage. Phosphorylation levels of ATM substrates were analyzed in U2OS cells treated with UNC0638 or control and irradiated with UV (+IDU). Proteins were extracted after DNA damage at the indicated times and western blot analysis was performed using indicated antibodies. ATM, KAP-1 and CHK2 phosphorylation levels were increased when cells were treated with UNC0638 in response to DNA damage when compared to DNA damage alone.

alone. In addition, phosphorylation levels were sustained for up to an hour after UV damage along with UNC0638 treatment.

This data demonstrates that catalytic inhibition of G9a results in increased phosphorylation of ATM substrates due to hyper-activation of ATM. Therefore, it suggests that under normal conditions G9a has a role in the regulation of ATM activity during the DNA damage repair pathway. We know from our previous work that G9a recruitment to sites of DNA damage is dependent on ATM phosphorylation (Chapter I and Ginjala et al. 2017). Taken together, this data suggests a negative feedback loop regulation where, after its ATM-dependent recruitment to DNA breaks, G9a plays a role in deactivating ATM, limiting in this way the DDR signal amplification and spreading.

HDAC inhibition results in increased phosphorylation of H2AX.

We then investigated if G9a effects on the DNA repair pathway is through methylation of HDAC1/2. Given that G9a inhibition resulted in ATM hyperactivation and consequently increased phosphorylation of ATM substrates, we set to determine if inhibition of HDAC1/2 would result in a similar phenotype. To confirm this, we looked for the effects of HDAC1/2 inhibition on phosphorylation levels of H2AX. U2OS cells were treated with either TSA (0.5uM, overnight), UNC0638 or control, and DNA damage was induced using UV laser followed by immunofluorescence using antibodies against endogenous pH2AX. Indeed, inhibition of HDAC1/2 resulted in increased phosphorylation of H2AX when compared to control cells. This further supports the idea that G9a-mediated methylation of HDAC1/2 is important for its role in regulating the DDR signal.

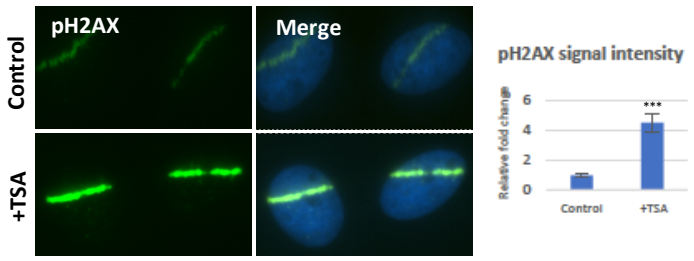

Figure 13. HDAC inhibition leads to increased phosphorylation of H2AX. U2OS cells were treated with the HDACi, TSA (0.5uM, overnight) and were subjected to laser micro-irradiation and pH2AX levels were analyzed by immunofluorescence. Inhibition of HDAC1/2 resulted in increased phosphorylation of H2AX compared to control cells.

Discussion

The importance of G9a in repressive complexes, and activator complexes as well, has been well established in the past years (reviewed by Shankar et al. 2013). Especially, the impact of its repressive function in the silencing of tumor suppressor genes and adhesions molecules during tumorigenesis and metastasis, respectively (Dong et al. 2012; Chen et al. 2010a). It was not until recently that G9a was reported to be recruited to sites of DNA damage where it affects early recruitment of DNA damage repair factors (chapter I and Ginjala et al. 2017). However, the precise function that G9a exerts during this process is still not fully understood. Here we presented additional evidence that G9a methyltransferase activity is an important factor in the regulation of the DNA damage response (DDR) signal that goes beyond its chromatin changing capabilities.

We have shown that catalytic inhibition of G9a resulted in both increased phosphorylation and signal spreading of pH2AX. Phosphorylation of H2AX by the PI3K-related kinases ATM or ATR is one of the first steps in the DNA damage response signal. This phosphorylation extends for up to 2 megabase pairs and, although not required for the recruitment of DDR proteins, it is important for their retention at the surrounding chromatin of DNA breaks (Celeste et al. 2003). The observation that H2AX phosphorylation is increased in the setting of G9a inhibition points towards a role for G9a in limiting the extent of the pH2AX signal spreading in response to DNA damage. Interestingly, we observed that after an hour a subset of cells recovered to normal levels of H2AX phosphorylation (Fig. 1A). It would be

interesting to determine which stage of the cell cycle these cells are in and evaluate if it has an effect on this phenomenon. From our previous work we know that recruitment of DDR factors was restored after an hour. It is possible that this observation correlates with the rescued levels of pH2AX seen in this study. The fact that G9a knockdown resulted in a lesser effect when compared to its catalytic inhibition suggests that its presence is important for this effect. G9a, although inactive, could still be important for key protein interactions that promote further phosphorylation of H2AX.

We also looked at pH2AX foci formation using DiVA cells to look at double stranded breaks specifically, as laser-induced DNA damage can create different types of damages. We found pH2AX foci formation to appeared blurrier in cells where G9a was inhibited when compared to control cells, also suggesting an abnormal spreading in this setting. Interestingly, in DiVA cells as well as in regular U2OS cells, treatment with UNC0638 alone did not cause detectable levels of pH2AX, suggesting that G9a effects over pH2AX is dependent on DNA damage.

Being a histone methyltransferase, it could be possible that histone H3 methylation levels at sites of DNA breaks are an important factor that controls the expansion of the signal. It is known that G9a promotes recruitment of HP1 and others to methylated histones to mediate heterochromatin formation. Keeping a close and condensed chromatin status could be one way in which G9a helps to restrain the signal spreading during the DNA repair process. It is also possible that the extent of pH2AX signal is demarcated by chromosomal domains defined by an unknown DNA component which is dependent on G9a activity. Importantly, it has

been shown that inability of the cell to dephosphorylate pH2AX results in deficient DNA repair and sensitivity to DNA damaging agents (Chowdhury et al. 2005). This is consistent with our data that shows that inhibition of G9a leads to inefficient HR- and NHEJ-mediated DNA repair. Either way it is demonstrated that lack of G9a activity results in both abnormal levels and amplification of phosphorylated H2AX which could have a great impact on the dynamics of DNA damage repair factors recruitment.

In this study we found that G9a inhibition resulted in increased phosphorylation of ATM and that this was required for the abnormal spreading of pH2AX. It is known that H2AX is a substrate of different kinases that are involved in the early steps of the DNA damage repair pathway. ATM, ATR or DNA-PKc phosphorylate the H2A histone variant at Serine 139 in response to DNA damage. We evaluated the effects of ATM inhibitor on the UNC0638-dependent abnormal pH2AX spreading and increased signal intensity. Surprisingly, we noticed that treatment with ATMi rescued the normal phosphorylation levels of H2AX, suggesting that ATM is required for the effects of G9a inhibition. In fact, we also observed a similar phenotype in ATM-deficient human fibroblasts, derived from A-T patients. In both cases, although other kinases that are able to phosphorylate H2AX were present, we failed to see the abnormal spreading and increased signal intensity, further supporting the idea that the effects of G9a on pH2AX is through ATM activity. Interestingly, we also observed that treatment with both G9a inhibitor and ATM inhibitor together resulted in increased phosphorylation levels of ATM compared to ATMi alone. This furthers supports the idea that lack of G9a activity

induces activation of ATM, which leads to the increased phosphorylation of H2AX. Another important point from this observation is that this data also suggests that G9a activity is important for maintaining appropriate phosphorylation/activation levels of ATM in response to DNA damage.

One puzzling observation in this study was the fact that, while recruitment of DDR factors downstream of MDC1 was affected (Chapter I and Ginjala et al. 2017), MDC1 itself was still recruited to sites of DNA breaks in the setting of G9a inhibition, although abnormally spread (Fig. 6). MDC1 is involved in the amplification of the repair signal by promoting further recruitment and activation of ATM (Stucki et al. 2005; Lou et al. 2006; Chapman & Jackson 2008). Notably, treatment with ATM inhibitor along with G9a inhibitor resulted in decreased UNC0638-dependent spreading of MDC1 (Fig. 6), suggesting that the abnormal spreading of MDC1 is dependent on ATM as well.

Despite the upregulated signaling in early steps of the repair pathway, early recruitment of downstream factors like 53BP1, RNF168 and BRCA1, was severely affected in cells treated with UNC0638 (this study and Ginjala et al. 2017). It is known that tight regulation of the dynamics of post-translation modifications like methylation and demethylation play an important role in the DNA repair pathway (Huang & Berger 2008). For instance, it was shown that MDC1 demethylation by JMJD1C is required for RNF8 interaction and recruitment of RAP80-BRCA1 (Watanabe et al. 2013). It is possible that G9a activity regulates methylation levels of key proteins which modulate the recruitment of factors downstream of the pathway. Also, dysregulation of pH2AX signal and other histone modifications by

G9a inhibition may lead to abnormal recruitment of downstream factors in the process. Further investigation is needed to determine how G9a is involved in this process and how it promotes downstream recruitment while limiting activation of ATM in early steps of the repair.

We have also shown several interacting partners of G9a during UV(+IDU)-induced DNA damage. These interactions were affected by inhibition of the catalytic activity of G9a, suggesting that they are dependent on methyltransferase activity. For proteins like PRMT5 and Ruvbl1/2 the effect was the opposite. It was interesting that CDYL was also found to be in complex with G9a during DNA damage. CDYL was recently found to possess crotonyl-CoA hydratase activity towards H3K9. It will be interesting to see whether regulation of histone crotonylation through G9a-CDYL association has an impact during DNA damage repair.

HDAC1/2 have been reported to be in a repressive complex with and to be a substrate of G9a (Rathert et al. 2008). Here we showed that methylation levels of HDAC1 were increased after DNA damage but not in the presence of G9a inhibitor, suggesting that G9a activity leads to HDAC1 methylation in response to DNA damage. Interestingly, catalytic inhibition of G9a resulted in increased acetylation (or delayed deacetylation) of H3K56, a substrate of HDAC1/2, after DNA damage. This suggests that methyltransferase activity of G9a is important in the dynamics of H3K56Ac; possibly through its interaction with and activation of HDAC1. It is probable that the same effects apply to HDAC2, as it has been published that HDAC1 and 2 have redundant activities and a decrease in H3K56Ac

was only observed in the absence of both proteins at the same time (Miller et al. 2011). Further investigation is needed to determine if G9a plays a direct or indirect role in this process. Either way, we clearly showed that H3K56 acetylation is increased by G9a inhibition, which suggests lack of HDAC1/2 deacetylase activity under these conditions.

In addition to detect increased levels of H3K56Ac we also observed increased levels of ATM acetylation; further supporting the idea that ATM is in a hyperactive status in the setting of G9a inhibition (Fig. 11). In fact, our data showed that phosphorylation levels of the known ATM substrates, CHK2 and KAP1, were robustly increased and/or sustained after inhibition of G9a in response to DNA damage (Fig. 12). The increased activation of ATM could be in part due to decreased HDAC1/2 activity in this setting and induced acetylation levels of H3K56Ac. Although no one has reported direct ATM deacetylation by HDAC1/2 it remains a possibility. HDAC1 has already been shown to immunoprecipitation with and be a substrate of ATM in response to DNA damage (Kim et al. 1999). Moreover, use of class I and II HDAC inhibitor, trichostatin A (TSA), has been shown to induce activation of the ATM pathway, as seen by increased pATM and pH2AX levels (Lee 2007; Bakkenist & Kastan 2003; Kaidi & Jackson 2013).

Taken together this data suggests that G9a regulates ATM activation in part by promoting methylation and deacetylase activity of HDAC1/2. It is possible that, after its ATM-dependent recruitment to sites of DNA breaks, G9a acts by recruiting and activating HDAC1. It is also possible that other factors are involved in this process. For instance, the class III deacetylase SIRT1, which is a substrate of G9a,

also deacetylates and activates HDAC1; contrary to this, SIRT1 deacetylates and negatively regulates Tip60 acetylatransferase (Moore et al. 2013; Dobbin et al. 2013; Wang & Chen 2010). It would be interesting to see if a mechanism involving G9a-HDAC1-SIRT1 is the responsible for limiting the ATM signal after DNA damage.

Moreover, activation of the ATM pathway leads to DNA repair but also to cell cycle arrest, apoptosis and senescence (Singh et al. 2012; Alexander et al. 2010). Similarly, the use of HDAC inhibitors has been shown to promote cell death, senescence, and autophagy among other cellular effects by inducing ATM activity (reviewed in Newbold et al. 2016). In comparison, G9a inhibition when combined with DNA damaging agents, has been found to repress cell proliferation and tumor growth in a number of tumors by inducing autophagy, apoptosis, and senescence (Ren et al. 2015; Ke et al. 2014b). Therefore, it is possible that the negative effects on tumor growth achieved through G9a inhibition may be in part due to decreased deacetylase activity of HDAC1/2 and hyperactivation of ATM kinase in response to DNA damage. Nonetheless, the effects of G9a inhibition could be more related to defects on early recruitment of DDR factors and the increased activation of ATM pathway could be actually a cellular response to overcome the effects of G9a inhibition. If this is the case, cancers harboring DNA repair defects that render them dependent on early recruitment of repair factors may be very sensitive to G9a inhibitors in combination with ATM inhibitors. Further investigation is needed to establish the efficacy of this approach.

Taken together our data suggests that G9a modulates ATM activation in part through regulation of HDAC1/2 activity and consequently acetylation levels of H3K56. We propose that, following its ATM-dependent recruitment to sites of DNA damage, G9a catalytic activity leads to methylation of HDAC1, a known partner of G9a. Methylation of HDAC1 is required for its deacetylase activity in response to DNA damage, and results in de-acetylation of histones and possibly ATM. G9a catalytic inhibition leads to loss of HDAC1 methylation which results in reduced HDAC1 activity, allowing increased acetylation of histones, and possibly ATM, resulting in its increased activation (Fig. 14).

This new understanding of the underlying mechanism helps in the design of better strategies to treat cancer according to repair defects specific for each case. Also, combination therapy with HDAC inhibitors would probably present a synergistic effect in these types of tumors.

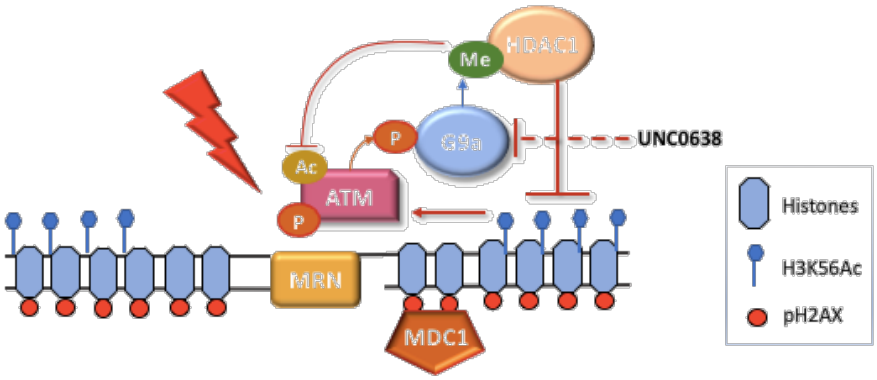

Figure 14. Proposed model for the role of G9a in the regulation of the ATM-dependent DNA damage response signal.

Methods

Cell Culture, reagents and treatments

U2OS, HEK293T and HeLa cells were grown on regular Dulbecco's modified Eagle's Medium (DMEM) supplemented with 10% fetal bovine serum (FBS) and 1% antimycotic/antibacaterial. DiVa (DSBs inducible via AsiSI) cells were a gift from Dr. Gaëlle Legube and were grown in same manner with the addition of 1μg/mL Puromycin (Sigma) as recommended. ATM mutated (GM05823) and normal (GM03349) human fibroblast cells were obtained from Coriell Institute and grown in regular DMEM supplemented with 15% FBS. Cells were kept in a humidified incubator at 37°C with 5% CO_2. Whenever indicated cells were treated with G9a small molecule inhibitor UNC0638 (Sigma, 1μM for 16-24 hour); ATM inhibitor KU-55933 (10 μM for 2 hours) and/or HDAC inhibitor TSA (Millipore, 0.5uM overnight). To induce DSBs on DiVa cells, cells were incubated with 300nM 4-hydroxytamoxifen for 4 hours prior to processing and analysis.

The antibodies (with concentrations) used were: rabbit anti-G9a (Bethyl Laboratories, 1:1000 for western blot), rabbit anti-G9a (Cell Signaling, 1:50 for immunofluorescence), mouse anti-pH2AX (Ser139) (Millipore®,1:4000 for western blot and 1:300 for IF), rabbit anti-pH2AX (Ser139) (Cell Signaling, 1:4000 for western blot and 1:300 for IF), mouse anti-pATM (Ser1981) (Millipore®,1:400 for IF), rabbit anti-pATM (Ser1981) (Cell Signaling, 1:4000 for western blot), mouse anti-MDC1 (Sigma, 1:300 for IF), anti-Actin (Sigma®, 1:10000 for western blot), rabbit anti-53BP1 (Bethyl Laboratories, 1:1000 for IF), anti-BRCA1 (check), anti-

RNF168 (Cell Signaling, 1:300 for IF), rabbit anti-HDAC2 (check), mouse anti-ATM (Santa Cruz, 1:4000), rabbit anti-pCHK2 (T68) (Cell Signaling, 1:4000), rabbit anti-CHK2 (Cell Signaling, 1:4000), rabbit anti pKAP1 (Bethyl Laboratories), rabbit anti-KAP1 (Bethyl Laboratories, 1:4000), mouse anti-H3K9me2 (Cell Signaling, 1:4000), rabbit anti-H3K36me2 (Active Motif, 1:4000), rabbit anti-H3K56Ac (Millipore®, 1:4000), rabbit and mouse anti-H3 (Cell Signaling).

UV(+IDU)-irradiation.

Whenever specified cells were subjected to DNA damage using a UV-crosslinker. Prior to UV-irradiation cells were incubated with 10μM IDU (5-iodo-2-hydroxyuridine) for 16-24 hours. Right before irradiation, media was completely removed, and plates were placed without lid inside UV-crosslinker. Cells were UV-irradiated with energy set to 100kJ. After irradiation, pre-warmed media was gently re-added to the cells and unless otherwise noted, cells were left to recover at 37°C for 15 min before collecting them.

Protein extraction and western blotting.

For whole cell extracts, cells were washed twice with cold PBS and collected with the addition of 1:1 2X Laemmli buffer (Sigma) and NETN (150mM NaCl, 1 mM EDTA, 120mM Tris-HCl and 0.5% N-P40) buffer. Samples were sonicated and boiled at 95°C for 10 minutes before loading. Protein extracts were resolved by SDS-PAGE (pre-cast 4-15% gradient gels, Bio-Rad) and transferred to PVDF membranes. Primary antibodies were incubated in 2.5% milk in TBST

overnight and secondary antibodies were incubated in TBST for 1 hour. Detection of antigens was performed with standard chemiluminescence (ECL Pico, Bio-Rad) and visualized using a Chemi-Doc (Bio-Rad) instrument. Secondary antibodies used were HRP conjugated goat anti-mouse or anti-rabbit (Bio-Rad).

Histone Extraction

Histone acid extractions was performed as previously (Shechter et al. 2007). Briefly, cells were grown in 10cm plates to be confluent the day of the experiment. Cells were washed twice and collected in 1X PBS supplemented with phosphatase inhibitor (Sigma). Hypotonic Buffer (Active Motif) was added to the pelleted cells and samples were incubated on ice for 15 min. Lysis of the cell was aided by adding detergent (Active Motif) and chromatin was pelleted by centrifugation. Acid extraction of the histones was performed by adding sulfuric acid to the samples and incubating overnight on a rocker at 4^{o}C. Histones were precipitated with TCA and pelleted by centrifugation at max speed in a cold centrifuge for 15 minutes. Histone pellets were washed twice with cold acetone (Sigma), air dried and resuspended in water.

Laser microirradiation.

A total of 60,000 cells per well were seeded in a 4 well chamber slide (Lab-Tek) 2 days before micro-irradiation and pre-sensitized with 5-iodo-2-hydroxyuridine (IDU) 24 hours before. Laser micro-irradiation was performed as before (Rogakou et al. 1999) using a PALM (Photo-activated Localization

Microscopy) UV-A pulsed laser (100 Hz, l 1⁄4 355 nm; P.A.L.M. Microlaser) integrated to a Zeiss Axiovert 200 microscope (Carl Zeiss AG). Targeted nuclei were selected using PALM Robo software (Zeiss) and generation of subnuclear DNA damage was achieved by focusing the laser through LD 40x to yield a spot size of ~1μm with laser output set to 50% which was the lowest power necessary to cause a detectable nuclear pH2AX stripe with minimal cellular toxicity. In average, at least 50 cells per well were irradiated within 5 minutes. Unless otherwise stated, cells were fixed with 4% paraformaldehyde (PFA) for 10 minutes after 10 minutes of recovery.

Immunofluorescence.

To analyze DNA damage response factors, cells were permeabilized with 0.5% Triton X-100 in PBS for 10 minutes after the 10 minutes fixation with 4% PFA. Cells were then incubated for 1 hour at room temperature with indicated antibodies diluted in 5% goat serum in PBS. After incubation with primary antibodies, cells were washed 4 times with PBS. Alexa Fluor Secondary 490 or 595 nm anti-mouse or rabbit (Thermofisher) diluted 1:500 in 5% goat serum in PBS were used as secondary antibodies and incubated for 1 hour at room temperature. Cells were washed 4 times with PBS and let dry for 10 min before mounted with Vectashield DAPI mounting media (Vector Laboratories). Images were taken with Nikon Eclipse 80i Microscope and fluorescence intensity was measured using ImageJ software.

Co-immunoprecipitation and Mass Spectrometry.

HeLa cells, HEK293T or HEK293 stably expressing Flag-G9a-V5 were seeded in 10 cm or 15 cm plates. Cells were not treated (control) or either UV-irradiated, UNC0638 treated or both and let to recover for 15 min at 37°C. After recovery, cells were immediately washed twice with cold PBS gently. Cells were collected and lysed with NETN (150mM NaCl, 1mM EDTA, 120mM Tris-HCl and 0.5% NP40) buffer supplemented with protease inhibitor cocktail 2 (Sigma) and protein inhibitor cocktail (Roche) for 30 min on ice with occasional vortex to aid lysis. Samples were centrifuged at 13rpm for 15 minutes and the protein-containing supernatant was collected. Protein concentration was measured using the Bradford colorimetric method from Bio-Rad. A total of 1-1.5 μg of protein lysate (4μg for MS analysis) was subjected to immunoprecipitation using antibodies against indicated proteins as follows. Briefly, samples were first precleared using Agarose A beads for at least 1 hour at 4°C in a rocker. Beads were discarded and precleared samples were incubated with agarose A beads and the indicated antibodies overnight for protein binding. For endogenous G9a immunoprecipitation 4μg of rabbit anti-G9a antibody (Bethyl Laboratories) were used; for methylated-lysine immunoprecipitation, 3μg of rabbit anti-methylated lysine (Abcam); for acetylated lysine immunoprecipitation, 4μg of mouse anti-acetylated lysine (Millipore®). Beads were pelleted and washed 3 times with ice-cold NETN buffer with protease and protein inhibitor cocktails. Proteins were eluted by boiling the beads at 95°C with Laemmli buffer and loaded into SDS-PAGE gels. Aliquots of original protein lysates were used as input controls and resolved directly by SDS-

PAGE. Resolved proteins were transferred to PVDF membranes and incubated with the indicated antibodies. For MS analysis, after the samples entered the gel, the sample-containing area of the gel was cut and sent to Biological Mass Spectrometry Facility at Rutgers University (Piscataway, New Jersey) where samples were analyzed by LC/MS-MS.

siRNA treatment.

Gene knockdown was achieved by transfecting Sigma esiRNA using Lipofectamine RNAiMax ® following the manufacturer's protocol. Briefly, cells were seeded to be 60-70% confluent on the day of transfection and 20pmol of esiRNA were transfected. Cells were incubated for 72 hours to allow for optimal knockdown prior to processing and analysis. Wester blotting with indicated antibodies was performed to analyze knockdown efficiency.

Chapter III: Regulation of DNA damage-associated marks by G9a; an ongoing work

Introduction

G9a methyltransferase has been well studied in the setting of gene transcription and how it is associated with cancer progression. More recent studies have found a link between G9a inhibition and sensitivity of tumor cells to DNA damaging agents. However, the underlying mechanism still not well understood. We have already presented evidence showing that G9a has a direct role in the DNA repair pathway. Moreover, we demonstrated that inhibition of G9a results in impairment of both HR and NHEJ mediated DNA repair. This new data uncovers a novel role for G9a in the DNA repair process and opens up the path for more questions about what its functional role is in response to DNA damage.

Given the little information about the effects of G9a on different DNA damage repair factors, as well as histone marks associated with this process, we decided to look at some of these factors upon G9a inhibition. Here we provide more evidence that helps to broaden our understanding about the role of G9a in response to DNA damage. We show that G9a inhibition results in increased H3K36me2, a known mark for DNA damage that was recently linked to ATM activation. We also provide data that shows that inhibition of G9a disrupts the normal dynamics of Poly(ADP)-ribosylation (PAR) at sites of DNA breaks, resulting in the retention of PAR signal for up to 30 minutes after laser scissors-induced breaks. Furthermore, we present surprising that shows that Mre11 inhibition results in unexpected increased phosphorylation levels of ATM at early time points after the induction of DNA breaks.

Results

G9a inhibition leads to increased methylation of H3K36

Modification on histones marks have been shown to play an important role during the DNA damage response. We wanted to understand how the local histone code at the surrounding chromatin of DNA breaks is affected by inhibition of G9a activity. Laser microirradiation was performed in U2OS cells followed by immunofluorescence using antibodies against several histones marks. Intriguingly, we observed that di-methylation levels of H3K36 were increased following inhibition of G9a in response of DNA damage compared to DNA damage alone. We also looked at global levels of H3K36me2 using similar conditions in UV(+IDU)-irradiated cells (pre-sensitized with IDU 24 hour prior to UV exposure). Global levels of H3K36me2 were increased after DNA damage in control cells. In cells treated with UNC063, levels of H3K36me2 were increased both untreated and post-DNA damage conditions, compared to cells not exposed to UNC0638.

H3K36me2 has been reported to be a mark for DNA damage and is detectable within 15 minutes after IR (Fnu et al. 2011). Furthermore, there is

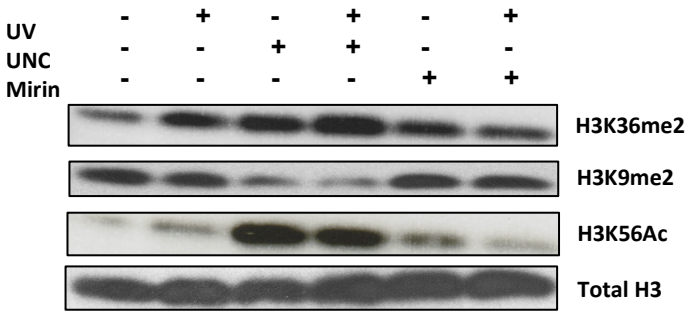

Figure 1. Mre11 inhibitor, Mirin, does not results in same chromatin changes as G9a inhibitor. U2OS cells were treated with either UNC0638 (1uM, overnight), Mirin (100uM, 1 hr) and irradiated with UV(+IDU). After 15 minutes recovery cells were processed for an acid histone extraction and histone marks were evaluated by western blot with indicated antibodies.

evidence that suggests that activation of ATM is required for induction of di-methylation of H3K36 in response to DNA damage (Cao et al. 2016). This is consistent with our data that shows G9a inhibition leads to both increased activation of ATM and increased H3K36 methylation.

Inhibition of Mre11 resembles effects of G9a inhibition on pATM, pH2AX and MDC1

It has been found that dimethylation of H3K36 promotes recruitment of MRN complex by directly associating with NBS1 (Cao et al. 2016). We investigated how inhibition of MRN by the small molecule mirin (Dupré et al. 2008) functionally interacts with G9a pathway in DNA repair. U2OS cells were treated with Mirin and then subjected to laser microirradiation followed by IF using antibodies for pATM,

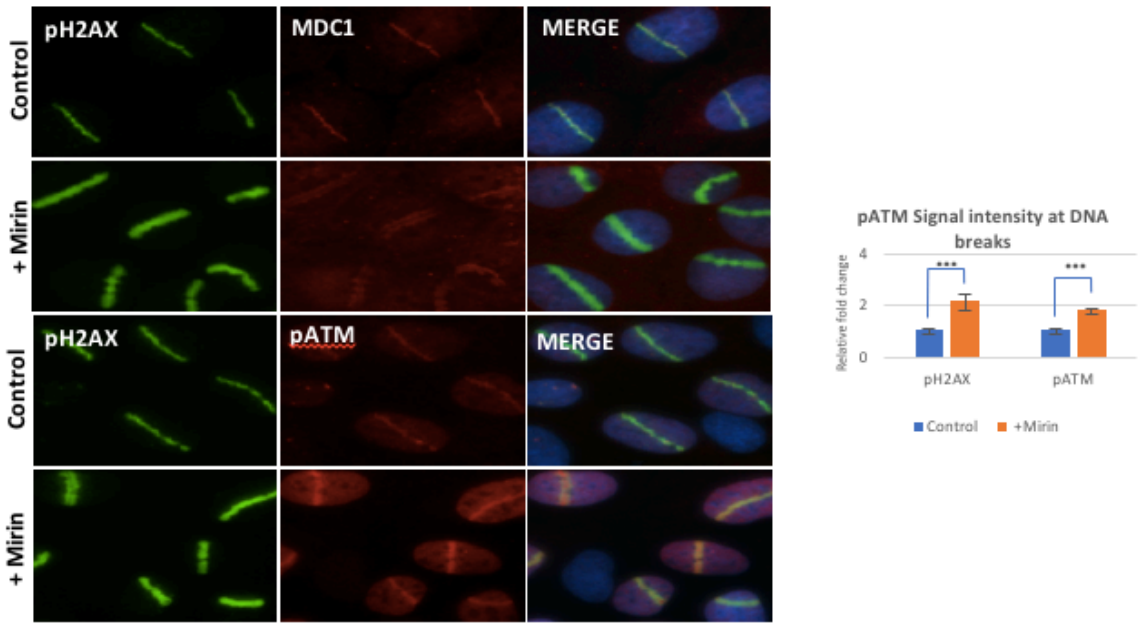

Figure 2. Inhibition of Mre11 exonuclease activity leads to increased pH2AX and pATM signal. U2OS cells were treated with Mirin (100uM, 1hr) followed by laser microirradiation and IF staining using the indicated antibodies. Quantification of pATM signal intensity is shown and expressed as the mean ± SD of two independent experiments. ***P≤ 0.01

pH2AX and MDC1. To our surprise we observed that the spreading of pH2AX was extended. Similarly, we observed that pATM signal was increased and MDC1 followed the same spreading pattern as that of pH2AX. These results resembled those of G9a inhibition at these early time points, suggesting that G9a activity may be required for MRN activation at DNA breaks.

To discard the possibility that Mirin was acting as an inhibitor of G9a we H3K36me2 and H3K56Ac, as we already found that these marks are induced by the catalytic inhibition of G9a. We observed that unlike G9a inhibition, Mre11 inhibition does not lead to decreased levels of H3K9me2 and does not induce H3K56Ac. Thus, although MRN inhibition with Mirin leads to similar effects on H2AX phosphorylation and ATM activation as UNC0638, Mirin does not affect the histone marks normally regulated by G9a. This finding suggests that G9a activity may be required for normal activation of the MRN complex, and that G9a inhibition may lead indirectly to inhibition of Mre11 activity.

G9a inhibition leads to retention of PAR signal at DSBs

During the course of this study, besides histone methylation, we evaluated other marks that are known to be important for efficient repair of DNA breaks. Surprisingly, we observed that catalytic inhibition of G9a resulted in retention of PAR (Poly-ADP-Ribose) signal at sites of laser scissors-induced DNA breaks. We performed a time course for up to an hour and evaluated PAR signal by immunofluorescence. In untreated cells PAR signal appeared rapidly within 5 minutes and was diminished by 15 minutes of the induced breaks. In contrast, in

cells treated with UNC0638, PAR signal was detectable for up to 30 minutes after DNA damage. This shows that PAR signal is sustained and enhanced in the setting of G9a inhibition.

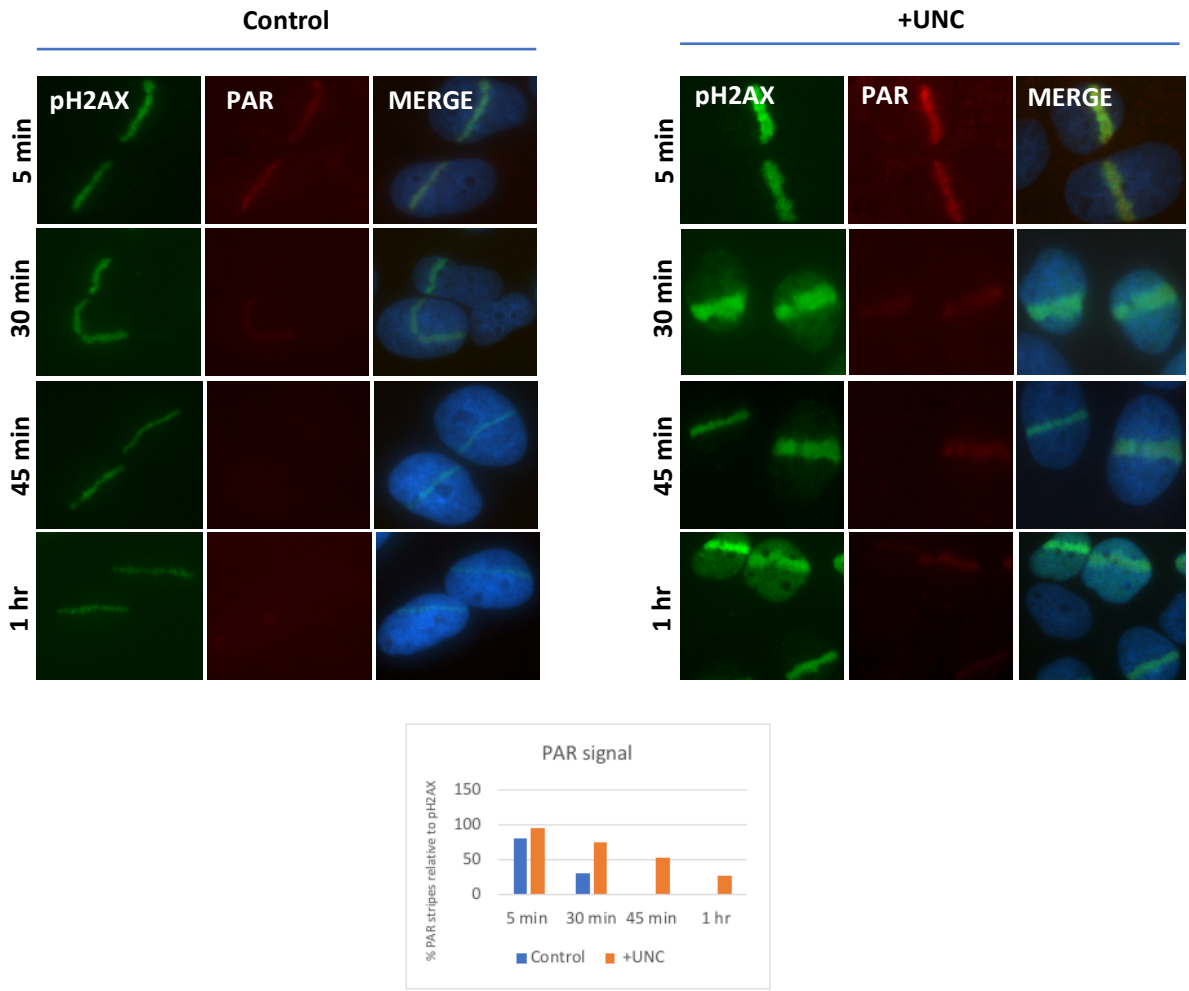

Figure 3. G9a inhibition resulted in retention of PAR signal. U2OS cells were treated with the UNC0638 (1uM, overnight) and were subjected to laser micro-irradiation followed by immunofluorescence using indicated antibodies.

Discussion

To get a deeper understanding on the role of G9a in the DNA repair pathway we decided to look at different signaling factors associated with this process. Given that G9a is a histone modifier, we looked a diverse histone methylation marks in the setting of DNA damage and evaluated whether the inhibition of G9a activity had any effect on them.

The histone mark H3K36me2 has been already linked to DNA damage. It is catalyzed by SETMAR (also known as Metnase) (Lee et al. 2005) and has been reported to be de-methylated by KDM8 and KDM2A (Amendola et al. 2017; Tsukada et al. 2005). It has been reported that H3K36me2 is important for the recruitment of Ku protein and thus, promotes NHEJ (Fnu et al. 2011). We observed an increase in the normal accumulation of H3K36me2 at sites of DNA breaks following catalytic inhibition of G9a. This shows that G9a catalytic activity is important to maintain the proper chromatin code in response to DNA damage. Interestingly, it has been reported that activation of ATM promoted methylation of H3K36 through phosphorylation of KDM2A. This phosphorylation impairs KDM2A recruitment to chromatin and thus led to enhanced levels H3K36me2. In turn this increased in H3K36me2 promoted recruitment of MRN complex by directly recruiting NBS1, a component of MRN complex (Cao et al. 2016). It is known that recruitment of MRN complex plays an important role in the activation of ATM after sensing of the DNA damage. We already showed an increase in ATM activation in response to DNA damage following inhibition of G9a. This data is consistent with

the previous report and suggests that the effects of G9a inhibition on levels of H3K36me2 is through hyperactivation of ATM. It is possible that there is a positive feedback loop regulation, in which upregulation of ATM leads to increased H3K36me2 and this in turn helps further activation of ATM through recruitment of MRN complex. Further investigation is needed to determine if G9a has a direct effect on H3K36 specific methyltransferase or demethylases.

Although there is evidence that shows the importance of H3K36me2 in the setting of DNA damage, there is a more recent study suggesting that its demethylation is equally important. Depletion of KDM8 or its catalytic inhibition resulted in increased levels of H3K36me2 and also in HR defects due to aberrant retention of RAD-51 at sites of DNA breaks, suggesting that demethylation of H3K36me2 is required for efficient DNA damage repair (Amendola et al. 2017). This could explain some of our observations regarding the inability of the cells to recruit DDR factors downstream of MDC1 (Chapter I and II) while still having upregulated activity of ATM in early stages of the repair.

An intriguing observation was that Mre11 inhibition using Mirin led to increased levels of pATM and pH2AX, as well as abnormal spreading of pH2AX and MDC1 in response to DNA damage; this resembled the same effects of UNC0638. It is possible that the similarity in these phenotypes is due to similar effects of G9a inhibitor and Mre11 in early stages of the repair. One possibility is that inhibition of Mre11 prevents resection from happening, and this causes an accumulation of pATM at sites of DNA breaks, but the signal cannot be transduced into further repair. Another possibility is G9a activity is required for Mre11/MRN

activity and thus, inhibiting either of them results in similar phenotypes. Importantly, Mirin did not affect H3K9me2, which is associated to G9a activity. This proves that Mirin does not affects G9a activity. Additionally, Mirin did not affect H3K56Ac or H3K36me2. It is important to note that while Mirin has been proposed to inhibit the MRN-dependent activation of ATM, these studies only looked at activation of ATM in much later time points, which could explain these discrepancies.

Preliminary data shows that G9a inhibition does not affect Mre11 localization to DNA damage sites. However, it is not known if its activity is affected. A recent study reported that G9a interacts with RPA and promotes HR (Yang et al. 2017). It could be possible that G9a has a role in the steps following resection, which would further support the idea that Mre11 and G9a have a role in the same pathway. It is still not known if, in our conditions, Mirin has an effect similar to UNC0638 in downstream DDR factors. Further investigation is needed in order to understand how the two are functionally related.

We have also shown that G9a catalytic inhibition resulted in retention of poly(ADP)-ribosylation (PAR) signal at sites of DNA breaks. Parylation is catalyzed mainly by PARP1 in response to DNA damage and mediate recruitment of DDR factors to sites of DNA breaks (reviewed on Wei & Yu 2016). We found that retention of PAR signal is prolonged upon G9a inhibition. It has been reported that FHA and BRCT protein domains recognize and interact with PAR chains which led to their recruitment to damaged DNA in early steps of the process. However, despite prolonged PARP activation, in the setting of G9 inhibition we see inhibition of the early phase of recruitment of DNA repair factors including 53BP1 and

BRCA1. This finding suggests that PAR signal alone is not sufficient to promote recruitment but requires concomitant activation of G9a. In addition, increased parylation can also induce further activation of ATM.

Further investigation is needed to understand how dysregulation of this marks via G9a inhibition affect DNA repair pathway and how we can take advantage of the new findings to design better targeted therapies in the clinic.

Methods

Cell Culture, reagents and treatments

U2OS cells were obtained from ATCC and grown on regular Dulbecco's modified Eagle's Medium (DMEM) supplemented with 10% fetal bovine serum (FBS) and 1% antimycotic/antibacaterial. Cells were kept in a humidified incubator at 37^{o}C with 5% CO_2. Whenever indicated cells were treated with G9a small molecule inhibitor UNC0638 (Sigma, 1μM for 16-24 hour) or Mre11 specific inhibitor Mirin (Sigma-Aldrish, 100μM for 1hr). The antibodies (with concentrations) used were: rabbit anti-G9a (Cell Signaling, 1:50 for immunofluorescence), mouse anti-pH2AX (Ser139) (Millipore®, 1:300), rabbit anti-pH2AX (Ser139) (Cell Signaling, 1:300), mouse anti-pATM (Ser1981) (Millipore®,1:400), mouse anti-MDC1 (Sigma, 1:300), mouse anti-H3K9me2 (Cell Signaling, 1:4000), rabbit anti-H3K36me2 (Active Motif, 1:4000), rabbit anti-H3K56Ac (Millipore®, 1:4000), rabbit and mouse anti-H3 (Cell Signaling).

Histone Extraction and western blot

Histone acid extractions was performed as previously (Shechter et al. 2007). Briefly, cells were grown in 10cm plates to be confluent the day of the experiment. Cells were washed twice and collected in 1X PBS supplemented with phosphatase inhibitor (Sigma). Hypotonic Buffer (Active Motif) was added to the pelleted cells and samples were incubated on ice for 15 min. Lysis of the cell was aided by adding detergent (Active Motif) and chromatin was pelleted by centrifugation. Acid extraction of the histones was performed by adding sulfuric

acid to the samples and incubating overnight on a rocker at 4°C. Histones were precipitated with TSA and pelleted by centrifugation at max speed in a cold centrifuge for 15 minutes. Histone pellets were washed twice with cold acetone (Sigma), air dried and resuspended in water. Protein extracts were resolved by SDS-PAGE (pre-cast 4-15% gradient gels, Bio-Rad) and transferred to PVDF membranes. Primary antibodies were incubated in 2.5% milk in TBST overnight and secondary antibodies were incubated in TBST for 1 hour. Detection of antigens was performed with standard chemiluminescence (ECL Pico, Bio-Rad) and visualized using a Chemi-Doc (Bio-Rad) instrument. Secondary antibodies used were HRP conjugated goat anti-mouse or anti-rabbit (Bio-Rad)

Laser microirradiation.

A total of 60,000 cells per well were seeded in a 4 well chamber slide (Lab-Tek, Nalge ® Nunc™ International) 2 days before microirradiation and pre-sensitized with 5-iodo-2-hydroxyuridine (IDU) 24 hours before. Laser microirradiation was performed as before (Rogakou et al. 1999) using a PALM (Photo-activated Localization Microscopy) UV-A pulsed laser (100 Hz, I 1⁄4 355 nm; P.A.L.M. Microlaser) integrated to a Zeiss Axiovert 200 microscope (Carl Zeiss AG). Targeted nuclei were selected using PALM Robo software (Zeiss) and generation of subnuclear DNA damage was achieved by focusing the laser through LD 40x to yield a spot size of ~1μm with laser output set to 50% which was the lowest power necessary to cause a detectable nuclear pH2AX stripe with minimal cellular toxicity. In average, at least 50 cells per well were irradiated within 5

minutes. Unless otherwise stated, cells were fixed with 4% paraformaldehyde (PFA) for 10 minutes after 10 minutes of recovery.

Immunofluorescence.

To analyze DNA damage response factors, cells were permeabilized with 0.5% Triton X-100 in PBS for 10 minutes after the 10 minutes fixation with 4% PFA. Cells were then incubated for 1 hour at room temperature with indicated antibodies diluted in 5% goat serum in PBS. After incubation with primary antibodies, cells were washed 4 times with PBS. Alexxa's 490 or 595 nm anti-mouse or rabbit (Thermofisher) diluted 1:500 in 5% goat serum in PBS were used as secondary antibodies and incubated for 1 hour at room temperature. Cells were washed 4 times with PBS and let dry for 10 min before mounted with Vectashield DAPI mounting media (Vector Laboratories). Images were taken with Nikon Eclipse 80i Microscope and fluorescence intensity was measured using ImageJ software.

General Conclusion

Here we have provided evidence that G9a plays a direct role in the DNA damage repair pathway in part by regulating normal levels of ATM activity, by controlling normal signal amplification, and by promoting the recruitment of DDR factors. We have demonstrated that catalytic inhibition of G9a resulted in a hyperactive ATM status, as seen by its increased phosphorylation and acetylation levels in response to DNA damage, which led to increased phosphorylation of the ATM substrates, H2AX, CHK2, and KAP1. Furthermore, we have demonstrated that G9a inhibition abrogated early recruitment of DDR factors to sites of DNA breaks, possibly as a result of the dysregulated ATM activity. In addition, we have shown that G9a activity regulates chromatin changes by maintaining appropriate levels of H3K36me2, H3K9me2 and H3K56ac. In particular, G9a may normally promote HDAC1/2 deacetylase activity by methylating it in response to DNA damage.

Taken together this data suggests that G9a regulates the DNA damage repair signal at different levels: through its direct association (and possibly regulation) with DDR factors, and by influencing chromatin landscape in response to DNA damage. G9a is recruited to sites of DNA breaks where it regulates ATM activity in part by limiting its phosphorylation and acetylation levels. The hyperactive status of ATM in the setting of G9a inhibition could explain the senescent phenotype, as well as cell death through apoptosis and activation of autophagy that others have reported as occurring in response to G9 inhibition. This

dysregulation of ATM activity can lead to impairment of recruitment of downstream factors despite hyperactivation of ATM. This impact in the recruitment of downstream factors, may explain why G9a inhibition sensitize tumor cells to exposure to DNA damaging agents. Alternatively, ATM activation may be a response of the cells to overcome G9a inhibition and the therapeutic effects of G9a inhibitors could be more related to defective recruitment of DDR factors. Also, sustained pH2AX leads to prolonged DSBs repair and chromatin instability (Li et al. 2015), which could be another way G9a inhibition may affect normal DNA repair processes.

In addition to this, we also found that at the chromatin level, G9a affects H3K9me2, H3K36me2 and H3K56Ac. These histone marks may influence the DNA repair pathway in different ways. There is evidence that suggests that inhibition of H3K9me2 results in decreased HP1 recruitment which reduces BRCA1 and BARD1 in sites of DNA breaks (Wu et al. 2015). In part, this could explain why, even with an upregulated ATM activity, recruitment of downstream factors is abrogated upon inhibition of G9a. Also, H3K56Ac, which is increased in the setting of G9a inhibition, has been associated with relaxed and open chromatin which has been suggested as being enough to induce ATM activation (Kaidi & Jackson 2013). Also, increased H3K56Ac levels suggest that HDAC1/2 deacetylase activity is decreased. Taking into consideration that HDAC1 is a substrate of both G9a and ATM, it is possible that this represents another way in which G9a promotes appropriate levels of ATM acetylation and thus, activation. In addition, H3K36me2 has been associated with DNA repair and to promote

recruitment of MRN complex. This is also consistent with our observations of increased activation of ATM. Even more, sustained levels of H3K36me2 has been reported to result in repair deficiency due to aberrant retention of RAD51.

Interestingly, we found that inhibition of Mre11 exonuclease activity using Mirin had effects similar to UNC0638 treatment. This suggests that one way in which G9a promotes recruitment of downstream factors is by regulating MRN complex activity. Further investigation is needed to establish a functional relationship between the two.

This new evidence helps to understand the role of G9a during DNA damage response. Furthermore, it provides new insights on how G9a can be, potentially, more efficiently used in the clinical setting. Particularly, having a deeper understanding of how G9a affects the DNA repair signal is useful to determine what types of cancer can be treated more efficiently with G9a inhibitors. For instance, our data suggests that tumors with pre-existent repair defects in the late phase of the response may be especially vulnerable to G9a inhibition. Given that it has been demonstrated the utility of G9a inhibition in treating tumors and knowing that it is directly involved in the DDR response, it would be beneficial the use of techniques like CRISPR to screen for functional synthetic lethality. The aim is to identify if impairment of specific DNA repair factors may lead to heightened sensitivity to G9a inhibition. This understanding will help to develop a more precise and effective strategy to treat cancer with G9a inhibitors in combinations with other therapies.

Bibliography

Abbotts, R. & Wilson, D.M., 2017. Coordination of DNA single strand break repair. *Free Radical Biology and Medicine*, 107, pp.228–244. Available at: http://www.sciencedirect.com/science/article/pii/S0891584916310735.

Agarwal, P. & Jackson, S.P., 2016. G9a inhibition potentiates the anti-tumour activity of DNA double-strand break inducing agents by impairing DNA repair independent of p53 status. *Cancer Letters*, 380(2), pp.467–475.

Alexander, A., Kim, J. & Walker, C.L., 2010. ATM engages the TSC2/mTORC1 signaling node to regulate autophagy. *Autophagy*, 6(5), pp.672–673.

Amendola, P.G. et al., 2017. JMJD-5/KDM8 regulates H3K36me2 and is required for late steps of homologous recombination and genome integrity. *PLoS Genetics*, 13(2), pp.1–24.

Antignano, F. et al., 2014. Methyltransferase G9A regulates T cell differentiation during murine intestinal inflammation. *The Journal of Clinical Investigation*, 124(5), pp.1945–1955. Available at: http://www.ncbi.nlm.nih.gov/pmc/articles/PMC4001530/.

Ayoub, N. et al., 2009. The Carboxyl Terminus of Brca2 Links the Disassembly of Rad51 Complexes to Mitotic Entry. *Current Biology*, 19(13), pp.1075–1085. Available at: http://www.ncbi.nlm.nih.gov/pmc/articles/PMC2719694/.

Ayrapetov, M.K. et al., 2014. DNA double-strand breaks promote methylation of histone H3 on lysine 9 and transient formation of repressive chromatin. *Proceedings of the National Academy of Sciences of the United States of America*, 111(25), pp.9169–9174. Available at: http://www.ncbi.nlm.nih.gov/pmc/articles/PMC4078803/.

Bakkenist, C.J. & Kastan, M.B., 2003. DNA damage activates ATM through intermolecular autophosphorylation and dimer dissociation.

Bennardo, N. et al., 2008. Alternative-NHEJ is a mechanistically distinct pathway of mammalian chromosome break repair. *PLoS genetics*, 4(6), p.e1000110.

Bennett, S.M. et al., 2012. Multiple protein-protein interactions within the DNA-PK complex are mediated by the C-terminus of Ku 80. *International Journal of Biochemistry and Molecular Biology*, 3(1), pp.36–45. Available at: http://www.ncbi.nlm.nih.gov/pmc/articles/PMC3325771/.

Bittencourt, D. et al., 2012. G9a functions as a molecular scaffold for assembly of transcriptional coactivators on a subset of Glucocorticoid Receptor target genes. *Proceedings of the National Academy of Sciences of the United States of America*, 109(48), pp.19673–19678. Available at: http://www.ncbi.nlm.nih.gov/pmc/articles/PMC3511704/.

Brown, S.E., Campbell, R.D. & Sanderson, C.M., 2001. Novel NG36/G9a gene products encoded within the human and mouse MHC class III regions. *Mammalian Genome*, 12(12), pp.916–924.

Bunting, S.F. et al., 2010. 53BP1 inhibits homologous recombination in Brca1-deficient cells by blocking resection of DNA breaks. *Cell*, 141(2), pp.243–254. Available at: http://www.ncbi.nlm.nih.gov/pmc/articles/PMC2857570/.

Burma, S. et al., 2001. ATM Phosphorylates Histone H2AX in Response to DNA Double-strand Breaks. *Journal of Biological Chemistry* , 276(45), pp.42462–

42467. Available at: http://www.jbc.org/content/276/45/42462.abstract.
Cao, L.L. et al., 2016. ATM-mediated KDM2A phosphorylation is required for the DNA damage repair. *Oncogene*, 35(3), pp.301–313.
Caron, P. et al., 2012. Cohesin protects genes against γH2AX induced by DNA double-strand breaks. *PLoS Genetics*, 8(1).
Carter, R.J. & Parsons, J.L., 2016. Base Excision Repair, a Pathway Regulated by Posttranslational Modifications. *Molecular and Cellular Biology* , 36(10), pp.1426–1437. Available at: http://mcb.asm.org/content/36/10/1426.abstract.
Casciello, F. et al., 2015. Functional role of G9a histone methyltransferase in cancer. , 6(September), pp.3–9.
Ceccaldi, R. et al., 2015. Homologous recombination-deficient tumors are hyper-dependent on POLQ-mediated repair. *Nature*, 518(7538), pp.258–262. Available at: http://www.ncbi.nlm.nih.gov/pmc/articles/PMC4415602/.
Cedar H, B.Y., 2009. Epigenetic silencing during early lineage commitment. *StemBook, ed. The Stem Cell Research Community*.
Celeste, A. et al., 2003. Histone H2AX phosphorylation is dispensable for the initial recognition of DNA breaks. *Nature Cell Biology*, 5(7), pp.675–679.
Chapman, J.R. et al., 2013. RIF1 Is Essential for 53BP1-Dependent Nonhomologous End Joining and Suppression of DNA Double-Strand Break Resection. *Molecular Cell*, 49(5), pp.858–871. Available at: http://www.ncbi.nlm.nih.gov/pmc/articles/PMC3594748/.
Chapman, J.R. & Jackson, S.P., 2008. Phospho-dependent interactions between NBS1 and MDC1 mediate chromatin retention of the MRN complex at sites of DNA damage. *EMBO Reports*, 9(8), pp.795–801.
Chaturvedi, C.-P. et al., 2012. Maintenance of gene silencing by the coordinate action of the H3K9 methyltransferase G9a/KMT1C and the H3K4 demethylase Jarid1a/KDM5A. *Proceedings of the National Academy of Sciences*, 109(46), p.18845 LP-18850. Available at: http://www.pnas.org/content/109/46/18845.abstract.
Chen, H., Lisby, M. & Symington, L.S., 2013. RPA coordinates DNA end resection and prevents formation of DNA hairpins. *Molecular cell*, 50(4), p.10.1016/j.molcel.2013.04.032. Available at: http://www.ncbi.nlm.nih.gov/pmc/articles/PMC3855855/.
Chen, M.W. et al., 2010a. H3K9 histone methyltransferase G9a promotes lung cancer invasion and metastasis by silencing the cell adhesion molecule Ep-CAM. *Cancer Research*, 70(20), pp.7830–7840.
Chen, M.W. et al., 2010b. H3K9 histone methyltransferase G9a promotes lung cancer invasion and metastasis by silencing the cell adhesion molecule Ep-CAM. *Cancer Research*, 70(20), pp.7830–7840.
Chen, X. et al., 2012. G9a/GLP-dependent histone H3K9me2 patterning during human hematopoietic stem cell lineage commitment. *Genes & Development*, 26(22), pp.2499–2511. Available at: http://www.ncbi.nlm.nih.gov/pmc/articles/PMC3505820/.
Chin, H.G. et al., 2007. Automethylation of G9a and its implication in wider substrate specificity and HP1 binding. *Nucleic Acids Research*, 35(21), pp.7313–7323.

Chin, H.G. et al., 2005. Sequence Specificity and Role of Proximal Amino Acids of the Histone H3 Tail on Catalysis of Murine G9a Lysine 9 Histone H3 Methyltransferase. *Biochemistry*, 44(39), pp.12998–13006. Available at: https://doi.org/10.1021/bi0509907.

Cho, H.-S. et al., 2011. Enhanced Expression of EHMT2 Is Involved in the Proliferation of Cancer Cells through Negative Regulation of SIAH1. *Neoplasia (New York, N.Y.)*, 13(8), pp.676–684. Available at: http://www.ncbi.nlm.nih.gov/pmc/articles/PMC3156658/.

Chowdhury, D. et al., 2005. γ-H2AX dephosphorylation by protein phosphatase 2A facilitates DNA double-strand break repair. *Molecular Cell*, 20(5), pp.801–809.

Collins, R.E. et al., 2008. The ankyrin repeats of G9a and GLP histone methyltransferases are mono- and dimethyllysine binding modules. *Nature structural & molecular biology*, 15(3), pp.245–250. Available at: http://www.ncbi.nlm.nih.gov/pmc/articles/PMC2586904/.

Deng, S.K. et al., 2014. RPA Antagonizes Microhomology-Mediated Repair of DNA Double-Strand Breaks. *Nature structural & molecular biology*, 21(4), pp.405–412. Available at: http://www.ncbi.nlm.nih.gov/pmc/articles/PMC3980576/.

Ding, J. et al., 2013. The Histone H3 Methyltransferase G9A Epigenetically Activates the Serine-Glycine Synthesis Pathway to Sustain Cancer Cell Survival and Proliferation. *Cell Metabolism*, 18(6), pp.896–907. Available at: http://dx.doi.org/10.1016/j.cmet.2013.11.004.

Dobbin, M.M. et al., 2013. SIRT1 collaborates with ATM and HDAC1 to maintain genomic stability in neurons. *Nature Neuroscience*, 16(8), pp.1008–1015.

Dong, C. et al., 2012. G9a interacts with Snail and is critical for Snail-mediated E-cadherin repression in human breast cancer. *The Journal of Clinical Investigation*, 122(4).

Dunham, I. et al., 1990. Characterization of the class III region in different MHC haplotypes by pulsed-field gel electrophoresis. *Immunogenetics*, 32(3), pp.175–182. Available at: https://doi.org/10.1007/BF02114970.

Dupré, A. et al., 2008. A forward chemical genetic screen reveals an inhibitor of the Mre11–Rad50–Nbs1 complex. *Nature chemical biology*, 4(2), pp.119–125. Available at: http://www.ncbi.nlm.nih.gov/pmc/articles/PMC3065498/.

Esashi, F. et al., 2007. Stabilization of RAD51 nucleoprotein filaments by the C-terminal region of BRCA2. *Nature Structural &Amp; Molecular Biology*, 14, p.468. Available at: http://dx.doi.org/10.1038/nsmb1245.

Escribano-Díaz, C. et al., 2013. A Cell Cycle-Dependent Regulatory Circuit Composed of 53BP1-RIF1 and BRCA1-CtIP Controls DNA Repair Pathway Choice. *Molecular Cell*, 49(5), pp.872–883.

Falck, J., Coates, J. & Jackson, S.P., 2005. Conserved modes of recruitment of ATM, ATR and DNA-PKcs to sites of DNA damage. *Nature*, 434(7033), pp.605–611. Available at: http://10.0.4.14/nature03442.

Feitelson, M.A. et al., 2015. Sustained proliferation in cancer: Mechanisms and novel therapeutic targets. *Seminars in Cancer Biology*, 35, pp.S25–S54. Available at:

http://www.sciencedirect.com/science/article/pii/S1044579X15000140.
Feldman, N. et al., 2006. G9a-mediated irreversible epigenetic inactivation of Oct-3/4 during early embryogenesis. *Nature Cell Biology*, 8, p.188. Available at: http://dx.doi.org/10.1038/ncb1353.
Fiszbein, A. et al., 2016. Alternative Splicing of G9a Regulates Neuronal Differentiation. *Cell Reports*, 14(12), pp.2797–2808. Available at: http://www.sciencedirect.com/science/article/pii/S221112471630184X.
Fnu, S. et al., 2011. Methylation of histone H3 lysine 36 enhances DNA repair by nonhomologous end-joining. *Proceedings of the National Academy of Sciences*, 108(2), pp.540–545. Available at: http://www.pnas.org/cgi/doi/10.1073/pnas.1013571108.
Ginjala, V. et al., 2017. Protein-lysine methyltransferases G9a and GLP1 promote responses to DNA damage. , pp.1–12.
Goldstein, M. & Kastan, M.B., 2015. Repair versus checkpoint functions of Brca1 are differentially regulated by site of chromatin binding. *Cancer research*, 75(13), pp.2699–2707. Available at: http://www.ncbi.nlm.nih.gov/pmc/articles/PMC4548823/.
Gupta, A. et al., 2005. Involvement of Human MOF in ATM Function. *Molecular and Cellular Biology* , 25(12), pp.5292–5305. Available at: http://mcb.asm.org/content/25/12/5292.abstract.
Hajdu, I. et al., 2011. Wolf–Hirschhorn syndrome candidate 1 is involved in the cellular response to DNA damage. *Proceedings of the National Academy of Sciences*, 108(32), p.13130 LP-13134. Available at: http://www.pnas.org/content/108/32/13130.abstract.
Harding, S.M., Coackley, C. & Bristow, R.G., 2011. ATM-dependent phosphorylation of 53BP1 in response to genomic stress in oxic and hypoxic cells. *Radiotherapy and Oncology*, 99(3), pp.307–312.
Hua, K.-T. et al., 2014. The H3K9 methyltransferase G9a is a marker of aggressive ovarian cancer that promotes peritoneal metastasis. *Molecular Cancer*, 13(1), p.189. Available at: http://www.molecular-cancer.com/content/13/1/189.
Huang, J. et al., 2010. G9a and Glp methylate lysine 373 in the tumor suppressor p53. *Journal of Biological Chemistry*, 285(13), pp.9636–9641.
Huang, J. & Berger, S.L., 2008. The emerging field of dynamic lysine methylation of non-histone proteins. *Current Opinion in Genetics and Development*, 18(2), pp.152–158.
Huang, T. et al., 2017. G9A promotes tumor cell growth and invasion by silencing CASP1 in non-small-cell lung cancer cells. *Cell Death &Amp; Disease*, 8, p.e2726. Available at: http://dx.doi.org/10.1038/cddis.2017.65.
Huen, M.S.Y. et al., 2007. The E3 ubiquitin ligase RNF8 transduces the DNA damage signal via an ubiquitin-dependent signaling pathway. *Cell*, 131(5), pp.901–914. Available at: http://www.ncbi.nlm.nih.gov/pmc/articles/PMC2149842/.
Huertas, P. & Jackson, S.P., 2009. Human CtIP Mediates Cell Cycle Control of DNA End Resection and Double Strand Break Repair. *The Journal of Biological Chemistry*, 284(14), pp.9558–9565. Available at:

http://www.ncbi.nlm.nih.gov/pmc/articles/PMC2666608/.
Iacovoni, J.S. et al., 2010. High-resolution profiling of γh2AX around DNA double strand breaks in the mammalian genome. *EMBO Journal*, 29(8), pp.1446–1457.
Jang, E.R. et al., 2010. ATM modulates transcription in response to histone deacetylase inhibition as part of its DNA damage response. *Experimental and Molecular Medicine*, 42(3), pp.195–204.
Kaidi, A. & Jackson, S.P., 2013. Tyrosine phosphorylation of KAT5 (Tip60) couples chromatin sensing to ATM-dependent checkpoint signaling. , 498(7452), pp.1–19.
Karanam, K. et al., 2012. Quantitative live cell imaging reveals a gradual shift between DNA repair mechanisms and a maximal use of HR in mid-S phase. *Molecular cell*, 47(2), pp.320–329. Available at: http://www.ncbi.nlm.nih.gov/pmc/articles/PMC3494418/.
Ke, X.X. et al., 2014a. Inhibition of H3K9 methyltransferase G9A repressed cell proliferation and induced autophagy in neuroblastoma. *PLoS ONE*, 9(9).
Ke, X.X. et al., 2014b. Inhibition of H3K9 methyltransferase G9A repressed cell proliferation and induced autophagy in neuroblastoma. *PLoS ONE*, 9(9).
Kim, G.D. et al., 1999. Sensing of Ionizing Radiation-induced DNA Damage by ATM through Interaction with Sensing of Ionizing Radiation-induced DNA Damage by ATM through Interaction with Histone Deacetylase *. , (5), pp.31127–31130.
Kim, H.-S. et al., 2015. The SET Domain Is Essential for Metnase Functions in Replication Restart and the 5' End of SS-Overhang Cleavage. *PLOS ONE*, 10(10), p.e0139418. Available at: https://doi.org/10.1371/journal.pone.0139418.
Kim, H., Chen, J. & Yu, X., 2007. Ubiquitin-Binding Protein RAP80 Mediates BRCA1-Dependent DNA Damage Response. *Science*, 316(5828), p.1202 LP-1205. Available at: http://science.sciencemag.org/content/316/5828/1202.abstract.
Kim, H. & Park, Y.J., 2017. G9a, an Epigenetic Modifier, Affects Cell Viability and Serine-Glycine Synthesis Pathway by Altering ATF4 Expression. *The FASEB Journal*, 31(1_supplement), p.lb331-lb331. Available at: http://www.fasebj.org/doi/abs/10.1096/fasebj.31.1_supplement.lb331.
Kim, J.-A. et al., 2007. Heterochromatin is refractory to γ-H2AX modification in yeast and mammals. *The Journal of Cell Biology*, 178(2), pp.209–218. Available at: http://www.ncbi.nlm.nih.gov/pmc/articles/PMC2064441/.
Kim, J.K. et al., 2009. UHRF1 binds G9a and participates in p21 transcriptional regulation in mammalian cells. *Nucleic Acids Research*, 37(2), pp.493–505. Available at: http://dx.doi.org/10.1093/nar/gkn961.
Kim, J.T. et al., 2013. Deregulation of Wnt/β-catenin signaling through genetic or epigenetic alterations in human neuroendocrine tumors. *Carcinogenesis*, 34(5), pp.953–961. Available at: http://www.ncbi.nlm.nih.gov/pmc/articles/PMC3643417/.
Kubicek, S. et al., 2007. Reversal of H3K9me2 by a Small-Molecule Inhibitor for the G9a Histone Methyltransferase. *Molecular Cell*, 25(3), pp.473–481.

Available at: http://www.sciencedirect.com/science/article/pii/S1097276507000408.
Lavin, M.F. et al., 2015. ATM-Dependent Phosphorylation of All Three Members of the MRN Complex: From Sensor to Adaptor W.-D. Heyer, T. Helleday, & F. Hanaoka, eds. *Biomolecules*, 5(4), pp.2877–2902. Available at: http://www.ncbi.nlm.nih.gov/pmc/articles/PMC4693261/.
Lee, J.S., 2007. Activation of ATM-dependent DNA damage signal pathway by a histone deacetylase inhibitor, trichostatin A. *Cancer Res Treat*, 39(3), pp.125–130. Available at: http://www.ncbi.nlm.nih.gov/pubmed/19746219%5Cnhttp://synapse.koreamed.org/Synapse/Data/PDFData/0036CRT/crt-39-125.pdf.
Lee, J.S. et al., 2011. Hypoxia-induced methylation of a pontin chromatin remodeling factor. *Proceedings of the National Academy of Sciences of the United States of America*, 108(33), pp.13510–13515. Available at: http://www.ncbi.nlm.nih.gov/pmc/articles/PMC3158161/.
Lee, J.S. et al., 2010. Negative Regulation of Hypoxic Responses via Induced Reptin Methylation. *Molecular Cell*, 39(1), pp.71–85.
Lee, S.-H. et al., 2005. The SET domain protein Metnase mediates foreign DNA integration and links integration to nonhomologous end-joining repair. *Proceedings of the National Academy of Sciences of the United States of America*, 102(50), pp.18075–18080. Available at: http://www.ncbi.nlm.nih.gov/pmc/articles/PMC1312370/.
Lee, S.H. et al., 2008. Hypoxic silencing of tumor suppressor RUNX3 by histone modification in gastric cancer cells. *Oncogene*, 28, p.184. Available at: http://dx.doi.org/10.1038/onc.2008.377.
Lehnertz, B. et al., 2010. Activating and inhibitory functions for the histone lysine methyltransferase G9a in T helper cell differentiation and function. *The Journal of Experimental Medicine*, 207(5), pp.915–922. Available at: http://www.ncbi.nlm.nih.gov/pmc/articles/PMC2867284/.
Li, G.-M., 2013. Decoding the Histone Code: Role of H3K36me3 in Mismatch Repair and Implications for Cancer Susceptibility and Therapy. *Cancer Research*, 73(21), p.6379 LP-6383. Available at: http://cancerres.aacrjournals.org/content/73/21/6379.abstract.
Li, X. et al., 2015. PP2A-B56 complex is involved in dephosphorylation of gamma-H2AX in the repair process of CPT-induced DNA double-strand breaks. *Toxicology*, 331(2015), pp.57–65.
Lindahl, T., 1993. Instability and decay of the primary structure of DNA. *Nature*, 362, p.709. Available at: http://dx.doi.org/10.1038/362709a0.
Ling, B.M.T. et al., 2012. Lysine methyltransferase G9a methylates the transcription factor MyoD and regulates skeletal muscle differentiation. *Proceedings of the National Academy of Sciences*, 109(3), p.841 LP-846. Available at: http://www.pnas.org/content/109/3/841.abstract.
Liu, C. et al., 2017. Histone Methyltransferase G9a Drives Chemotherapy Resistance by Regulating the Glutamate – Cysteine Ligase Catalytic Subunit in Head and Neck Squamous Cell Carcinoma. , pp.1421–1435.
Liu, F. et al., 2013. Discovery of an in vivo Chemical Probe of the Lysine

Methyltransferases G9a and GLP. *Journal of medicinal chemistry*, 56(21), p.10.1021/jm401480r. Available at: http://www.ncbi.nlm.nih.gov/pmc/articles/PMC3880643/.

Liu, J. et al., 2012. Structural mechanism of the phosphorylation-dependent dimerization of the MDC1 forkhead-associated domain. *Nucleic Acids Research*, 40(9), pp.3898–3912. Available at: http://www.ncbi.nlm.nih.gov/pmc/articles/PMC3351156/.

Liu, S. et al., 2017. Chromodomain Protein CDYL Acts as a Crotonyl-CoA Hydratase to Regulate Histone Crotonylation and Spermatogenesis. *Molecular Cell*, 67(5), p.853–866.e5.

Lou, Z. et al., 2006. MDC1 maintains genomic stability by participating in the amplification of ATM-dependent DNA damage signals. *Molecular Cell*, 21(2), pp.187–200.

Mahaney, B.L. et al., 2013. XRCC4 and XLF form long helical protein filaments suitable for DNA end protection and alignment to facilitate DNA double strand break repair. *Biochemistry and cell biology = Biochimie et biologie cellulaire*, 91(1), pp.31–41. Available at: http://www.ncbi.nlm.nih.gov/pmc/articles/PMC3725335/.

Maier, V.K. et al., 2015. Functional Proteomic Analysis of Repressive Histone Methyltransferase Complexes Reveals ZNF518B as a G9A Regulator. *Molecular & cellular proteomics : MCP*, 14(6), pp.1435–46. Available at: http://www.ncbi.nlm.nih.gov/pubmed/25680957%0Ahttp://www.pubmedcentral.nih.gov/articlerender.fcgi?artid=PMC4458711.

Mao, Z. et al., 2008. DNA repair by nonhomologous end joining and homologous recombination during cell cycle in human cells. *Cell Cycle*, 7(18), pp.2902–2906.

Marteijn, J.A. et al., 2014. Understanding nucleotide excision repair and its roles in cancer and ageing. *Nature Reviews Molecular Cell Biology*, 15(7), pp.465–481. Available at: http://10.0.4.14/nrm3822.

Massip, L. et al., 2010. Deciphering the chromatin landscape induced around DNA double strand breaks. *Cell Cycle*, 9(15), pp.2963–2972.

Matsuoka, S. et al., 2007. ATM and ATR Substrate Analysis Reveals Extensive Protein Networks Responsive to DNA Damage. *Science*, 316(May), pp.1160–1167.

Mauger, O. et al., 2015. Alternative splicing regulates the expression of G9A and SUV39H2 methyltransferases, and dramatically changes SUV39H2 functions. *Nucleic Acids Research*, 43(3), pp.1869–1882. Available at: http://www.ncbi.nlm.nih.gov/pmc/articles/PMC4330376/.

Maze, I. et al., 2010. Essential Role of the Histone Methyltransferase G9a in Cocaine-induced Plasticity. *Science (New York, N.Y.)*, 327(5962), p.213. Available at: http://www.ncbi.nlm.nih.gov/pmc/articles/PMC2820240/.

Miller, K.M. et al., 2011. Human HDAC1 and HDAC2 function in the DNA-damage response to promote DNA non-homologous end-joining. *Nature Structural & Molecular Biology*, 17(9), pp.1144–1151.

Milner, C.M. & Duncan Campbell, R., 1993. The G9a gene in the human major histocompatibility complex encodes a novel protein containing ankyrin-like

repeats. *Biochemical Journal*, 292(Pt 3), p.952. Available at: http://www.ncbi.nlm.nih.gov/pmc/articles/PMC1134208/.

Modrich, P., 1991. Mechanisms and Biological Effects of Mismatch Repair. *Annual Review of Genetics*, 25(1), pp.229–253. Available at: https://doi.org/10.1146/annurev.ge.25.120191.001305.

Moore, K.E. et al., 2013. General Molecular Affinity Strategy for Global Detection and Proteomic Analysis of Lysine Methylation.

Nakada, S., 2016. Opposing roles of RNF8/RNF168 and deubiquitinating enzymes in ubiquitination-dependent DNA double-strand break response signaling and DNA-repair pathway choice. *Journal of Radiation Research*, 57(Suppl 1), pp.i33–i40. Available at: http://www.ncbi.nlm.nih.gov/pmc/articles/PMC4990112/.

Nakajima, N.I. et al., 2017. Inhibition of the HDAC/Suv39/G9a pathway restores the expression of DNA damage-dependent major histocompatibility complex class I-related chain A and B in cancer cells. *Oncology Reports*, 38(2), pp.693–702. Available at: http://www.ncbi.nlm.nih.gov/pmc/articles/PMC5562072/.

Nakanishi, K. et al., 2005. Human Fanconi anemia monoubiquitination pathway promotes homologous DNA repair. *Proceedings of the National Academy of Sciences*, 102(4), pp.1110–1115. Available at: http://www.pnas.org/cgi/doi/10.1073/pnas.0407796102.

Nakanishi, K. et al., 2005. Human Fanconi anemia monoubiquitination pathway promotes homologous DNA repair. *Proceedings of the National Academy of Sciences of the United States of America*, 102(4), pp.1110–5.

Newbold, A. et al., 2016. How do tumor cells respond to HDAC inhibition? *FEBS Journal*, 283(22), pp.4032–4046.

Nishio, H. & Walsh, M.J., 2004. CCAAT displacement protein/cut homolog recruits G9a histone lysine methyltransferase to repress transcription. *Proceedings of the National Academy of Sciences of the United States of America*, 101(31), p.11257 LP-11262. Available at: http://www.pnas.org/content/101/31/11257.abstract.

Ochi, T. et al., 2015. PAXX, a paralog of XRCC4 and XLF, interacts with Ku to promote DNA double-strand break repair. *Science (New York, N.Y.)*, 347(6218), pp.185–188. Available at: http://www.ncbi.nlm.nih.gov/pmc/articles/PMC4338599/.

Ogawa, H. et al., 2002. A Complex with Chromatin Modifiers That Occupies E2F- and Myc-Responsive Genes in G_0 Cells. *Science*, 296(5570), pp.1132–1136. Available at: http://www.jstor.org.proxy.libraries.rutgers.edu/stable/3076711.

Oh, S.-T. et al., 2014. H3K9 histone methyltransferase G9a-mediated transcriptional activation of *p21*. *FEBS Letters*, 588(5), pp.685–691. Available at: http://doi.wiley.com/10.1016/j.febslet.2014.01.039 [Accessed March 14, 2018].

Osipovich, O. et al., 2004. Targeted inhibition of V(D)J recombination by a histone methyltransferase. *Nature Immunology*, 5, p.309. Available at: http://dx.doi.org/10.1038/ni1042.

Patnaik, D. et al., 2004. Substrate Specificity and Kinetic Mechanism of Mammalian G9a Histone H3 Methyltransferase. *Journal of Biological Chemistry* , 279(51), pp.53248–53258. Available at: http://www.jbc.org/content/279/51/53248.abstract.

Pei, H. et al., 2011. MMSET regulates histone H4K20 methylation and 53BP1 accumulation at DNA damage sites. *Nature*, 470(7332), pp.124–128. Available at: http://www.ncbi.nlm.nih.gov/pmc/articles/PMC3064261/.

Pellegrini, M. et al., 2006. Autophosphorylation at serine 1987 is dispensable for murine Atm activation in vivo. *Nature*, 443(7108), pp.222–225. Available at: http://10.0.4.14/nature05112.

Petit, C. & Sancar, A., 1999. Nucleotide excision repair: From E. coli to man. *Biochimie*, 81(1), pp.15–25. Available at: http://www.sciencedirect.com/science/article/pii/S0300908499800340.

Pierce, A.J. et al., 1999. XRCC3 promotes homology-directed repair of DNA damage in mammalian cells. *Genes and Development*, 13(20), pp.2633–2638.

Pierce, A.J. et al., 1999. XRCC3 promotes homology-directed repair of DNA damage in mammalian cells. *Genes & development*, 13(20), pp.2633–8.

Pilch, D.R. et al., 2003. Characteristics of γ-H2AX foci at DNA double-strand breaks sites. *Biochemistry and Cell Biology*, 81(3), pp.123–129. Available at: http://dx.doi.org/10.1139/o03-042.

Pless, O. et al., 2008. G9a-mediated Lysine Methylation Alters the Function of CCAAT/Enhancer-binding Protein-β. *Journal of Biological Chemistry* , 283(39), pp.26357–26363. Available at: http://www.jbc.org/content/283/39/26357.abstract.

Polato, F. et al., 2014. CtIP-mediated resection is essential for viability and can operate independently of BRCA1. *The Journal of Experimental Medicine*, 211(6), p.1027 LP-1036. Available at: http://jem.rupress.org/content/211/6/1027.abstract.

Purcell, D.J. et al., 2012. Recruitment of coregulator G9a by Runx2 for selective enhancement or suppression of transcription. *Journal of Cellular Biochemistry*, 113(7), pp.2406–2414. Available at: http://www.ncbi.nlm.nih.gov/pmc/articles/PMC3350606/.

Rada, M. et al., 2016. Human EHMT2/G9a activates p53 through methylation-independent mechanism. *Oncogene*, 36, p.922. Available at: http://dx.doi.org/10.1038/onc.2016.258.

Rao, V.K. et al., 2016. G9a promotes proliferation and inhibits cell cycle exit during myogenic differentiation. *Nucleic Acids Research*, 44(17), pp.8129–8143. Available at: http://dx.doi.org/10.1093/nar/gkw483.

Rathert, P. et al., 2008. Protein lysine methyltransferase G9a acts on non-histone targets. *Nature chemical biology*, 4(6), pp.344–346.

Ren, A. et al., 2015. Inhibition of H3K9 methyltransferase G9a induces autophagy and apoptosis in oral squamous cell carcinoma. *Biochemical and Biophysical Research Communications*, 459(1), pp.10–17.

Rogakou, E.P. et al., 1998. DNA Double-stranded Breaks Induce Histone H2AX Phosphorylation on Serine 139. *Journal of Biological Chemistry* , 273(10),

pp.5858–5868. Available at: http://www.jbc.org/content/273/10/5858.abstract.
Rogakou, E.P. et al., 1999. Megabase chromatin domains involved in DNA double-strand breaks in vivo. *Journal of Cell Biology*, 146(5), pp.905–915.
Savic, V. et al., 2009. Formation of Dynamic γ-H2AX Domains along Broken DNA Strands is Distinctly Regulated by ATM and MDC1 and Dependent upon H2AX Densities in Chromatin. *Molecular cell*, 34(3), pp.298–310. Available at: http://www.ncbi.nlm.nih.gov/pmc/articles/PMC2744111/.
Shahbazian, M.D. & Grunstein, M., 2007. Functions of Site-Specific Histone Acetylation and Deacetylation. *Annual Review of Biochemistry*, 76(1), pp.75–100. Available at: http://www.annualreviews.org/doi/10.1146/annurev.biochem.76.052705.162114.
Shankar, S.R. et al., 2013. G9a, a multipotent regulator of gene expression. *Epigenetics*, 8(1), pp.16–22.
Shechter, D. et al., 2007. Extraction, purification and analysis of histones. *Nature Protocols*, 2(6), pp.1445–1457.
Shiloh, Y. & Ziv, Y., 2013. The ATM protein kinase: regulating the cellular response to genotoxic stress, and more. *Nature Reviews Molecular Cell Biology*, 14, p.197. Available at: http://dx.doi.org/10.1038/nrm3546.
Simsek, D. & Jasin, M., 2010. Alternative end-joining is suppressed by the canonical NHEJ component Xrcc4/ligase IV during chromosomal translocation formation. *Nature structural & molecular biology*, 17(4), pp.410–416. Available at: http://www.ncbi.nlm.nih.gov/pmc/articles/PMC3893185/.
Singh, K. et al., 2012. Autophagy-dependent senescence in response to DNA damage and chronic apoptotic stress. *Autophagy*, 8(2).
So, S., Davis, A.J. & Chen, D.J., 2009. Autophosphorylation at serine 1981 stabilizes ATM at DNA damage sites. *The Journal of Cell Biology*, 187(7), pp.977–990. Available at: http://www.ncbi.nlm.nih.gov/pmc/articles/PMC2806275/.
Sobhian, B. et al., 2007. RAP80 Targets BRCA1 to Specific Ubiquitin Structures at DNA Damage Sites. *Science (New York, N.Y.)*, 316(5828), pp.1198–1202. Available at: http://www.ncbi.nlm.nih.gov/pmc/articles/PMC2706583/.
Spies, T., Bresnahan, M. & L Strominger, J., 1989. *Human Major Histocompatibility Complex Contains a Minimum of 19 Genes between the Complement Cluster and HLA-B*,
Stewart, G.S. et al., 2009. The RIDDLE Syndrome Protein Mediates a Ubiquitin-Dependent Signaling Cascade at Sites of DNA Damage. *Cell*, 136(3), pp.420–434.
Stucki, M. et al., 2005. MDC1 directly binds phosphorylated histone H2AX to regulate cellular responses to DNA double-strand breaks. *Cell*, 123(7), pp.1213–1226.
Sun, Y. et al., 2005. A role for the Tip60 histone acetyltransferase in the acetylation and activation of ATM. *Proceedings of the National Academy of Sciences of the United States of America*, 102(37), pp.13182–13187.

Available at: http://www.pnas.org/content/102/37/13182.full.
Sun, Y. et al., 2007. DNA Damage-Induced Acetylation of Lysine 3016 of ATM Activates ATM Kinase Activity. *Molecular and Cellular Biology* , 27(24), pp.8502–8509. Available at: http://mcb.asm.org/content/27/24/8502.abstract.
Sun, Y. et al., 2009. Histone H3 methylation links DNA damage detection to activation of the Tip60 tumor suppressor. *Nature cell biology*, 11(11), pp.1376–1382. Available at: http://www.ncbi.nlm.nih.gov/pmc/articles/PMC2783526/.
Sweis, R.F. et al., 2014. Discovery and Development of Potent and Selective Inhibitors of Histone Methyltransferase G9a. *ACS Medicinal Chemistry Letters*, 5(2), pp.205–209. Available at: http://www.ncbi.nlm.nih.gov/pmc/articles/PMC4027767/.
Tachibana, M. et al., 2007. Functional dynamics of H3K9 methylation during meiotic prophase progression. *The EMBO Journal*, 26(14), pp.3346–3359. Available at: http://www.ncbi.nlm.nih.gov/pmc/articles/PMC1933398/.
Tachibana, M. et al., 2008. G9a/GLP complexes independently mediate H3K9 and DNA methylation to silence transcription. *The EMBO Journal*, 27(20), pp.2681–2690. Available at: http://www.ncbi.nlm.nih.gov/pmc/articles/PMC2572175/.
Tachibana, M. et al., 2002. G9a histone methyltransferase plays a dominant role in euchromatic histone H3 lysine 9 methylation and is essential for early embryogenesis. *Genes and Development*, 16(14), pp.1779–1791.
Tachibana, M. et al., 2005. Histone methyltransferases G9a and GLP form heteromeric complexes and are both crucial for methylation of euchromatin at H3-K9. *Genes and Development*, 19(7), pp.815–826.
Tachibana, M. et al., 2001. SET Domain-containing Protein, G9a, is a Novel Lysine-preferring Mammalian Histone Methyltransferase with Hyperactivity and Specific Selectivity to Lysines 9 and 27 of Histone H3. *Journal of Biological Chemistry*, 276(27), pp.25309–25317.
Thorslund, T. et al., 2015. Histone H1 couples initiation and amplification of ubiquitin signalling after DNA damage. *Nature*, 527(7578), pp.389–393. Available at: http://10.0.4.14/nature15401.
Tonini, T. et al., 2004. Determination of Functional Viral Titer by Drug-Resistance Colony Assay, Expression of Green Fluorescent Protein, and $β$-Galactoside Staining. In A. Giordano & G. Romano, eds. *Cell Cycle Control and Dysregulation Protocols: Cyclins, Cyclin-Dependent Kinases, and Other Factors*. Totowa, NJ: Humana Press, pp. 149–153. Available at: https://doi.org/10.1385/1-59259-822-6:149.
Tsukada, Y. et al., 2005. Histone demethylation by a family of JmjC domain-containing proteins. *Nature*, 439, p.811. Available at: http://dx.doi.org/10.1038/nature04433.
Ueda, J. et al., 2006. Zinc finger protein Wiz links G9a/GLP histone methyltransferases to the co-repressor molecule CtBP. *Journal of Biological Chemistry*, 281(29), pp.20120–20128.
Uziel, T. et al., 2003. Requirement of the MRN complex for ATM activation by DNA damage. *The EMBO Journal*, 22(20), pp.5612–5621. Available at:

http://www.ncbi.nlm.nih.gov/pmc/articles/PMC213795/.
Vedadi, M., Barsyte-Lovejoy, D., Liu, F., Rival-Gervier, S., Allali-Hassani, A., Labrie, V., Wigle, T.J., DiMaggio, P.A., et al., 2011. A chemical probe selectively inhibits G9a and GLP methyltransferase activity in cells. *Nature Chemical Biology*, 7, p.566. Available at: http://dx.doi.org/10.1038/nchembio.599.
Vedadi, M., Barsyte-Lovejoy, D., Liu, F., Rival-Gervier, S., Allali-Hassani, A., Labrie, V., Wigle, T.J., Dimaggio, P.A., et al., 2011. A chemical probe selectively inhibits G9a and GLP methyltransferase activity in cells. *Nature chemical biology*, 7(8), pp.566–74. Available at: http://www.pubmedcentral.nih.gov/articlerender.fcgi?artid=3184254&tool=pmcentrez&rendertype=abstract.
Wang, J. & Chen, J., 2010. SIRT1 regulates autoacetylation and histone acetyltransferase activity of TIP60. *Journal of Biological Chemistry*, 285(15), pp.11458–11464.
Wang, M. et al., 2006. PARP-1 and Ku compete for repair of DNA double strand breaks by distinct NHEJ pathways. *Nucleic Acids Research*, 34(21), pp.6170–6182. Available at: http://www.ncbi.nlm.nih.gov/pmc/articles/PMC1693894/.
Watanabe, S. et al., 2013. JMJD1C demethylates MDC1 to regulate the RNF8 and BRCA1-mediated chromatin response to DNA breaks. *Nature Structural and Molecular Biology*, 20(12), pp.1425–1433.
Wei, H. & Yu, X., 2016. Functions of PARylation in DNA Damage Repair Pathways. *Genomics, Proteomics & Bioinformatics*, 14(3), pp.131–139. Available at: http://linkinghub.elsevier.com/retrieve/pii/S1672022916300705.
Weiss, T. et al., 2010. Histone H1 variant-specific lysine methylation by G9a/KMT1C and Glp1/KMT1D. *Epigenetics & Chromatin*, 3(1), p.7. Available at: https://doi.org/10.1186/1756-8935-3-7.
Willemsen, M.H. et al., 2012. Update on Kleefstra syndrome. *Molecular Syndromology*, 2(3–5), pp.202–212.
Wu, H. et al., 2011. Histone methyltransferase G9a contributes to H3K27 methylation in vivo. *Cell Research*, 21(2), pp.365–367. Available at: http://www.ncbi.nlm.nih.gov/pmc/articles/PMC3193445/.
Wu, H. et al., 2013. Short-Form CDYLb but not long-form CDYLa functions cooperatively with histone methyltransferase G9a in hepatocellular carcinomas. *Genes, Chromosomes and Cancer*, 52(7), p.n/a-n/a. Available at: http://doi.wiley.com/10.1002/gcc.22060 [Accessed March 11, 2018].
Wu, W. et al., 2015. Interaction of BARD1 and HP1 is required for BRCA1 retention at sites of DNA damage. *Cancer Research*, 75(7), pp.1311–1321.
Xia, B. et al., 2006. Control of BRCA2 Cellular and Clinical Functions by a Nuclear Partner, PALB2. *Molecular Cell*, 22(6), pp.719–729. Available at: http://www.sciencedirect.com/science/article/pii/S1097276506003376.
Yang, Q. et al., 2017. G9a coordinates with the RPA complex to promote DNA damage repair and cell survival. *Proceedings of the National Academy of Sciences*, p.201700694. Available at: http://www.pnas.org/lookup/doi/10.1073/pnas.1700694114.

Yu, Y. et al., 2012. Histone H3 Lysine 56 Methylation Regulates DNA Replication through Its Interaction with PCNA. *Molecular Cell*, 46(1), pp.7–17. Available at: http://www.ncbi.nlm.nih.gov/pmc/articles/PMC3327800/.

Yuan, Y. et al., 2012. A Small-Molecule Probe of the Histone Methyltransferase Induces Cellular Senescence in Pancreatic Adenocarcinoma. *ACS Chemical Biology*.

Yun, M.H. & Hiom, K., 2009. CtIP-BRCA1 modulates the choice of DNA double-strand break repair pathway throughout the cell cycle. *Nature*, 459(7245), pp.460–463. Available at: http://www.ncbi.nlm.nih.gov/pmc/articles/PMC2857324/.

Zhang, F. et al., 2009. PALB2 Links BRCA1 and BRCA2 in the DNA-Damage Response. *Current biology : CB*, 19(6), pp.524–529. Available at: http://www.ncbi.nlm.nih.gov/pmc/articles/PMC2750839/.

Zhang, J. et al., 2015. Down-regulation of G9a triggers DNA damage response and inhibits colorectal cancer cells proliferation. *Oncotarget*, 6(5), pp.2917–27. Available at: http://www.pubmedcentral.nih.gov/articlerender.fcgi?artid=4413627&tool=pmcentrez&rendertype=abstract.

Zhou, H. et al., 2012. Toward a Comprehensive Characterization of a Human Cancer Cell Phosphoproteome. *Journal of Proteome Research*, 12(1), pp.260–271. Available at: http://dx.doi.org/10.1021/pr300630k.